https://www.mdc-berlin.de/de/veroeffentlichungstypen/clinical-journal-club

Als gemeinsame Einrichtung von MDC und Charité fördert das Experimental and Clinical Research Center die Zusammenarbeit zwischen Grundlagenwissenschaftlern und klinischen Forschern. Hier werden neue Ansätze für Diagnose, Prävention und Therapie von Herz-Kreislauf- und Stoffwechselerkrankungen, Krebs sowie neurologischen Erkrankungen entwickelt und zeitnah am Patienten eingesetzt. Sie sind eingelanden, um uns beizutreten. Bewerben Sie sich!

A 78-year-old man presented to the emergency department with weakness on the left side that had developed 90 minutes earlier. An ischemic stroke in the territory of the right middle cerebral artery was diagnosed, and treatment was initiated. After some time, examination showed the following change in the patient's tongue. What is the most likely diagnosis?

Tissue plasminogen activator-associated angioedema

Lingual artery thrombosis

Lingual dystonia

Unilateral hypoglossal nerve palsy

Melkersson-Rosenthal syndrome

Orolingual angioedema is a known potential adverse effect of intravenous tissue plasminogen activator (t-PA). The swelling can be asymmetric at first and can develop in a location contralateral to the ischemic lesion following a stroke. The mechanism is incompletely understood. Treatment in this case included intravenous antihistamines and glucocorticoids, without need for advanced airway management. The tongue swelling resolved, but at a follow-up visit 3 months after presentation, some neurologic deficits resulting from the stroke remained.

Melkersson-Rosenthal-Syndrom

Chronische, systemische, granulomatöse Entzündung mit der klassischen Symptomentrias: Cheilitis granulomatosa, Fazialisparese, Lingua plicata. Das Vollbild des Syndroms ist selten, häufiger sind unterschiedlich ausgeprägte Minusvarianten. Das von E. Melkersson und C. Rosenthal erstbeschriebene Krankheitsbild wird heute zunehmend unter dem umfassenderen Begriff "orofaziale Granulomatose" geführt und allgemeiner als: "rezidivierende uni- oder bilaterale, orofaziale Schwellung mit Hirnnervendysfunktionen oder -paresen" definiert.

Krankheitsbeginn in Kindheit oder früher Adoleszenz

verstärkt gefurchte Zunge (Lingua plicata)

anfallsartig auftretende Schwellungen im Bereich der Lippen, durch vergrößerte Lippenspeicheldrüsen (als Cheilitis granulomatosa) bzw. des Gesichts (Bereich der Augen, Wangen, Stirn oder Gaumen) mit granulomatöser Entzündung (Arteriitis).

anfallsartig auftretende periphere Fazialislähmung nur in 10 % der Fälle (verursacht durch eine Schwellung des Nervus facialis im Canalis n. VII). Eine Parese tritt jedoch gar nicht oder erst sehr viel später auf. Eine Trias trifft man nur in seltenen Fällen an. Meist ist es ein monosymptomatischer Verlauf (als Cheilitis granulomatosa).

Angioedema is a localized, non-pitting, non-dependent, submucosal, and subcutaneous swelling resulting from the extravasation of fluid into the interstitium due to the increased production of plasma kinins and histamine. It can present with urticaria or anaphylaxis and is usually associated with angiotensin-converting enzyme inhibitors (ACEis), complement deficiencies, or the side effects of tissue plasminogen activator (tPA). Orolingual angioedema following tPA for acute ischemic stroke is a transient, self-resolving hemifacial swelling contralateral to neurological deficits that can rarely progress to the airway, compromising it and leading to a life-threatening situation if not managed promptly.

Plasminogen activation is essential for fibrinolysis—the breakdown of fibrin polymers in blood clots. Besides this important function, plasminogen activation participates in a wide variety of inflammatory conditions. One of these conditions is hereditary angioedema (HAE), a rare disease with characteristic attacks of aggressive tissue swelling due to unregulated production and activity of the inflammatory mediator bradykinin. Plasmin was already implicated in this disease decades ago, but a series of recent discoveries have made it clear that plasmin actively contributes to this pathology. Collective evidence points toward an axis in which the plasminogen activation system and the contact system (which produces bradykinin) are mechanistically coupled. This is amongst others supported by findings in subtypes of HAE that are caused by gain-of-function mutations in the genes that respectively encode factor XII or plasminogen, as well as clinical experience with the antifibrinolytic agents in HAE. The concept of a link between plasminogen activation and the contact system helps us to explain the inflammatory side effects of fibrinolytic therapy, presenting as angioedema or tissue edema. Furthermore, these observations motivate the development and characterization of therapeutic agents that disconnect plasminogen activation from bradykinin production.

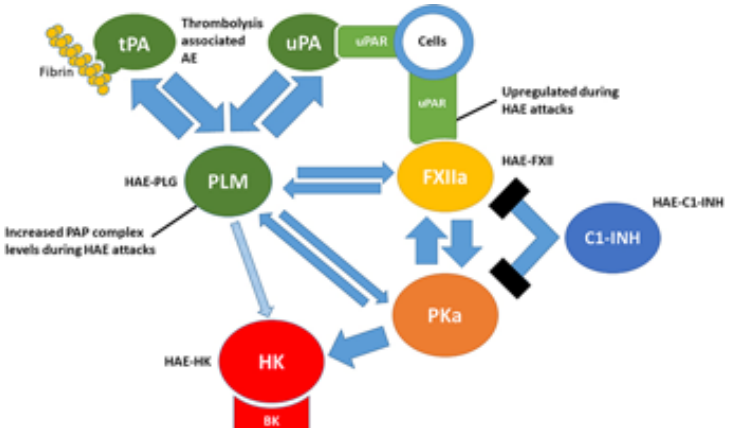

Die akute intermittierende Porphyrie

Die akute intermittierende Porphyrie (AIP) ist die häufigste akute Porphyrie. Symptomatische Patienten und asymptomatische Genträger weisen eine Reduktion der Aktivität des Enzyms Porphobilinogen-Desaminase (PBG-D) von 50 Prozent auf, die für die Porphyrinsynthese ausreicht. Akute Porphyrieattacken treten auf, wenn die Hämsynthese durch Medikamente, Alkohol oder Infektionen gesteigert wird, die PBG-Desaminase die Vorstufen aufgrund ihrer Reduktion nicht entsprechend umsetzen kann, so daß PBG akkumuliert.

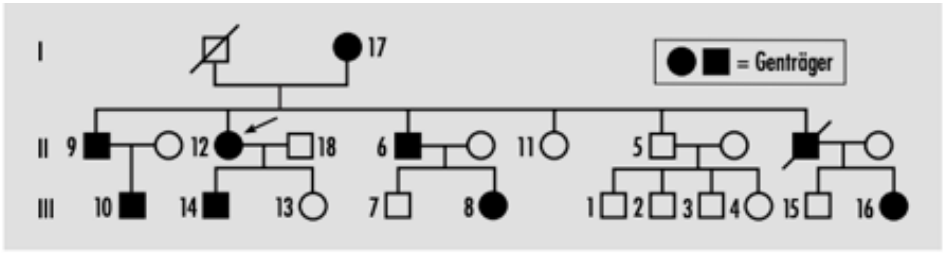

Stammbaum der Familie der Patientin (Pfeil) mit akuter intermittierender Porphyrie (die Zahlen beziehen sich auf die Abbildung).

Symptome bei der akuten intermittierenden Porphyrie (in abfallender Häufigkeit)

- Bauchschmerzen
- Tachykardie
- periphere Lähmung
- Parästhesien
- Erbrechen
- Obstipation
- Diarrhö
- Muskelschwäche
- Krämpfe
- Atemlähmung
- Mentale Symptome (Verwirrtheit, Halluzinationen)
- Hochdruck
- epileptische Anfälle
- Koma

Medikamente, die Porphyrieattacken auslösen können*

- Barbiturate (zum Beispiel Luminaletten)
- Carbamazepin (zum Beispiel Tegretal)
- Diclofenac (zum Beispiel Voltaren)
- Phenytoin (zum Beispiel Zentropil)
- Griseofulvin (zum Beispiel Flucin)
- Meprobamat (zum Beispiel Visano)
- Phenylbutazon (zum Beispiel Ambene)
- Sulfonamid-Antibiotika
- Valproinsäure (zum Beispiel Ergenyl)

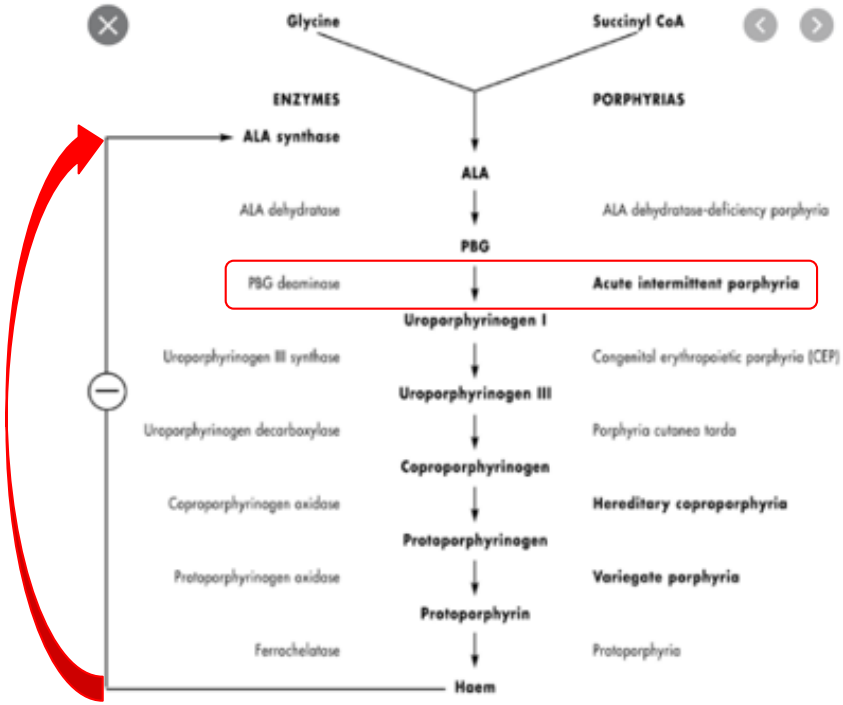
Glycine
Succinyl CoA
ENZYMES
PORPHYRIAS
ALA synthase
ALA
ALA dehydratase
ALA dehydratase-deficiency porphyria
PBG
PBG deaminase
Acute intermittent porphyria
Uroporphyrinogen I
Uroporphyrinogen III synthase
Congenital erythropoietic porphyria (CEP)
Uroporphyrinogen III
Uroporphyrinogen decarboxylase
Porphyria cutanea tarda
Coproporphyrinogen
Coproporphyrinogen oxidase
Hereditary coproporphyria
Protoporphyrinogen
Protoporphyrinogen oxidase
Variegate porphyria
Protoporphyrin
Ferrochelatase
Protoporphyria
Haem

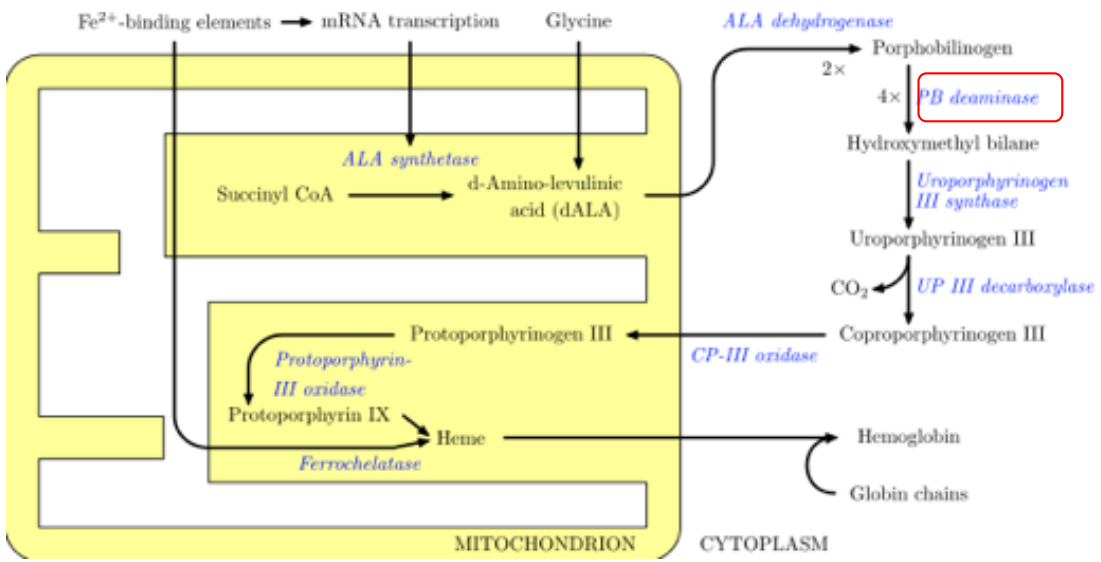
Fe^{2+}-binding elements
mRNA transcription
Glycine
ALA dehydrogenase
Porphobilinogen
2×
4×
PB deaminase
Hydroxymethyl bilane
Uroporphyrinogen III synthase
Uroporphyrinogen III
CO_2
UP III decarboxylase
Coproporphyrinogen III
CP-III oxidase
Protoporphyrinogen III
Protoporphyrin-III oxidase
Protoporphyrin IX
Heme
Ferrochelatase
Hemoglobin
Globin chains
ALA synthetase
Succinyl CoA
d-Amino-levulinic acid (dALA)
MITOCHONDRION
CYTOPLASM

Hämine (Chloroeisen(III)-Porphyrin-Koordinationskomplexe) sind Komplexverbindungen der Häme mit dem Eisen-Ion in der Oxidationsstufe (+III) und einem Chlorid-Ion als axialen Liganden. Für die Synthese des Hämins erhielt der deutsche Chemiker Hans Fischer 1930 den Nobelpreis für Chemie. Humanes, aus menschlichem Blut gewonnenes Hämin wird in Form eines Infusionslösungskonzentrats (Normosang®, Orphan Europe, Frankreich) zur Behandlung akuter Schübe bei Patienten mit akuter hepatischer Porphyrie eingesetzt und unterliegt der ärztlichen Verschreibungspflicht. Porphyrien sind meist angeborene Bildungsstörungen der Häm-Gruppe, gekennzeichnet durch den teilweisen Ausfall von Enzymen, die die 8 nacheinander folgenden Schritte des Häm-Aufbaus katalysieren. Bei einer Störung des Synthesewegs aber führt die positive Rückkopplung zu einer Anreicherung des Stoffwechselproduktes, das nicht mit der normalen Rate umgesetzt (weiterverarbeitet) werden kann und ein Porphyrie-Schub entsteht (Porphyrinvorläufer sind toxisch für den Körper). Hämin-Arginat besetzt die positive Rückkopplungsstelle im Syntheseweg (es suggeriert dem Körper, dass eine ausreichende Menge Häm vorhanden ist) und bewirkt eine Entkopplung der Rückkopplung.

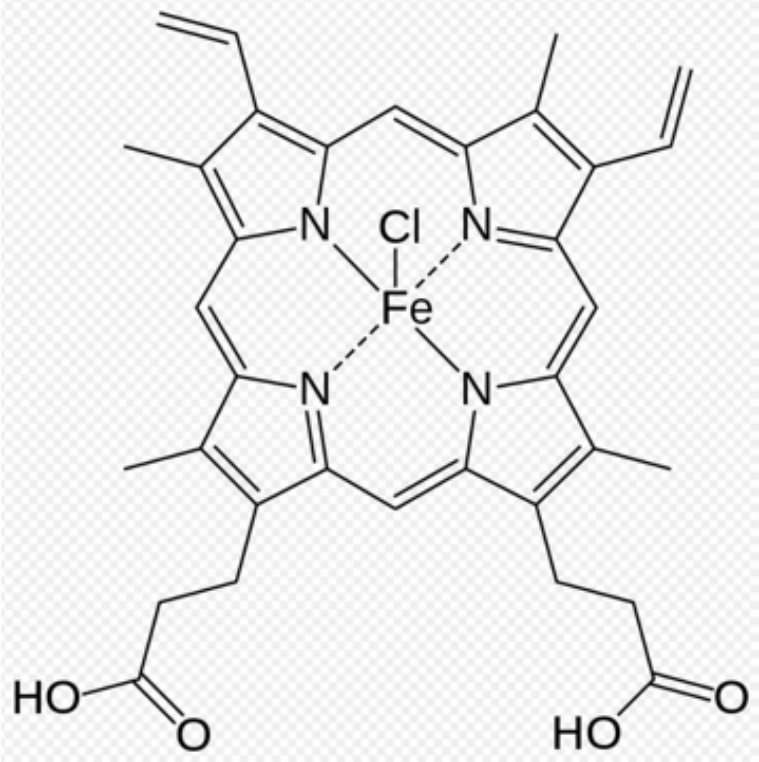

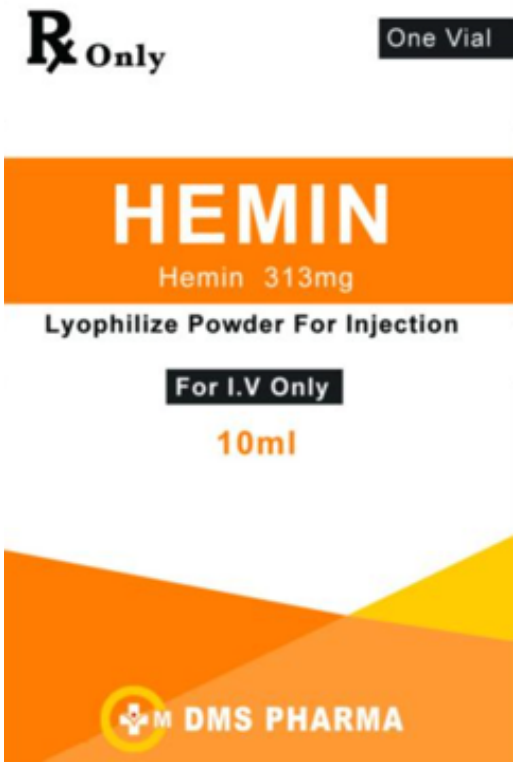

Givosiran ist ein Arzneistoff, der als Givlaari (Hersteller Alnylam Pharmaceuticals) zur Behandlung der akuten intermittierenden Porphyrie (AIP) zugelassen wurde. Es ist ein Vertreter einer vergleichsweise neuen Wirkstoffklasse, deren Wirkung auf RNA-Interferenz (RNAi) beziehungsweise RNA-Silencing (Gen-Stilllegung) beruht.

In den Biowissenschaften hat sich RNA-Interferenz als eine experimentelle Möglichkeit zur vorübergehenden Stilllegung von Genen („Gen-Knockdown“) etabliert. Man spricht bei dieser Substanzklasse von RNAi-Therapeutika.

Givosiran ist eine doppelsträngige, kleine interferierende Ribonukleinsäure (small interfering RNA, siRNA). Givosiran ist angezeigt zur Behandlung der akuten intermittierenden Porphyrie (AIP) bei Patienten ab 12 Jahren. Intermittierend bedeutet phasenhaft, siehe auch Krankheitsverlauf. Die AIP ist eine sehr seltene Krankheit (ultra rare disease) und eine Form der Porphyrien. Dabei handelt es sich um meist angeborene Störungen der Häm-Biosynthese, bei denen es aufgrund eines Enzym-Defektes zur Überproduktion, Anhäufung und vermehrten Ausscheidung von Zwischenprodukten der Hämsynthese, den sogenannten Porphyrinen, kommt. Unterschieden werden erythropoetische (die Blutbildung betreffende) und hepatische (die Leber betreffende) Porphyrien.

Givosiran inhibiert die Aminolävulinsäuresynthase, welche in der Hämoglobinsynthese eine relevante Rolle spielt.

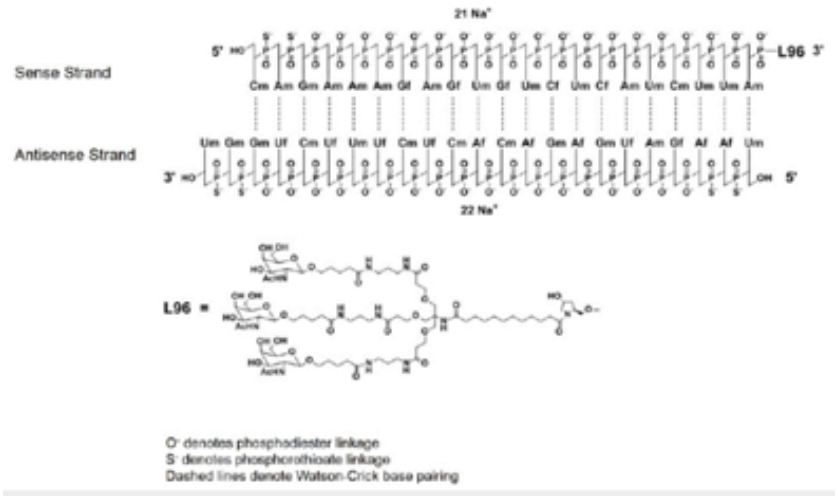

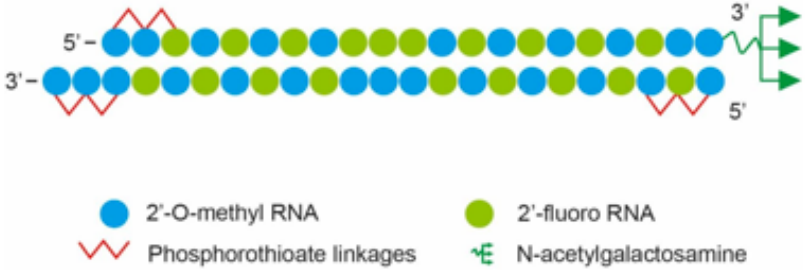

Phase 3 Trial of RNAi Therapeutic Givosiran for Acute Intermittent Porphyria

Up-regulation of hepatic delta-aminolevulinic acid synthase 1 (ALAS1), with resultant accumulation of delta-aminolevulinic acid (ALA) and porphobilinogen, is central to the pathogenesis of acute attacks and chronic symptoms in acute hepatic porphyria. Givosiran, an RNA interference therapy, inhibits ALAS1 expression.

In this double-blind, placebo-controlled, phase 3 trial, we randomly assigned symptomatic patients with acute hepatic porphyria to receive either subcutaneous givosiran (2.5 mg per kilogram of body weight) or placebo monthly for 6 months. The primary end point was the annualized rate of composite porphyria attacks among patients with acute intermittent porphyria, the most common subtype of acute hepatic porphyria. (Composite porphyria attacks resulted in hospitalization, an urgent health care visit, or intravenous administration of hemin at home.) Key secondary end points were levels of ALA and porphobilinogen and the annualized attack rate among patients with acute hepatic porphyria, along with hemin use and daily worst pain scores in patients with acute intermittent porphyria.

Characteristic	Patients with Acute Hepatic Porphyria			Patients with Acute Intermittent Porphyria		
	Placebo (N=46)	Givosiran (N=48)	Overall (N=94)	Placebo (N=43)	Givosiran (N=46)	Overall (N=89)
Age — yr	37.4±10.5	40.1±12.1	38.8±11.4	37.3±10.5	40.7±12.0	39.0±11.4
Female sex — no. (%)	41 (89)	43 (90)	84 (89)	39 (91)	41 (89)	80 (90)
Body-mass index†	25.5±6.4	24.3±5.2	24.9±5.8	25.7±6.3	24.3±5.2	24.9±5.8
Race — no. (%)‡						
White	34 (74)	39 (81)	73 (78)	33 (77)	37 (80)	70 (79)
Black	1 (2)	0	1 (1)	0	0	0
Asian	7 (15)	8 (17)	15 (16)	6 (14)	8 (17)	14 (16)
Other	4 (9)	1 (2)	5 (5)	4 (9)	1 (2)	5 (6)
Acute intermittent porphyria with identified mutation — no. (%)	43 (93)	46 (96)	89 (95)	43 (100)	46 (100)	89 (100)
Nonacute intermittent porphyria§						
All subtypes	3 (7)	2 (4)	5 (5)	NA	NA	NA
Hereditary coproporphyria	0	1 (2)	1 (1)			
Variegate porphyria	1 (2)	1 (2)	2 (2)			
Acute hepatic porphyria without identified mutation	2 (4)	0	2 (2)¶			
No. of yr since diagnosis	8.3±8.5	11.1±11.2	9.7±10.0	8.4±8.7	11.5±11.3	10.0±10.2
Previous hemin prophylaxis — no. (%)						
Yes	18 (39)	20 (42)	38 (40)	17 (40)	20 (43)	37 (42)
No	28 (61)	28 (58)	56 (60)	26 (60)	26 (57)	52 (58)
Historical annualized attack rate‖						
High — no. (%)	21 (46)	24 (50)	45 (48)	20 (47)	23 (50)	43 (48)
Low — no. (%)	25 (54)	24 (50)	49 (52)	23 (53)	23 (50)	46 (52)
Median rate (IQR)	7 (4–14)	8 (4–18)	8 (4–16)	8 (4–14)	8 (4–18)	8 (4–16)
Previous chronic symptoms — no. (%)**						
Yes	26 (57)	23 (48)	49 (52)	24 (56)	22 (48)	46 (52)
No	20 (43)	25 (52)	45 (48)	19 (44)	24 (52)	43 (48)
Previous long-term opioid use — no. (%)††						
Yes	13 (28)	14 (29)	27 (29)	12 (28)	14 (30)	26 (29)
No	33 (72)	34 (71)	67 (71)	31 (72)	32 (70)	63 (71)

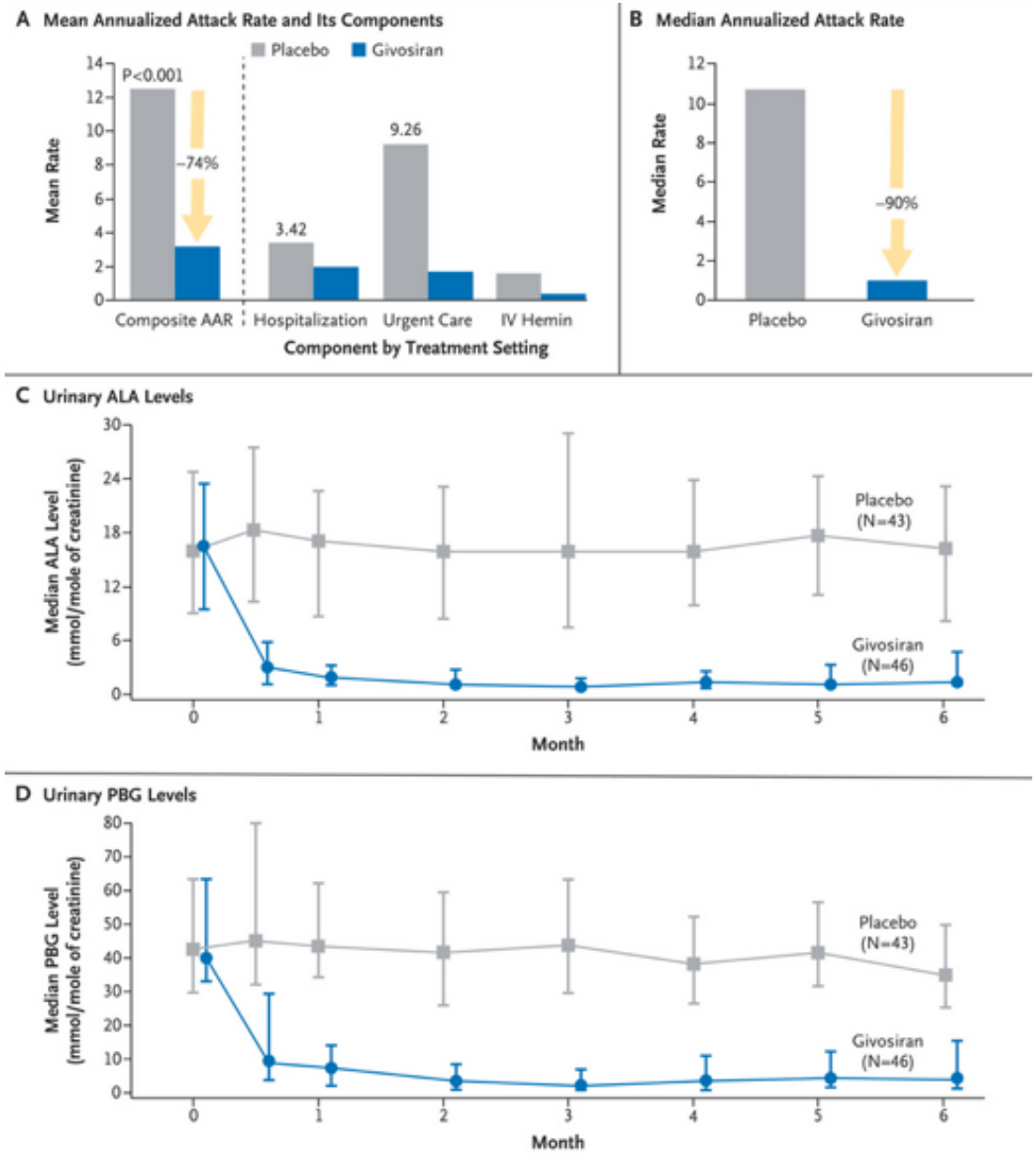

Figure 1. Annualized Attack Rate (AAR) and Urinary Levels of Neurotoxic Heme Intermediates in Patients with Acute Intermittent Porphyria.

Panel A shows the mean annualized rate of composite porphyria attacks (the primary end point) among the 89 patients with acute intermittent porphyria who received either givosiran or placebo. A composite porphyria attack was defined as an attack that resulted in hospitalization, an urgent health care visit, or intravenous administration of hemin at home. IV denotes intravenous. Panel B shows the median annualized attack rate, which was calculated from the individual patients' annualized attack rates. Also shown are the median levels of urinary delta-aminolevulinic acid (ALA) (Panel C) and porphobilinogen (PBG) (Panel D) in patients with acute intermittent porphyria. In Panels C and D, the I bars denote the interquartile range.

Secondary End Points	Placebo (N=43)	Givosiran (N=46)	Difference†	P Value
Urinary ALA — mmol/mole of creatinine				
Mean (±SD) level at baseline	17.5±10.9	20.0±16.8		
Month 3				
Least-squares mean (±SE)	20.0±1.5	1.8±1.4	−18.2±2.0	<0.001
Median (IQR)	15.7 (7.5 to 28.9)	0.8 (0.5 to 1.7)	−14.6 (−18.0 to 9.6)‡	<0.001
Month 6				
Least-squares mean (±SE)	23.2±2.5	4.0±2.4	−19.1±3.5	<0.001
Median (IQR)	16.2 (8.0 to 23.0)	1.3 (0.9 to 4.6)	−12.8 (−16.1 to −7.8)‡	<0.001
Urinary porphobilinogen — mmol/mole of creatinine				
Mean (±SD) at baseline	46.8±24.3	50.4± 34.3		
Least-squares mean (±SE) at 6 mo	49.1±5.0	12.9±4.6	−36.2±6.8	<0.001
Median (IQR) at 6 mo	35.1 (25.6 to 50.0)	4.4 (1.6 to 15.3)	−27.5 (−34.0 to −21.0)‡	<0.001
Annualized no. of days of hemin use				
Mean (95% CI)	29.7 (18.4 to 47.9)	6.8 (4.2 to 10.9)	0.23 (0.11 to 0.45)§	<0.001
Median (IQR)¶	27.6 (2.1 to 47.6)	0.0 (0.0 to 10.8)		
Annualized attack rate in patients with acute hepatic porphyria				
Mean (95% CI)	12.3 (9.2 to 16.3)	3.4 (2.4 to 4.7)	0.27 (0.17 to 0.43)§	<0.001
Median (IQR)¶	10.7 (2.2 to 25.9)	1.0 (0.0 to 6.4)		
Daily worst score for pain‖				
Median of change in AUC from baseline (IQR)	5.3 (−23.0 to 11.1)	−11.5 (−29.2 to 3.0)	−10.1 (−22.8 to 0.9)‡	0.046
Median of average change from baseline (IQR)	0.2 (−1.0 to 0.5)	−0.5 (−1.3 to 0.1)	−0.4 (−1.0 to 0.1)‡	0.049
Daily worst score for fatigue‖				
Least-squares mean (±SE) of change in AUC from baseline	−4.2±4.7	−11.1±4.5	−6.9±6.5	NS
Least-squares mean (±SE) of average change from baseline	−0.2±0.2	−0.5±0.2	−0.3±0.3	NS
Daily worst score for nausea‖				
Least-squares mean (±SE) of change in AUC from baseline	−4.0±3.5	1.5±3.3	5.5±4.8	NT
Least-squares mean (±SE) of average change from baseline	−0.2±0.2	0.1±0.1	0.2±0.2	NT
SF-12**				
Mean (±SD) at baseline	38.4±9.4	39.4±9.6		NT
Least-squares mean (±SE) of change from baseline at 6 mo	1.4±1.2	5.4±1.2	3.9±1.7	NT

Adverse Events	Placebo (N=46)	Givosiran (N=48)
	no. of patients (%)	
Any adverse event	37 (80)	43 (90)
Any severe adverse event	5 (11)	8 (17)
Any serious adverse event	4 (9)	10 (21)
Any adverse event leading to discontinuation of the trial regimen	0	1 (2)
Death	0	0
Adverse events with higher frequency (≥5 percentage points) in the givosiran group		
Injection-site reaction†	0	12 (25)
Nausea	5 (11)	13 (27)
Chronic kidney disease	0	5 (10)
Decreased eGFR	0	3 (6)
Rash	0	3 (6)
Increased alanine aminotransferase	1 (2)	4 (8)
Fatigue	2 (4)	5 (10)
Adverse events with higher frequency (≥5 percentage points) in the placebo group		
Pyrexia	6 (13)	1 (2)
Hypoesthesia	4 (9)	0
Dyspepsia	4 (9)	0
Vomiting	5 (11)	2 (4)
Urinary tract infection	6 (13)	3 (6)
Back pain	4 (9)	1 (2)
Adverse events of interest		
Hepatic‡	1 (2)	6 (13)
Renal§		
Any event	3 (7)	7 (15)
Increased serum creatinine or decreased eGFR¶	2 (4)	7 (15)

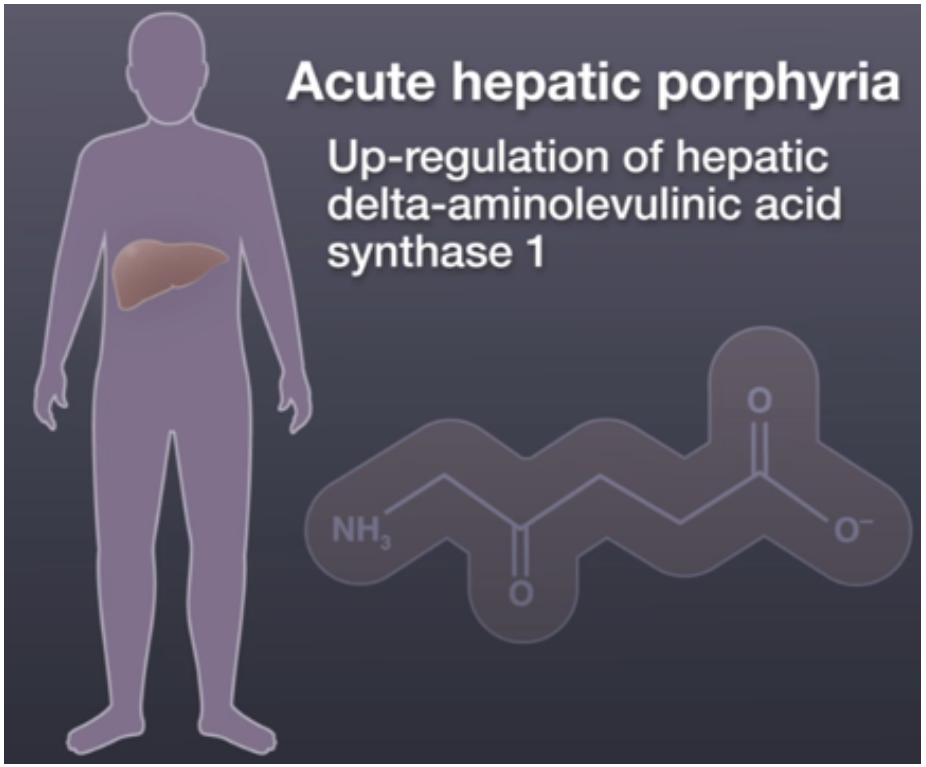
Acute hepatic porphyria
Up-regulation of hepatic delta-aminolevulinic acid synthase 1
NH3
O⁻

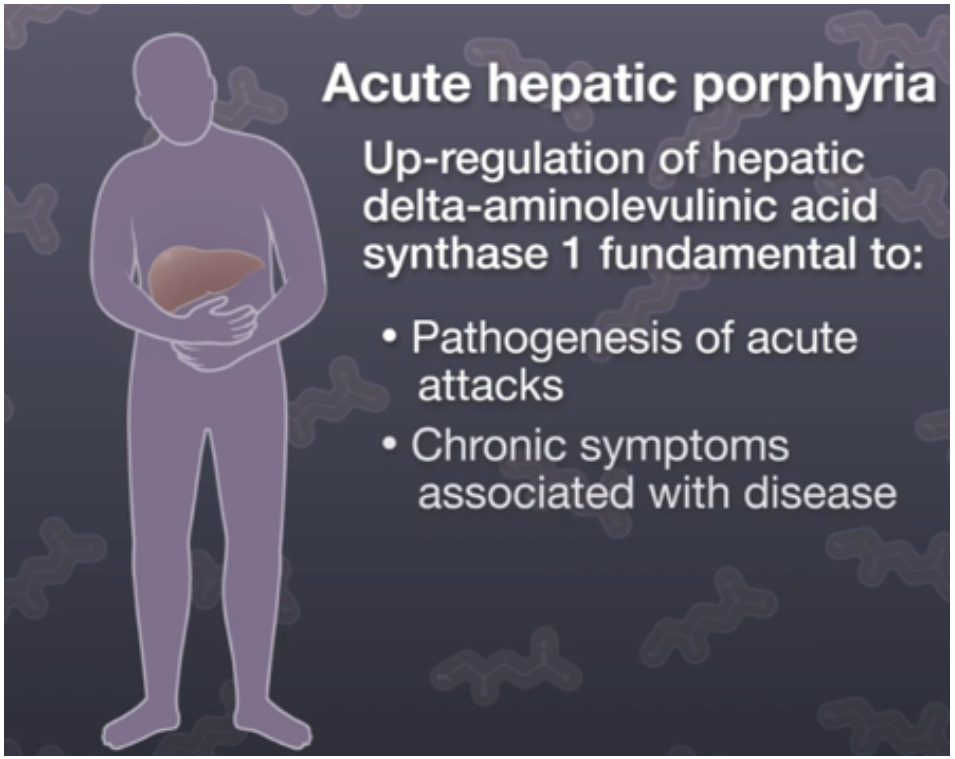
Acute hepatic porphyria
Up-regulation of hepatic delta-aminolevulinic acid synthase 1 fundamental to:
• Pathogenesis of acute attacks
• Chronic symptoms associated with disease

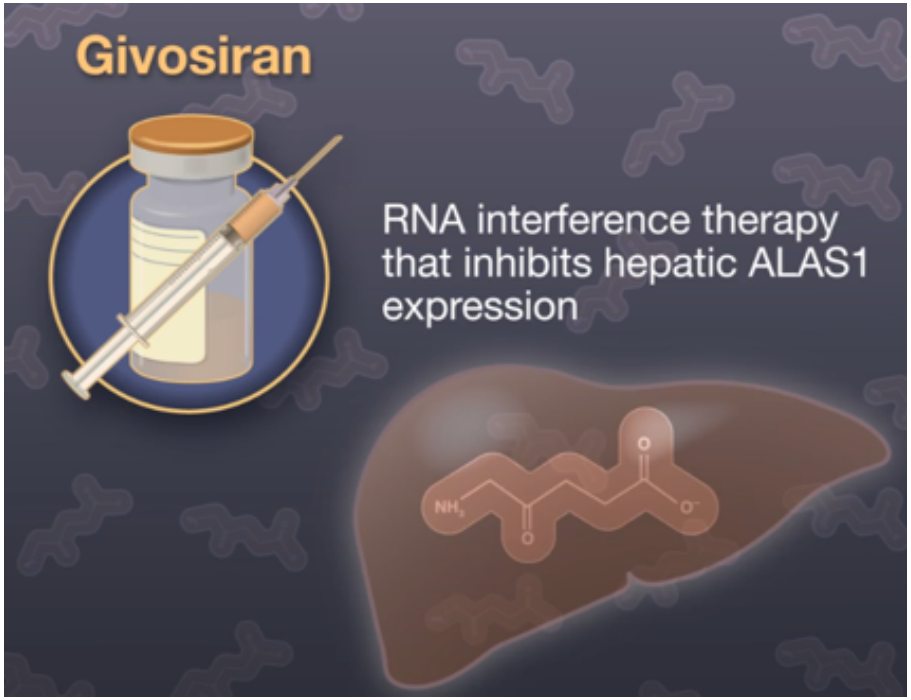
Givosiran
RNA interference therapy that inhibits hepatic ALAS1 expression


Givosiran
Placebo
Monthly, for 6 months

Primary end point:

Annualized rate of porphyria attacks in patients with **acute intermittent porphyria**

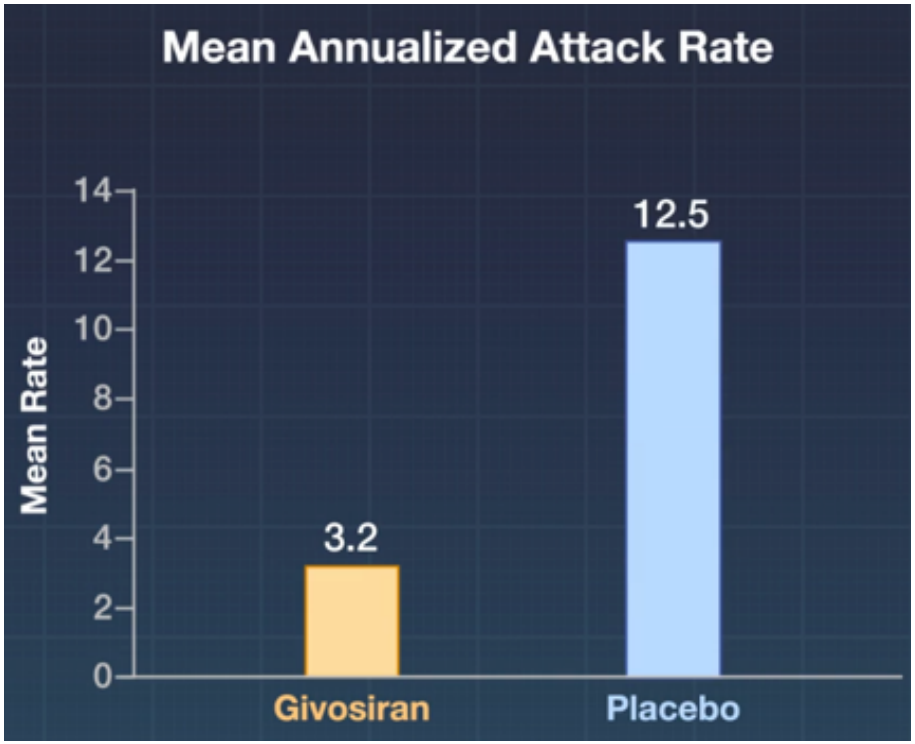

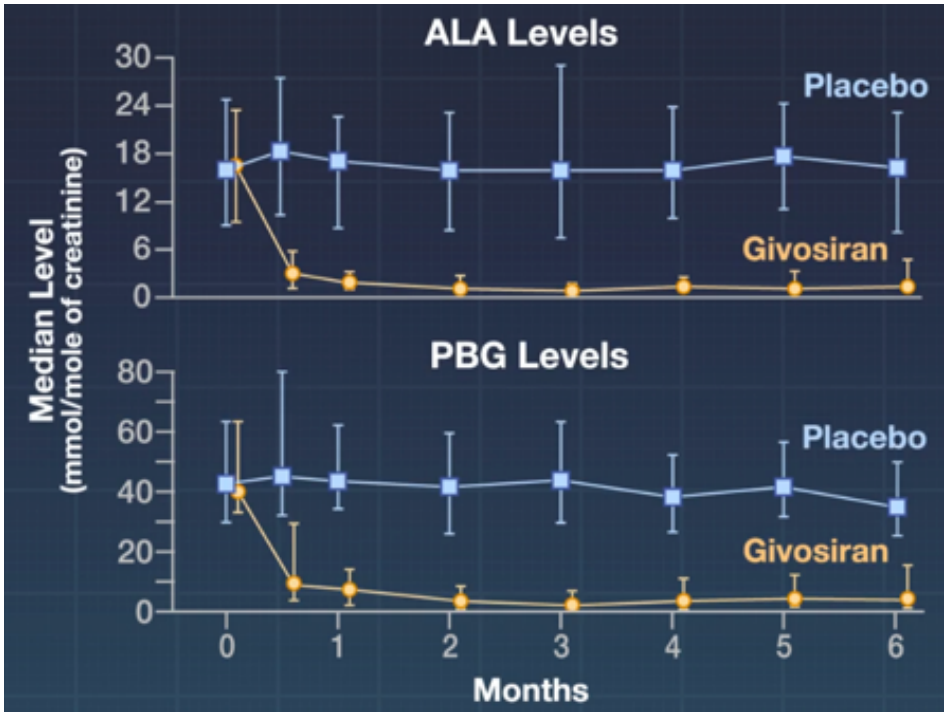

Adverse events more common in the givosiran group included:

- Injection-site reactions
- Nausea
- Chronic kidney disease
- Decreased glomerular filtration rate
- Rash
- Increased alanine aminotransferase
- Fatigue

Spread of SARS-CoV-2 in the Icelandic Population

During the current worldwide pandemic, coronavirus disease 2019 (Covid-19) was first diagnosed in Iceland at the end of February. However, data are limited on how SARS-CoV-2, the virus that causes Covid-19, enters and spreads in a population (in size about the same as Spandau in Berlin, ie <300,000 persons). We targeted testing to persons living in Iceland who were at high risk for infection (mainly those who were symptomatic, had recently traveled to high-risk countries, or had contact with infected persons). We also carried out population screening using two strategies: issuing an open invitation to 10,797 persons and sending random invitations to 2283 persons. We sequenced SARS-CoV-2 from 643 samples.

Children under 10 years of age were less likely to receive a positive result than were persons 10 years of age or older, with percentages of 6.7% and 13.7%, respectively, for targeted testing; in the population screening, no child under 10 years of age had a positive result, as compared with 0.8% of those 10 years of age or older. Fewer females than males received positive results both in targeted testing (11.0% vs. 16.7%) and in population screening (0.6% vs. 0.9%). The haplotypes of the sequenced SARS-CoV-2 viruses were diverse and changed over time. The percentage of infected participants that was determined through population screening remained stable for the 20-day duration of screening.

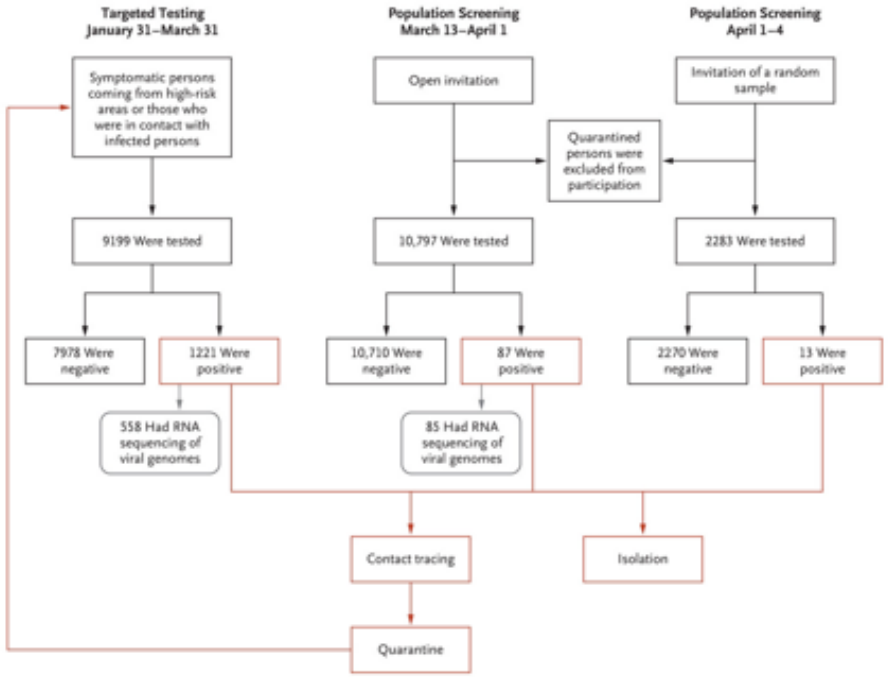

Figure 1. Study Design for Targeted Testing and Population Screening.

In Iceland, targeted testing for severe acute respiratory syndrome coronavirus 2 (SARS-CoV-2) began on January 31, 2020, and involved persons who were deemed to be at high risk for infection (i.e., those who were symptomatic, had traveled to high-risk countries, or had contact with infected persons). In the population screening, data from the open-invitation subgroup and random-sample subgroup were evaluated separately.

Variable	Targeted Testing January 31–March 15		Population Screening March 13–April 1		Targeted Testing March 16–31		Random-Sample Population Screening April 1–4	
	All Persons (N=1924)	SARS-CoV-2 Positive (N=177)	All Persons (N=10,797)	SARS-CoV-2 Positive (N=87)	All Persons (N=7275)	SARS-CoV-2 Positive (N=1044)	All Persons (N=2283)	SARS-CoV-2 Positive (N=13)
SARS-CoV-2 positivity — no. (%)	177 (9.2)	—	87 (0.8)	—	1044 (14.4)	—	13 (0.6)	—
SARS-CoV-2 sequencing performed — no. (%)	—	157 (88.7)	—	59 (67.8)	—	361 (34.6)	—	0
Male sex — no. (%)	835 (43.4)	92 (52.0)	5004 (46.3)	46 (52.9)	2795 (38.4)	516 (49.4)	864 (37.8)	9 (69.2)
Mean age — yr	40.0	44.4	38.6	40.8	40.4	41.3	45.4	50.5
Any international travel — no. (%)	—	115 (65.0)	939 (8.7)	20 (23.0)	—	162 (15.5)	11 (0.5)	0
Specific country of international travel — no.*								
China (high-risk area)	—	1	2	0	—	0	0	0
Austria (high-risk area February 29)	—	43	16	0	—	34	0	0
Italy (high-risk area February 29)	—	45	7	1	—	3	0	0
Switzerland (high-risk area February 29)	—	9	11	0	—	2	1	0
United Kingdom	—	7	193	12†‡	—	44	0	0
United States	—	7	160	3	—	18	1	0
Denmark	—	2	90	1	—	2	2	0
Germany (high-risk area March 12)	—	1	36	1	—	2	0	0
Spain (high-risk area March 14)	—	0	142	1‡	—	34	3	0
The Netherlands	—	0	26	2†	—	5	1	0
Poland	—	0	45	1	—	0	0	0
Other	—	0	247	0	—	14	4	0
Known contact with infected person — no. (%)	—	71 (40.1)	281 (2.6)	6 (6.9)	—	629 (60.2)	60 (2.6)	1 (7.7)
Reported any symptoms — no. (%)‡	—	153 (86.4)	3579 (33.1)	51 (58.6)	—	985 (94.3)	271 (11.9)	6 (46.2)
Reported specific symptoms — no.	—	78	3579	51	—	950	271	6
Distribution of symptoms reported — no. (%)								
Fever	—	38 (42.1)§	410 (3.8)	17 (19.5)	—	491 (48.8)§	21 (0.9)	0
Cough	—	23 (25.5)§	1769 (16.4)	32 (36.8)	—	313 (31.1)§	87 (3.8)	3 (23.1)
Body aches	—	26 (28.8)§	537 (5.0)	19 (21.8)	—	310 (30.8)§	43 (1.9)	1 (7.7)
Headache	—	21 (23.3)§	1,086 (10.1)	18 (20.7)	—	239 (23.7)§	89 (3.9)	2 (15.4)
Sore throat	—	15 (16.6)§	1,558 (14.4)	26 (29.9)	—	123 (12.2)§	107 (4.7)	0
Rhinorrhea	—	14 (15.5)§	1,784 (16.5)	24 (27.6)	—	126 (12.5)§	139 (6.1)	4 (30.8)
Fatigue¶	—	12 (13.3)§	—	—	—	207 (20.6)§	—	—
Loss of smell or taste‖	—	2 (2.2)§	—	—	—	116 (11.5)§	13 (0.6)	1 (7.7)
Other	—	14 (15.5)§	911 (8.4)	15 (17.2)	—	254 (25.2)§	88 (3.9)	3 (23.1)

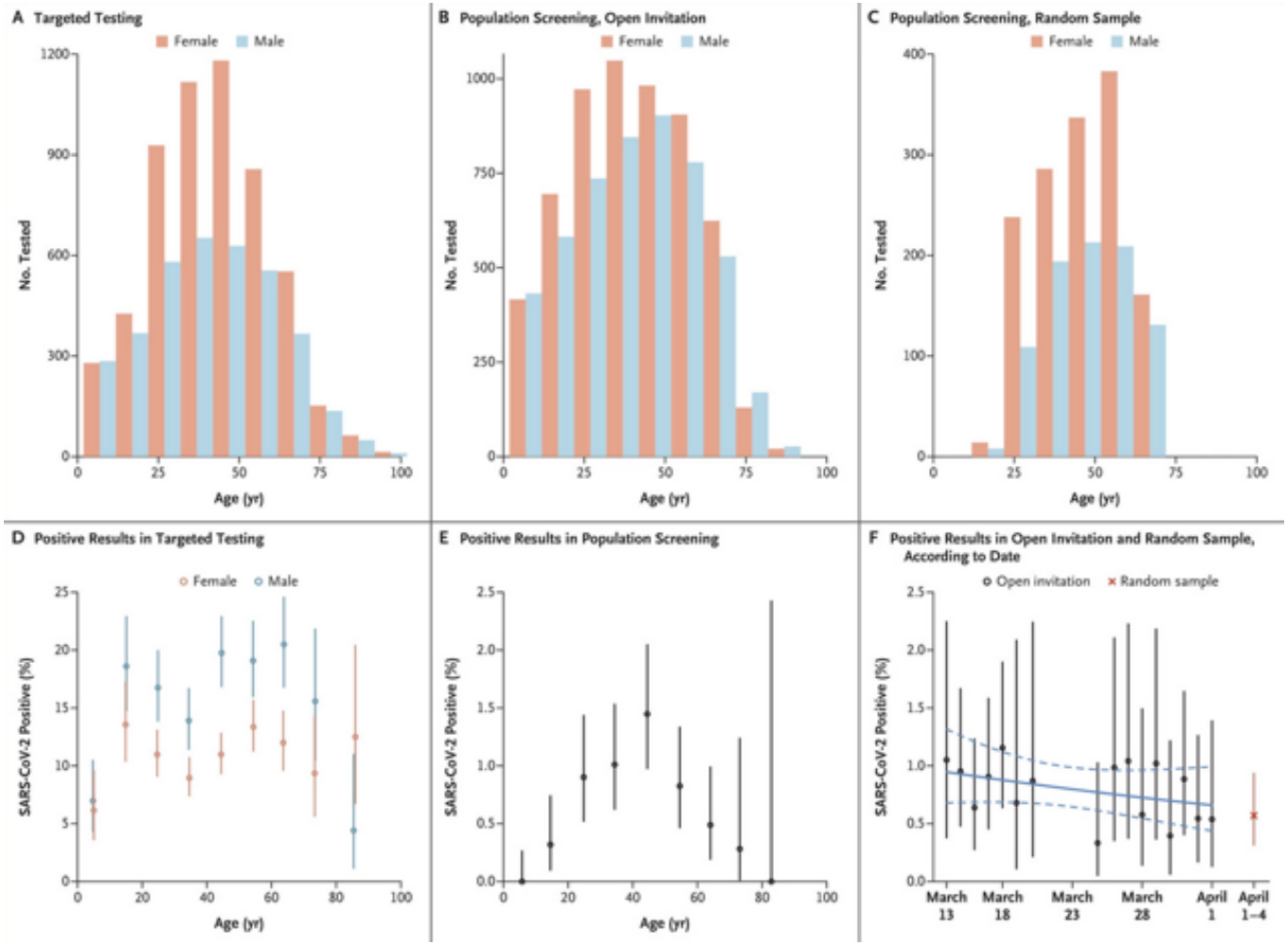

Figure 2. Distribution of Targeted Testing and Population Screening for SARS-CoV-2 and Percentages of Positive Results, According to Age and Sex.

Shown is the distribution according to age and sex among all the participants in the study who were targeted for testing for the presence of SARS-CoV-2 (Panel A), among those who participated in the open invitation of the population screening (Panel B), and among those who participated in the random sample (Panel C). Also shown are the percentages of participants who tested positive stratified according to sex in the targeted-testing group (Panel D) and in the population-screening group (Panel E). In addition, the percentage of participants who tested positive in the population screening is shown according to sampling date in the open invitation (black) and the random sampling (red) (Panel F). The solid blue curve in Panel F indicates the logistic-regression line, and the dashed lines indicate the 95% confidence intervals (CI) of the logistic regression. The logistic-regression slope corresponds to a change of −2% (95% CI, −5 to 1) in the infection rate per day. The vertical bars indicate 95% confidence intervals for age groups (in Panels D and E) and for individual dates (in Panel F).

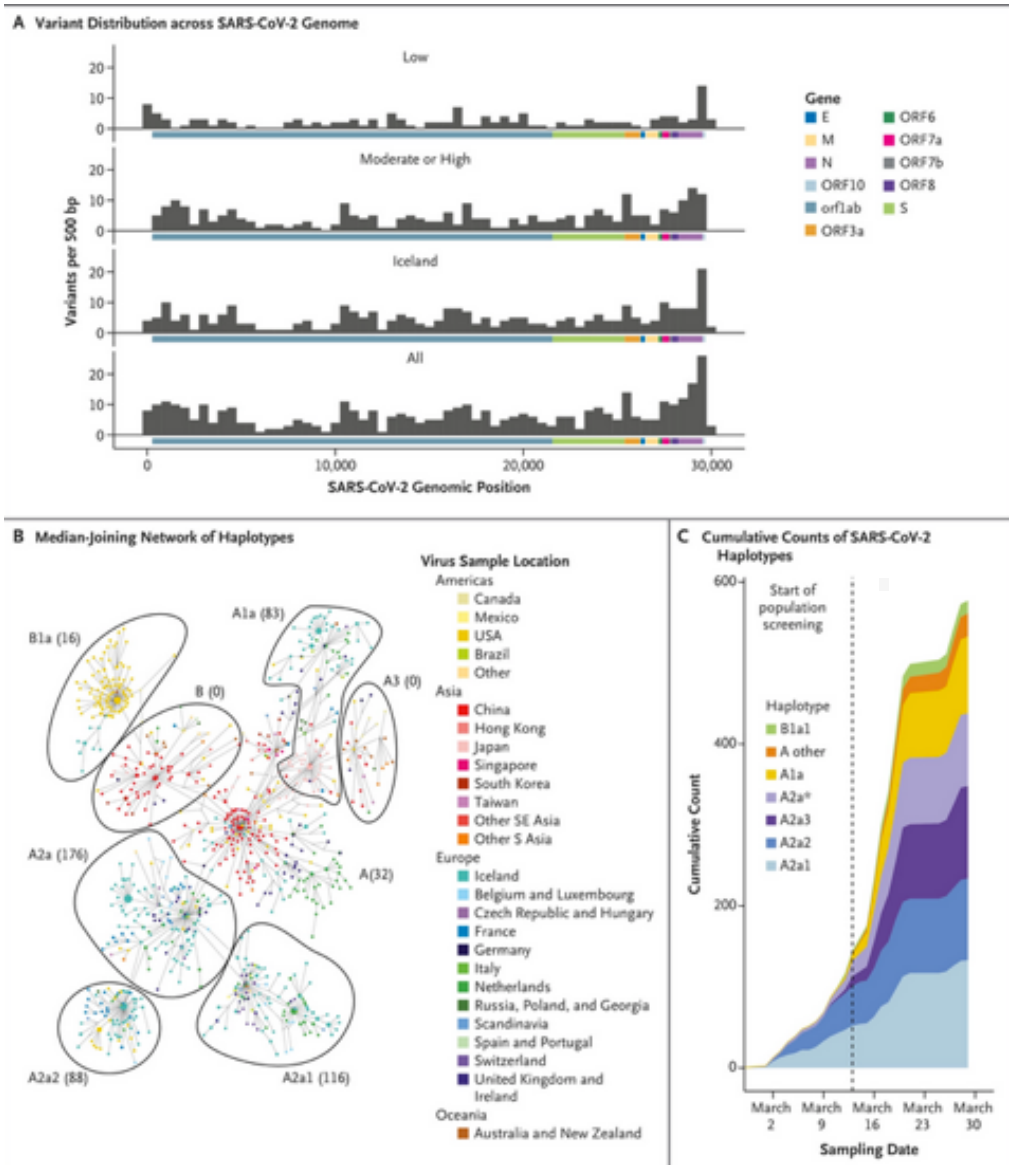

Genome, a Median-Joining Network of Haplotypes, and Cumulative Counts from Targeted Testing and Population Screening.

Panel A shows the distribution of variants across the SARS-CoV-2 genome. The genes of SARS-CoV-2 are E (envelope small membrane protein), M (membrane protein), N (nucleoprotein), S (spike protein), and ORFs (open reading frames) 10, 1ab, 3a, 6, 7a, 7b, and 8. The different subsets that were considered included all variants, variants only observed in Iceland, and variants that were determined by the variant effect predictor to have a low effect (synonymous variants), a moderate effect (missense variants), or a high effect (loss-of-function variants). Panel B shows a median-joining network of 802 haplotypes from 1547 SARS-CoV-2 sequences (of which 513 are from Iceland). Each circle represents a different sequence type, in which the size of the circle reflects the number of carrier hosts, and the lines between circles represent one or more mutations that differentiate the sequence types. Circles are colored according to the regions where samples were obtained. The principal clades are outlined and labeled, with the number of sequences from Icelanders shown in parentheses. Haplotypes from clade A are not outlined. Panel C shows the cumulative counts of SARS-CoV-2 haplotypes from targeted testing and population screening as a function of sampling date. A2a* refers to all A2a haplotypes except A2a1, A2a2, and A2a3. The dashed vertical line indicates the start of the population screening.

Haplotype	Early Targeted Testing January 31–March 15			Population Screening March 13–April 1			Later Targeted Testing March 16–31		
	Imported	Country of Origin	Local	Imported	Country of Origin	Local	Imported	Country of Origin	Local
	no. (%)		*no. (%)*	*no. (%)*		*no. (%)*	*no. (%)*		*no. (%)*
All haplotypes	101 (100)	IT:42, AT:38	56 (100)	16 (100)	UK:9, US:3	43 (100)	83 (100)	AT:28, UK:23	278 (100)
A2a1	36 (35.6)	IT:29, AT:3	16 (28.6)	5 (31.2)	UK:4, DE:1	8 (18.6)	17 (20.5)	AT:6, UK:4	51 (18.3)
A2a2	33 (32.7)	AT:28, DK:2	18 (32.1)	2 (12.5)	US:2	1 (2.3)	19 (22.9)	AT:9, UK:5	28 (10.1)
A2a3	5 (5.0)	CH:5	11 (19.6)	0		11 (25.6)	5 (6.0)	ES:2	82 (29.5)
A2a	19 (18.8)	IT:11, AT:6	5 (8.9)	2 (12.5)	NL:1, DK:1	1 (2.3)	30 (36.1)	AT:13, UK:10	33 (11.9)
A1a	2 (2.0)	CH:1, IT:1	6 (10.7)	4 (25.0)	UK: 4	19 (44.2)	4 (4.8)	UK:2, ES:2	60 (21.6)
Other clade A	2 (2.0)	UK:1, AT:1	0	2 (12.5)	UK:2	3 (7.0)	2 (2.4)	US:1, UK:1	19 (6.8)
B1a1	4 (4.0)	US:4	0	1 (6.2)	US:1	0	6 (7.2)	US:6	5 (1.8)

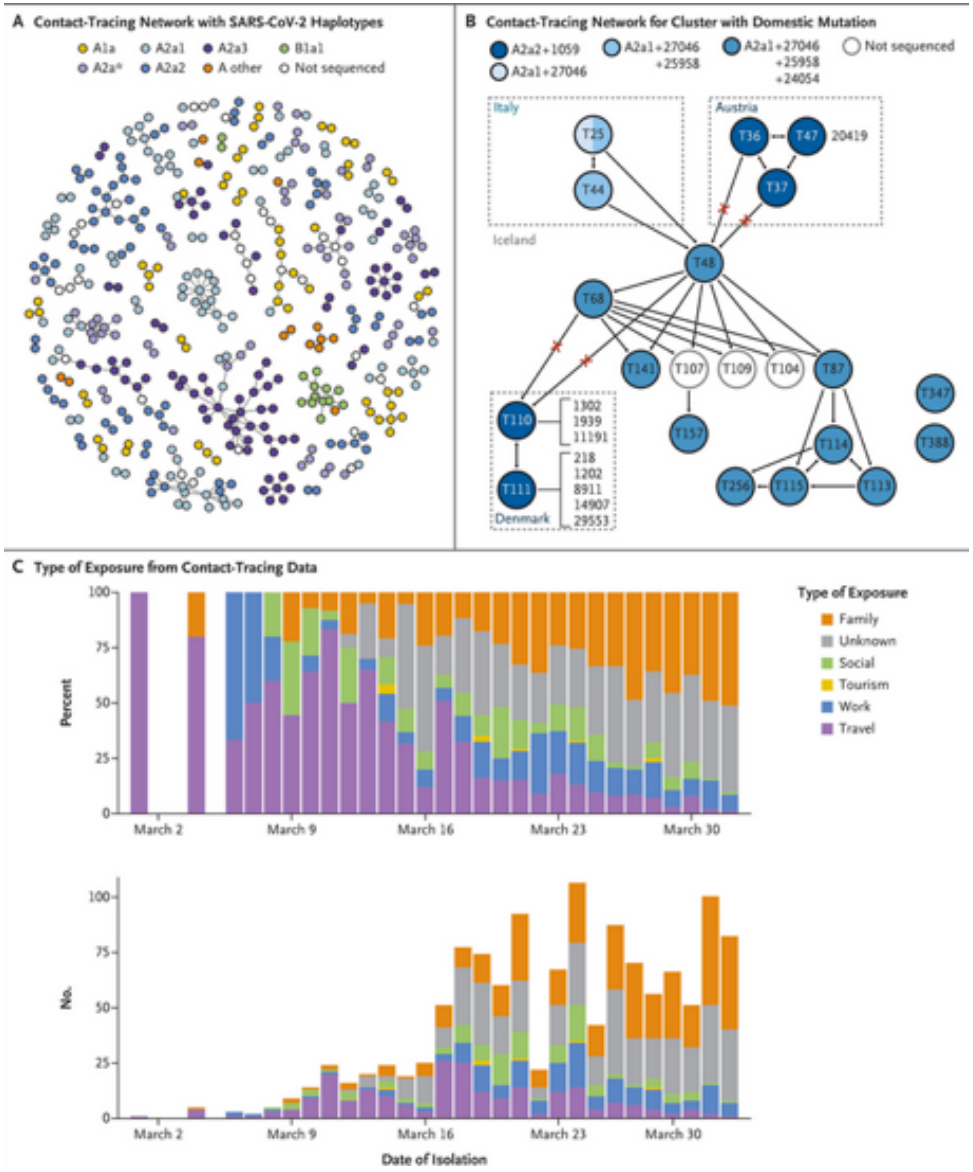

Figure 4. Overall Clusters in the Contact-Tracing Network, a Network Cluster Including a Novel Domestic Mutation, and Source of Exposure.

Panel A shows an overview of all clusters in t
contact-tracing network with SARS-CoV-2 ha
Panel B shows a contact-tracing network for a cluster that included a novel domestic mutation (24054C→T). Person T25 carried both the A2a1a strain and the A2a1a+25958 strain. Contact-tracing networks show infected persons as nodes and a connection between two nodes where a transmission of infection or contact has been established. In cases in which the direction of transmission was ambiguous, a bidirectional arrow is shown. Persons who traveled internationally are indicated in boxes representing their travel destination. The colors of nodes represent the haplotype of the viral strain, either as a clade or a clade plus one or more mutations. Additional mutations are represented by a position number beside each node. The labels on the nodes are identifiers given in increasing order of identification (e.g., T6 is the sixth case reported). Red X marks indicate recorded contacts that are inconsistent with the viral haplotypes carried by each person. Panel C shows the type of exposure from contact-tracing data according to the date of isolation and percentage (top graph) and total number (bottom graph). The type of exposure is classified for each positive case into the following categories: family, unknown, social, work (including schools), tourism (reported working domestically in tourism), and travel (international travel).

In Iceland, the prevalence of SARS-CoV-2 infection among persons at high risk for infection and the stability of the infection rate in the general population provide grist for both assurance and alarm. The percentage of participants who tested positive in population screening remained stable (0.8%) over the course of 20 days, and the infection rates in the two screening groups (recruited through open invitation and through random sampling) were not substantially different. These results were consistent with a slow spread of SARS-CoV-2 through the Icelandic population.

The lack of increase in the incidence of infection over time may be due to containment efforts by the Icelandic health care authorities and their nimble response to the outbreak abroad. Testing of exposed persons with symptoms had been carried out for 1 month before the first SARS-CoV-2 case was identified in Iceland. Self-isolation, quarantining, and other social-distancing measures may also have helped to prevent an increase in the infection rate.

The haplotype composition of the viruses from persons who were identified through population screening was different from that of viruses infecting persons who tested positive in the early phase of targeted testing, so we conclude that the haplotypes of the virus that were propagating in the general population came from a different source (as compared with those infecting high-risk persons in the early phase of targeted testing), perhaps brought into Iceland by persons arriving from countries that had not yet been designated as high-risk areas.

Thus, the frequency of the SARS-CoV-2 infection in the overall Icelandic population was stable from March 13 to April 1, a finding that appears to indicate that the containment measures had been working. However, the virus has spread to the extent that unless we continue to test and isolate, track contacts, and quarantine, we are likely to fail in our efforts to contain the virus.

Thrombectomy for Stroke in the Public Health Care System of Brazil

Randomized trials involving patients with stroke have established that outcomes are improved with the use of thrombectomy for large-vessel occlusion. These trials were performed in high-resource countries and have had limited effects on medical practice in low- and middle-income countries. We studied the safety and efficacy of thrombectomy in the public health system of Brazil. In 12 public hospitals, patients with a proximal intracranial occlusion in the anterior circulation that could be treated within 8 hours after the onset of stroke symptoms were randomly assigned in a 1:1 ratio to receive standard care plus mechanical thrombectomy (thrombectomy group) or standard care alone (control group). The primary outcome was the score on the modified Rankin scale (range, 0 [no symptoms] to 6 [death]) at 90 days.

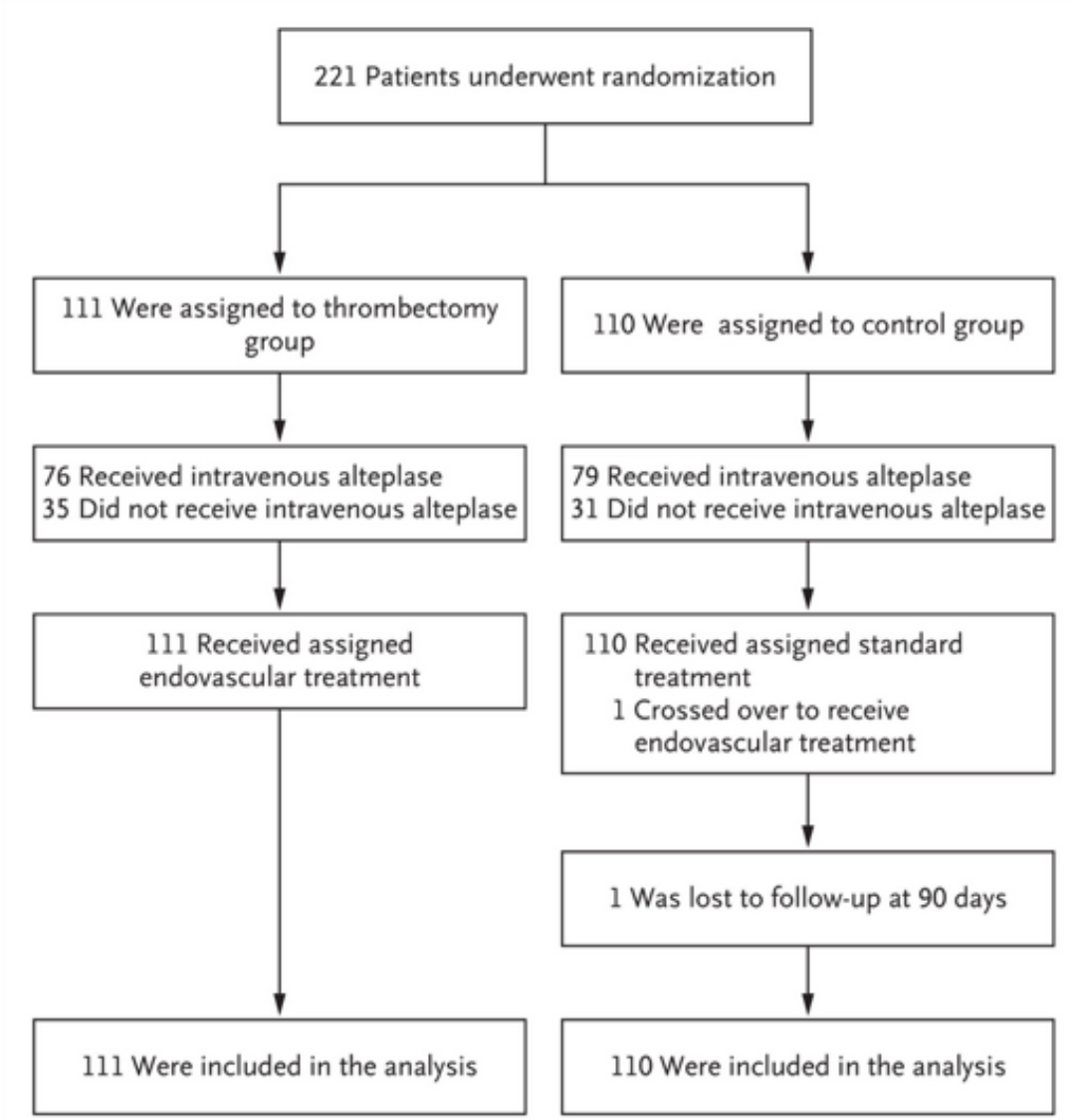

Variable	Thrombectomy (N=111)	Control (N=110)
Age — yr		
Median (IQR)	65 (54–77)	67 (53–73)
Range	22–93	20–92
Female sex — no. (%)	51 (45.9)	53 (48.2)
White race — no. (%)†	62 (55.9)	56 (50.9)
NIHSS score‡		
Median (IQR)	18 (14–21)	18 (14–21)
Range	6–30	8–29
Location of stroke in left hemisphere — no. (%)	64 (57.7)	63 (57.3)
Medical history — no. (%)		
History of ischemic stroke or TIA	14 (12.6)	11 (10.0)
Atrial fibrillation	15 (13.5)	12 (10.9)
Diabetes mellitus	23 (20.7)	37 (33.6)
Hypertension	70 (63.1)	75 (68.2)
Current or past tobacco use	17 (15.3)	22 (20.0)
Heart failure	22 (19.8)	21 (19.1)
Prestroke score on the modified Rankin scale of 0 — no. (%)§	91 (82.0)	98 (89.1)
Transferred from another hospital — no. (%)	26 (23.4)	27 (24.5)
Median systolic blood pressure (IQR) — mm Hg	144 (130–162)	140 (127–160)
Median glucose level at hospital arrival (IQR) — mmol/liter	124 (108–148)	125 (104–157)
Treatment with intravenous alteplase — no. (%)	76 (68.5)	79 (71.8)
Baseline ASPECTS¶		
Median (IQR)	8 (7–9)	8 (7–9)
Range	4–10	5–10
CT or CTA performed — no. (%)	110 (99.1)	108 (98.2)
CT perfusion performed — no. (%)	50 (45.0)	50 (45.5)
MRI or MRA performed — no. (%)	1 (0.9)	2 (1.8)
Intracranial arterial occlusion — no. (%)		
Intracranial ICA	23 (20.7)	19 (17.3)
M1 middle cerebral artery segment	88 (79.3)	89 (80.9)
M2 middle cerebral artery segment‖	0	4 (3.6)
Extracranial ICA occlusion — no. (%)	9 (8.1)	4 (3.6)
Median time from stroke onset to randomization (IQR) — min	237 (175–295)	237 (164–295)
Median time from stroke onset to start of intravenous alteplase (IQR) — min	170 (132–213)	161 (115–219)

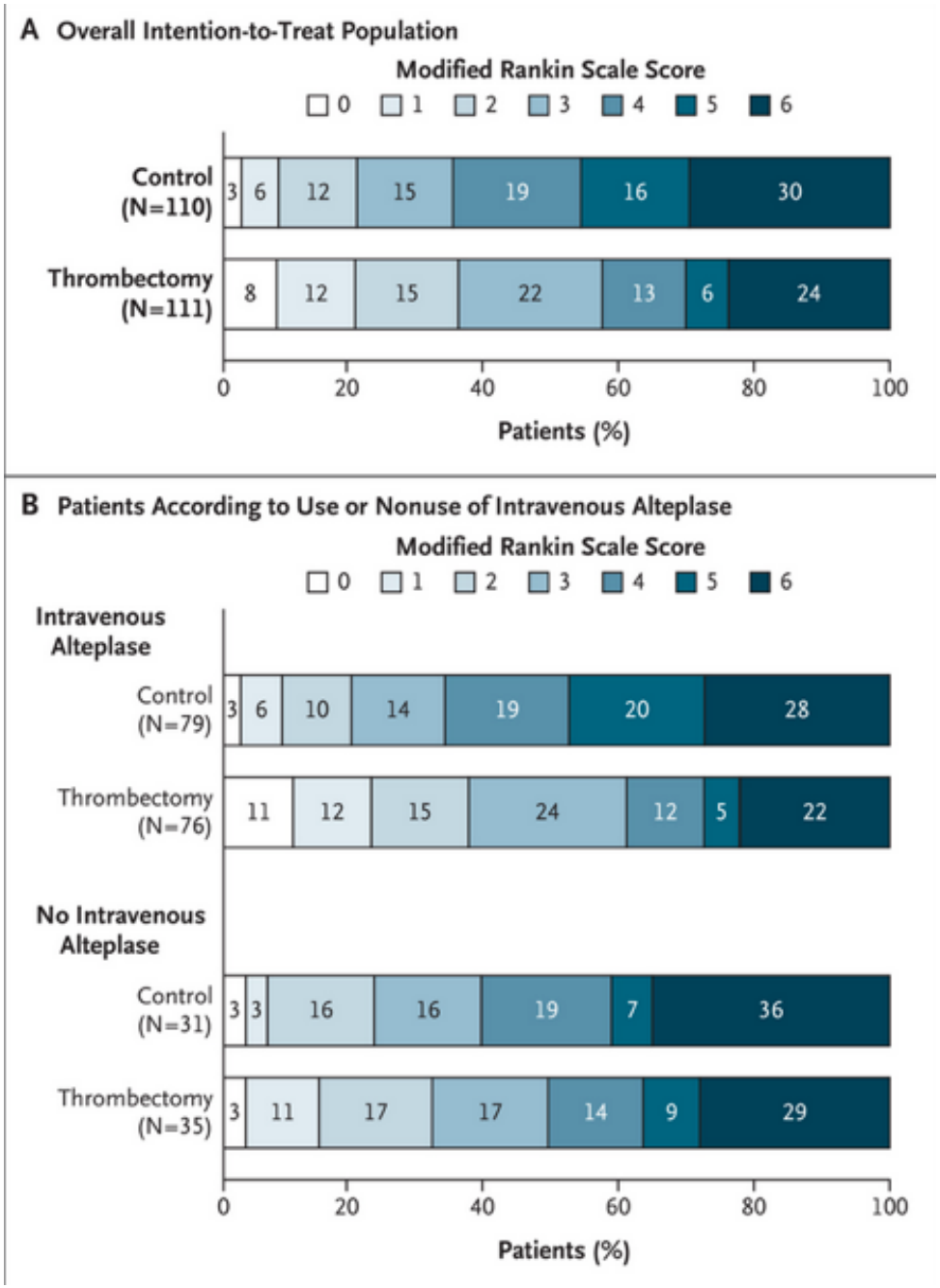

Figure 2. Distribution of Scores on the Modified Rankin Scale at 90 Days.

Panel A shows the distribution of scores for disability on the modified Rankin scale (on which scores range from 0 to 6, with higher scores indicating more severe disability) among patients in the thrombectomy group and the control group in the overall intention-to-treat population. A significant difference between the thrombectomy group and the control group was noted in the overall distribution of scores (adjusted common odds ratio for a decrease of ≥1 point in the score on the modified Rankin scale, 2.28; 95% confidence interval [CI], 1.41 to 3.69). For the main secondary efficacy end point, functional independence was defined as a score of 0, 1, or 2 on the modified Rankin scale, and the incidence was significantly higher in the thrombectomy group than in the control group (35.1% vs. 20.0%; adjusted odds ratio, 2.55; 95% CI, 1.34 to 4.88). Panel B shows the distribution of scores at 90 days in the thrombectomy and control groups according to the use of intravenous alteplase treatment. In this analysis, there was no evidence of heterogeneity of effect (P=0.47 for interaction by the Wald test). In both panels, the percentages may not total 100 because of rounding.

Outcome	Thrombectomy (N=111)	Control (N=110)	Odds Ratio (95% CI)
Primary outcome: score on the modified Rankin scale at 90 days	NA	NA	2.28 (1.41 to 3.69)†
Secondary outcomes‡			
Score on the modified Rankin scale of 0 to 2 at 90 days — no. (%)	39 (35.1)	22 (20.0)	2.55 (1.34 to 4.88)§
Median change in ASPECTS from baseline to 24 hr on CT or MRI (IQR)	−2 (−4 to −1)	−3 (−6 to −1)	NA
Dramatic neurologic improvement at 24 hr — no./total no. (%)¶	33/105 (31.4)	26/108 (24.1)	1.45 (0.79 to 2.67)
Median EQ-5D score at 90 days (IQR)‖	0.458 (0 to 0.737)	0.235 (0 to 0.522)	NA
Vessel recanalization at 24 hr on CT or MRA — no./total no. (%)**	65/81 (80.2)	38/82 (46.3)	5.23 (2.53 to 10.82)
Successful recanalization immediately after thrombectomy — no. (%)††	91 (82.0)	NA	NA

Safety

Outcome	Thrombectomy (N=111)	Control (N=110)	Risk Difference (95% CI)	Odds Ratio (95% CI)
	number (percent)		*percentage points*	
Death at 90 days	27 (24.3)	33 (30.0)	−5.7 (−18.3 to 6.9)	0.75 (0.41 to 1.36)†
Symptomatic ICH according to SITS-MOST criteria‡	5 (4.5)	5 (4.5)	0.0 (−6.4 to 6.3)	0.99 (0.26 to 3.78)
Symptomatic ICH according to ECASS III criteria§	8 (7.2)	6 (5.5)	1.7 (−5.6 to 9.1)	1.35 (0.39 to 4.88)
Asymptomatic ICH	57 (51.4)	27 (24.5)	26.8 (13.6 to 40.0)	3.24 (1.77 to 6.01)
ICH imaging classification¶				
Subarachnoid hemorrhage	4 (3.6)	0	3.6 (−0.8 to 8.0)	NA
Intracerebral hemorrhage remote from stroke	1 (0.9)	1 (0.9)	0.0 (−3.4 to 3.4)	0.99 (0.01 to 78.49)
Parenchymal hematoma‖				
Any	6 (5.4)	7 (6.4)	−1.0 (−8.1 to 6.2)	0.84 (0.26 to 2.68)
Type 1	1 (0.9)	1 (0.9)	0.0 (−3.4 to 3.4)	0.99 (0.01 to 78.49)
Type 2	5 (4.5)	6 (5.5)	−1.0 (−7.6 to 5.7)	0.82 (0.19 to 3.33)
Procedure-related complications				
Distal embolization in a new territory	4 (3.6)	NA	NA	NA
Arterial dissection	3 (2.7)	NA	NA	NA
Arterial perforation	1 (0.9)	NA	NA	NA
Groin hematoma	1 (0.9)	NA	NA	NA

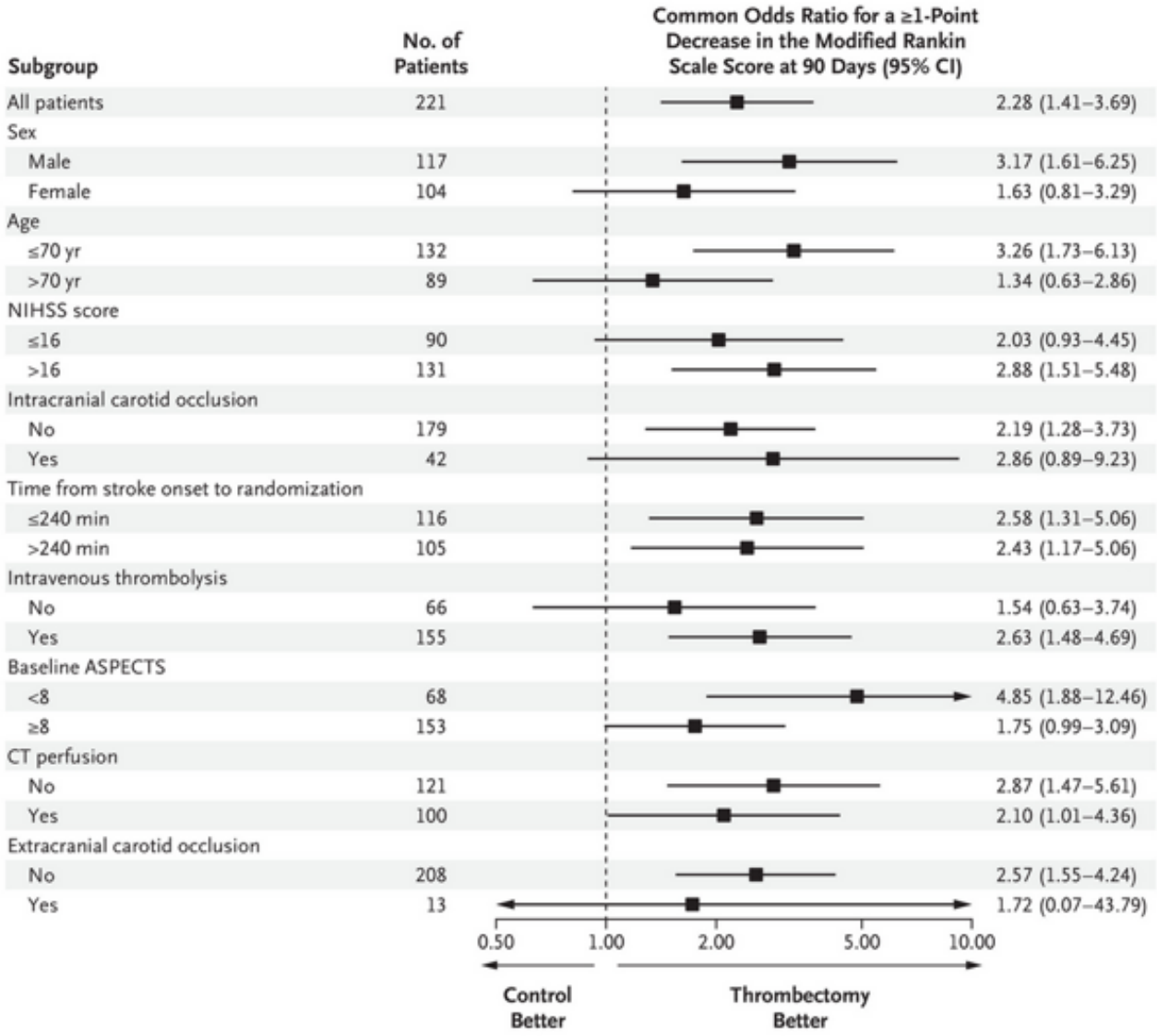

The forest plot shows the effect size in the primary outcome variable (common odds ratio for a better distribution of scores on the modified Rankin scale at 90 days, analyzed according to ordinal logistic regression and adjusted for minimization factors) across the prespecified subgroups and according to the Alberta Stroke Program Early Computed Tomography Score (ASPECTS; range, 0 to 10, with higher values indicating a smaller infarct core) and the use or nonuse of computed tomographic (CT) perfusion. Scores on the National Institutes of Health Stroke Scale (NIHSS) range from 0 to 42, with higher scores indicating more severe neurologic deficits. The cutoff values and categories of the subgroups are those specified in the minimization factors obtained before randomization. The threshold for ASPECTS corresponds to the median value according to the core laboratory evaluation. The measurement of effect size was a cumulative logistic-regression odds ratio (shift analysis). Squares indicate point estimates for the treatment effect.

Thrombectomy for Stroke in Brazil's Public Health Care System

MULTICENTER, RANDOMIZED, CONTROLLED TRIAL

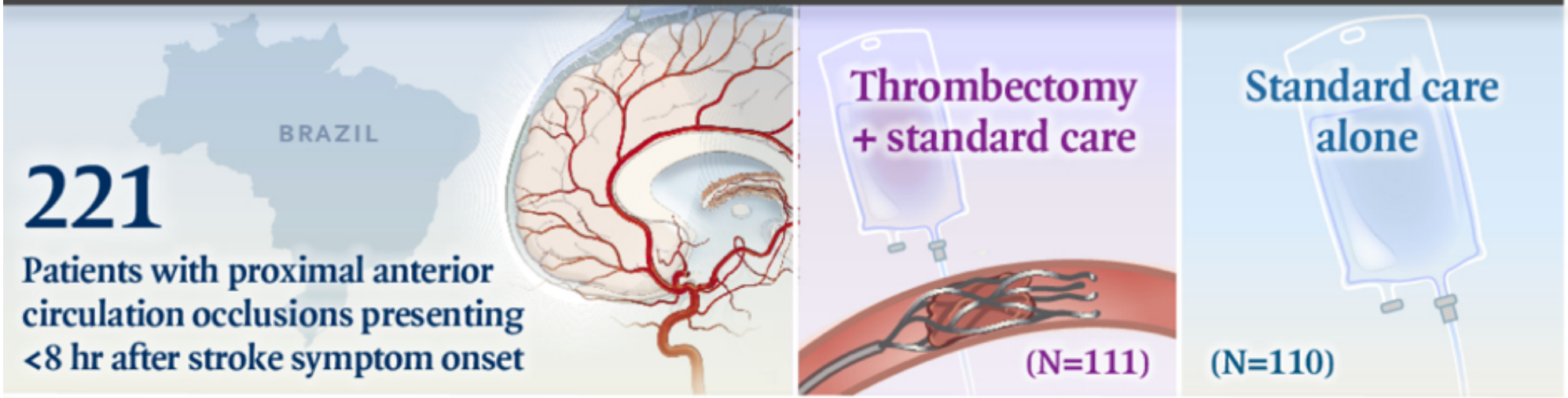

Disability as shown by distribution of modified Rankin scores at 90 days	Common OR for better scores with thrombectomy 2.28 (95% CI, 1.41 to 3.69; P=0.001)	
Modified Rankin score of 0–2 at 90 days (no or minor neurologic deficit)	35.1%	20.0%
	Difference, 15.1 percentage points; 95% CI, 2.6 to 27.6	

Stopped early for efficacy showing benefit of thrombectomy in this underresourced system

Abstract

T helper type 1 (Th1) lymphocytes secrete secrete interleukin (IL)-2, interferon-γ, and lymphotoxin-α and stimulate type 1 immunity, which is characterized by intense phagocytic activity. Conversely, Th2 cells secrete IL-4, IL-5, IL-9, IL-10, and IL-13 and stimulate type 2 immunity, which is characterized by high antibody titers. Type 1 and type 2 immunity are not strictly synonymous with cell-mediated and humoral immunity, because Th1 cells also stimulate moderate levels of antibody production, whereas Th2 cells actively suppress phagocytosis. For most infections, save those caused by large eukaryotic pathogens, type 1 immunity is protective, whereas type 2 responses assist with the resolution of cell-mediated inflammation. Severe systemic stress, immunosuppression, or overwhelming microbial inoculation causes the immune system to mount a type 2 response to an infection normally controlled by type 1 immunity. In such cases, administration of antimicrobial chemotherapy and exogenous cytokines restores systemic balance, which allows successful immune responses to clear the infection.

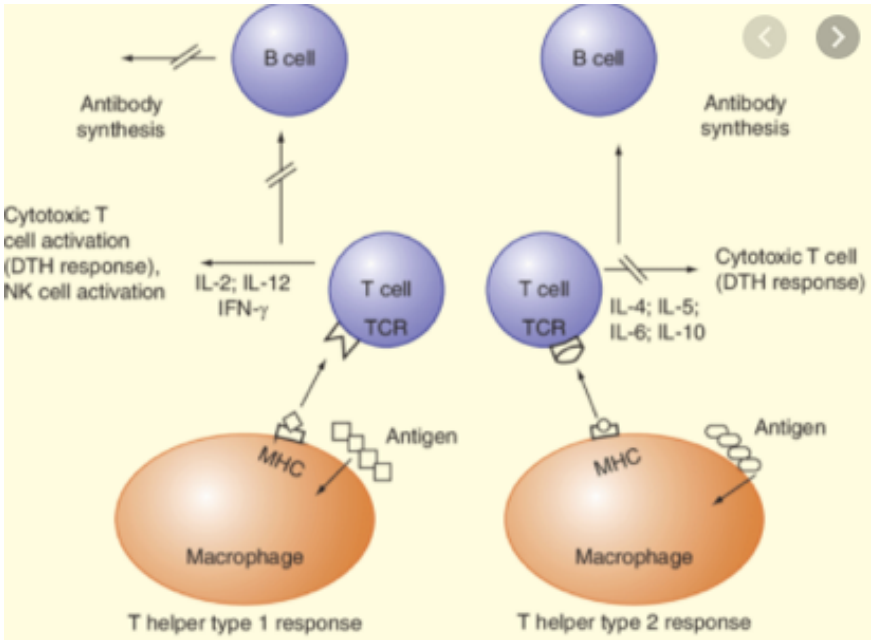

Immune responses often can be characterized as type 1 or type 2

- Type 1 immune responses: Killing microbes
  - Pro-inflammatory; neutrophils and macrophages
  - Antibody classes involved in phagocytosis and complement activ.
  - Macrophage activation
- Type 2 immune responses: Defense at epithelium
  - Allergic inflammation: eosinophils, basophils
  - Antibody classes: IgE and IgG1 (mast cell activation)
  - Expulsion type reactions (diarrhea, coughing, sneezing, etc.).

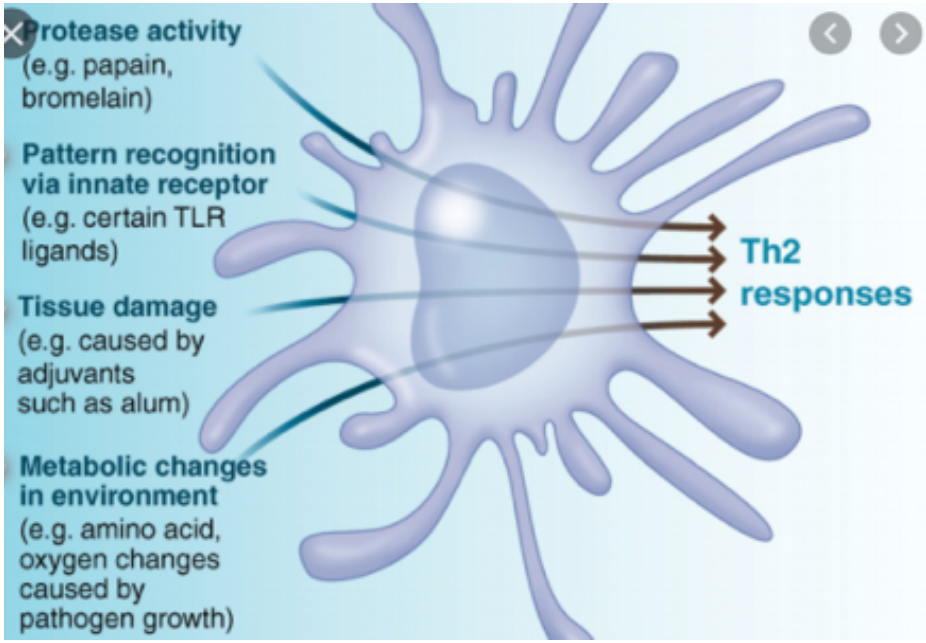

Disseminated Coccidioidomycosis Treated with Interferon-γ and Dupilumab

We describe a case of life-threatening disseminated coccidioidomycosis in a previously healthy child. Like most patients with disseminated coccidioidomycosis, this child had no genomic evidence of any known, rare immune disease. However, comprehensive immunologic testing showed exaggerated production of interleukin-4 and reduced production of interferon-γ. Supplementation of antifungal agents with interferon-γ treatment slowed disease progression, and the addition of interleukin-4 and interleukin-13 blockade with dupilumab resulted in rapid resolution of the patient's clinical symptoms. This report shows that blocking of type 2 immune responses can treat infection. This immunomodulatory approach could be used to enhance immune clearance of refractory fungal, mycobacterial, and viral infections.

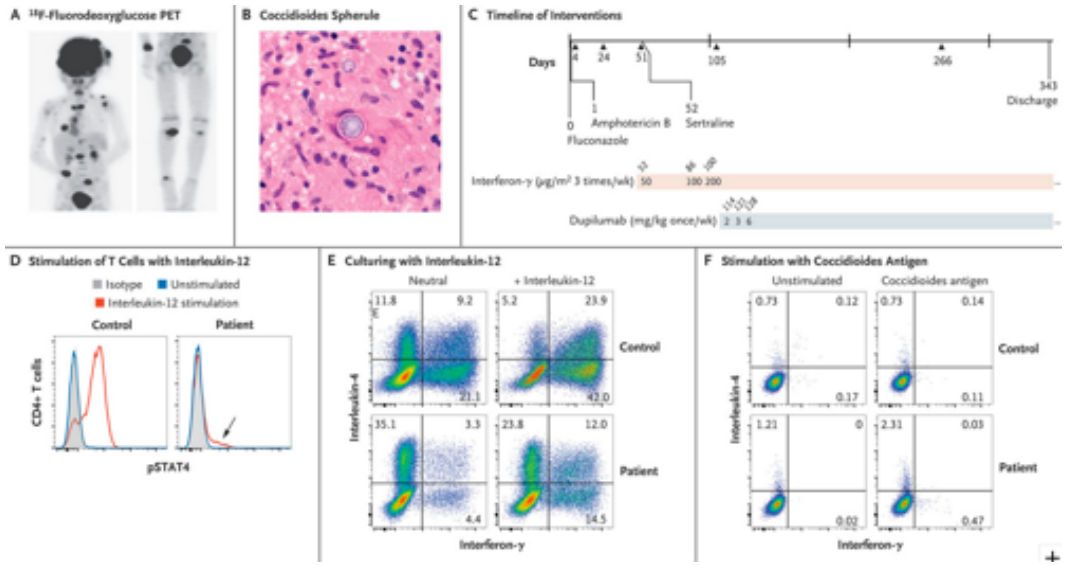

Figure 1. A Case of Disseminated Coccidioidomycosis Characterized by Defective Interleukin-12 Signaling and Th1 Response.

Panel A shows an ^{18}F-fluorodeoxyglucose positron-emission tomographic scan showing disseminated infection with multiple lesions of the spine, clavicle, ribs, paratracheal lymph nodes, right distal radius, and right leg. Panel B shows a coccidioides spherule obtained from surgical biopsy of a scalp lesion. Panel C shows the timeline of interventions in our patient. Initial treatment included fluconazole and liposomal amphotericin B, and sertraline was added at day 52 after admission. Treatment with subcutaneous interferon-γ was also started on day 52, and treatment with dupilumab was started on day 114. Triangles represent major débridement surgical procedures. Doses of interferon-γ and dupilumab are indicated in the shaded bars; numbers above the bars are days after admission. Panel D shows stimulation of helper T cells with interleukin-12, which led to a poor phosphorylated STAT4 (pSTAT4) response; however, the loss of function was not absolute (arrow). Panel E shows intracellular cytokine staining of CD4+ T-cell effectors generated in neutral conditions and stimulated with phorbol myristate acetate (PMA) and ionomycin. Interleukin-4 production was greatly enhanced relative to interferon-γ production in the patient as compared with a control. A normal response was only partially restored by culturing in type 1 helper T (Th1) cell conditions (i.e., with interleukin-12). Panel F shows stimulation of peripheral-blood mononuclear cells with T27K coccidioidal antigen, which led to increased production of interleukin-4 over interferon-γ in helper T cells.

Sertralin ist eine tricyclische chemische Verbindung

	Baseline (admission)	Reference Ranges
Lymphocyte Counts		
CD3+ T lymphocytes	2,193 (75%)	1,400-3,700 (56-75%)
CD4+ T-cell helper subset	1,235 (43%)	700-2,200 (28-47%)
CD8+ Cytotoxic T cell subset	842 (29%)	490-1,300 (16-30%)
CD19+ B lymphocytes	545 (19%)	390-1,400(14-33%)
NK lymphocytes	141 (5%)	130-720 (4-17%)
Immunoglobulins		
IgG	2,060 mg/dL	540-1,330 mg/dL
IgA	257 mg/dL	30-160 mg/dL
IgM	89 mg/dL	40-140 mg/dL
IgE	2,396 kIU/L	<20 kIU/L
Neutrophil oxidative burst	96% positive	>90% positive

Table S2. Responses to treatment

	Baseline (admission)	Antifungals +IFN-γ	Antifungals + IFN-γ + Dupilumab
IgE (kIU/L)	2,396	354	109
IgG (mg/dL)	2,190	2,060	1,350
CRP	9.5	3.0 (wk 10)	1.0 (wk 20)

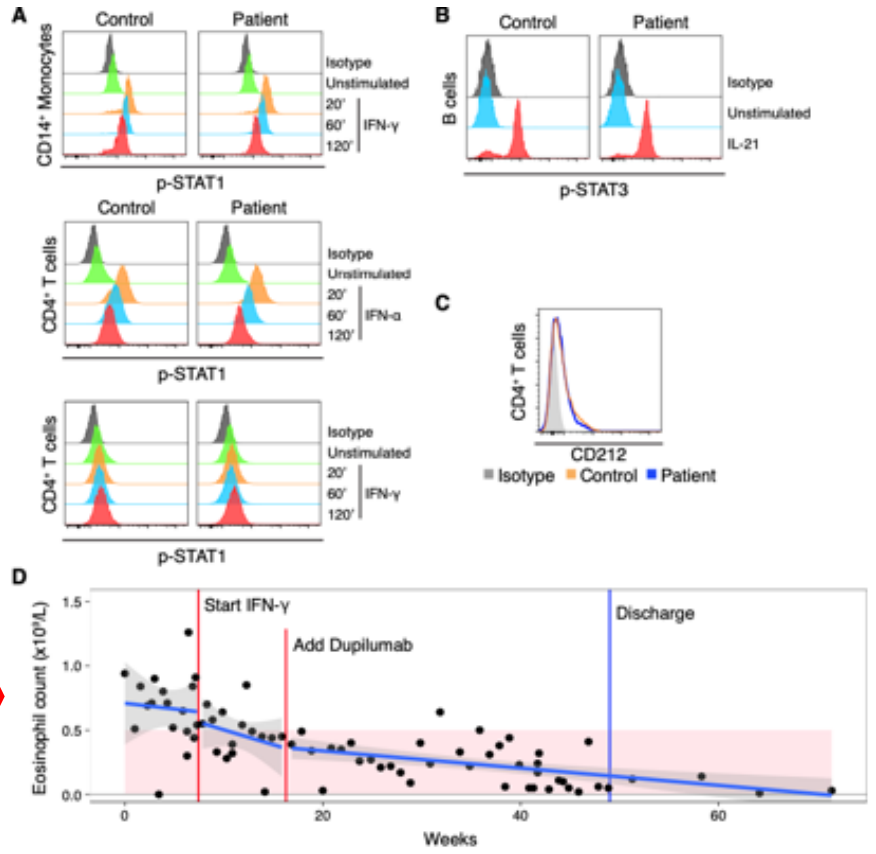

Fig. S1. Normal responses of STAT1 and STAT3 in the proband. (A) Peripheral blood cells were stimulated with IFN-α and IFN-γ and phosphorylation of STAT1 evaluated by flow cytometry as a function of time. (B) Peripheral blood B cells from the patient or a healthy control were stimulated with IL-21 and phosphorylation of STAT3 evaluated by flow cytometry. (C) Expression of CD212 (IL12RB1) by flow cytometry. (D) Patient's absolute eosinophil counts over time.

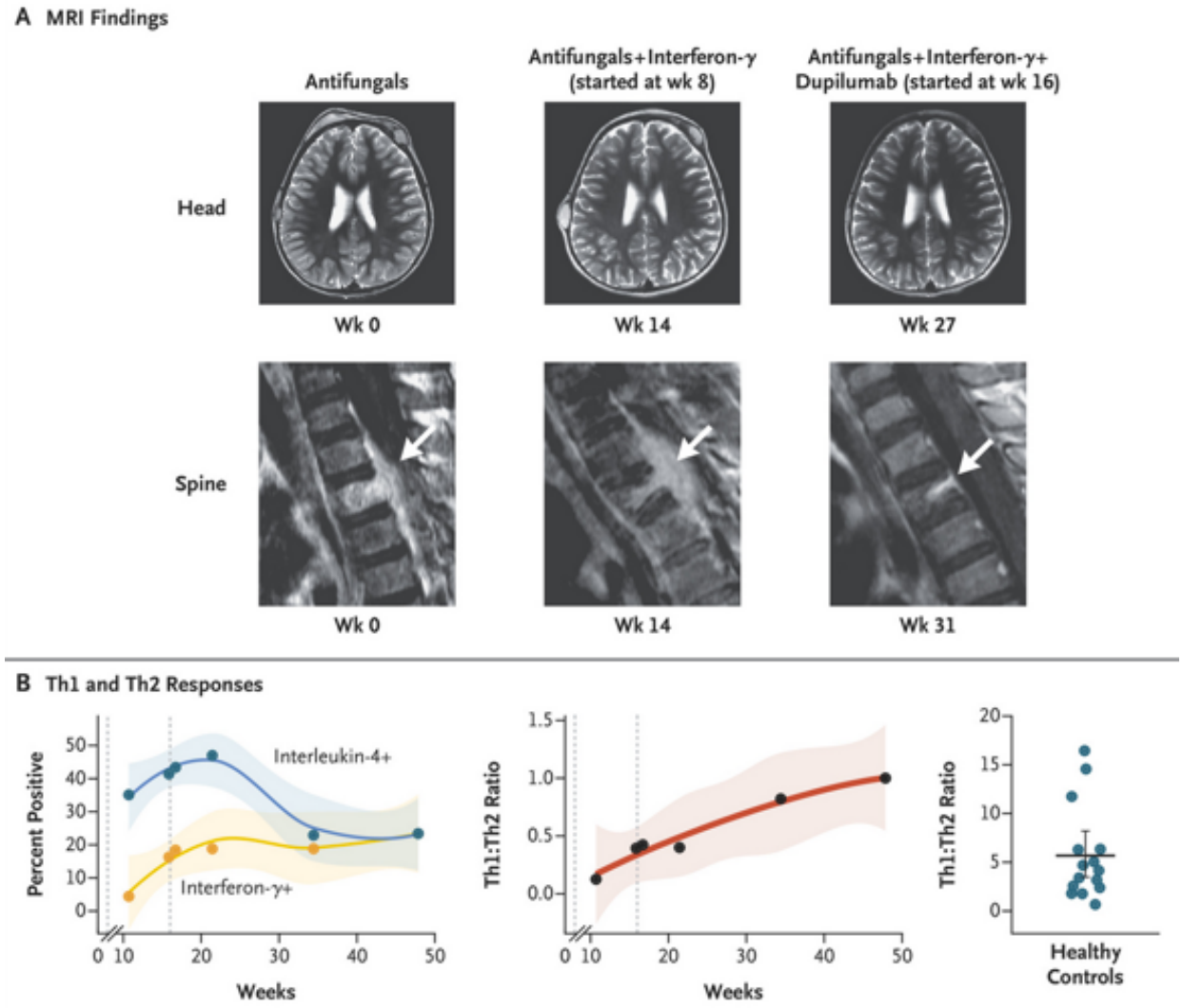

Figure 2. Resolution of Disseminated Coccidioidomycosis after Treatment with Interferon-γ and Dupilumab.

Panel A shows magnetic resonance imaging (MRI) of the head and spine at baseline and during treatment. A spinal lesion is indicated by the arrow. Panel B shows the percentage of CD4+ T cells producing interferon-γ (Th1 cells) or interleukin-4 (type 2 helper T [Th2] cells) (left) and their ratio (center) over time. The ratio does not include double-positive (i.e., positive for interferon-γ and interleukin-4) cells. The first dashed line represents the initiation of interferon-γ treatment, and the second dashed line represents the initiation of dupilumab treatment. Shading indicates the 95% confidence interval. For comparison, the Th1:Th2 ratio for 15 healthy controls is shown on the right. The horizontal line indicates the bootstrapped mean, and the I bar indicates the 95% confidence interval.

Discussion

Risk factors for disseminated coccidioidomycosis include pregnancy, immunosuppression, HIV and acquired immunodeficiency syndrome, and monogenic defects of the interleukin-12–interferon-γ axis — all states in which type 2 immunity dominates over type 1 immunity. In this report, we showed that treatment with interferon-γ (augmenting type 1 immunity) in combination with dupilumab (suppressing type 2 immunity) resulted in complete resolution of disease in a patient with life-threatening disseminated coccidioidomycosis who had no known monogenic immunodeficiency. These observations imply that a relative insufficiency of type 1 immunity combined with strong type 2 responses confers susceptibility to disseminated coccidioidomycosis. We propose that restoring the balance between type 1 and type 2 immunity enables clinical improvement and that the relative differentiation state of helper T cells may serve as a useful biomarker in this disease.

Th1 cells produce interferon-γ, which augments microbial killing by macrophages and other innate cells. A direct correlation between disease resolution and production of interferon-γ by lymphocytes in response to coccidioides antigen has been found in patients with disseminated coccidioidomycosis. Consequently, interferon-γ has been used with success as adjunctive therapy in a few cases of disseminated coccidioidomycosis. In our patient, however, this approach was insufficient to eliminate disease, despite the improvement of interleukin-12 signaling and some restoration of helper T-cell differentiation.

Type 2 immune responses have been shown to be deleterious in animal models of coccidioidomycosis. Interleukin-4 suppresses Th1 development and reduces the antifungal activity of phagocytes and neutrophils. We therefore reasoned that inhibiting the Th2 milieu could halt the relentless dissemination of the disease in this patient. Indeed, the addition of dupilumab accelerated clinical improvement, with resolution of bone and soft-tissue lesions. Whether dupilumab exerts disease control by altering T-cell differentiation and function, phagocyte microbicidal activity, or both remains to be determined.

In our patient, genome sequencing did not identify any plausible rare variants that could explain a susceptibility to disseminated coccidioidomycosis. We found that the combination of interferon-γ and dupilumab successfully controlled a severe case of disseminated coccidioidomycosis. We propose that this immunomodulatory approach may have therapeutic potential for other severe fungal infections, and we speculate it may also be useful in other infections where type 1 immunity is important, including viral and mycobacterial infections.

A 59-year-old man with metastatic colon cancer was referred to the dermatology clinic for a possible case of shingles. He had a 10-week history of painless and nonpruritic skin lesions coalescing around a large abdominal scar from a hemicolectomy performed 3 years earlier. A subsequent liver resection and cholecystectomy had also been performed through this incision. On examination, the lesions were firm, pink to violaceous in color, and vesicular-appearing; the presence of ascites was also evident. In this clinical context, cutaneous metastases were considered most likely, and a skin biopsy confirmed the diagnosis of metastatic colon adenocarcinoma. The most common site of cutaneous metastases in colon adenocarcinoma is the abdominal skin, sometimes in or around surgical scars, as was seen in this case. The patient ultimately received hospice care and died 5 months after this presentation.

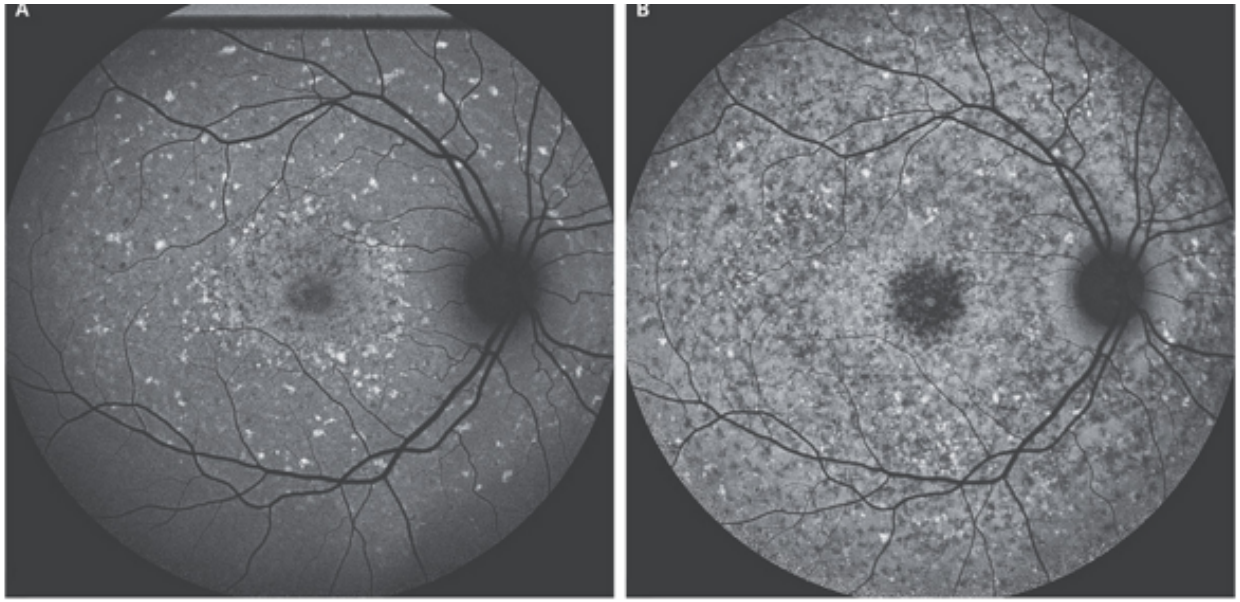

A 13-year-old boy was referred to the ophthalmology clinic with enlarging blind spots in the central vision in both eyes. He had no family history of eye problems. At presentation, the visual acuity was 20/40 in the right eye and 20/50 in the left eye. Fundus examination of both eyes showed widespread, yellow, pisciform flecks. Short-wavelength autofluorescence imaging showed diffuse hyperautofluorescent lesions suggestive of bisretinoid accumulation and patchy central areas of atrophy of the retinal pigment epithelium with peripapillary sparing (Panel A). These findings are consistent with a diagnosis of Stargardt juvenile macular degeneration (also called Stargardt's disease), an autosomal recessive disorder caused by mutations in the gene encoding ATP-binding cassette subfamily A member 4 (*ABCA4*). Dysfunction of the ABCA4 transporter leads to the accumulation of toxic bisretinoids with consequent degeneration of the retinal pigment epithelium and photoreceptors. Vision loss typically begins during childhood and progresses. The diagnosis was confirmed with sequencing of *ABCA4*. The patient was advised to avoid vitamin A supplementation, which may accelerate bisretinoid accumulation. At 6-year follow-up, visual acuity was 20/70 in the right eye and 20/50 in the left eye, with worsening central scotomata. Autofluorescence imaging showed progressive atrophy in the previously identified areas of pisciform flecks with the maintenance of peripapillary sparing (Panel B).

Down Syndrome

Down syndrome, also called Down's syndrome (DS), is the most common chromosomal condition associated with intellectual disability and is characterized by a variety of additional clinical findings. It occurs in approximately 1 of 800 births worldwide. In the United States, DS accounts for approximately 500 live births annually, and more than 200,000 persons are living with the disorder. The original description of the syndrome, in 1866, has been attributed to John Langdon Down, a physician from Cornwall, England. More than 90 years later, the chromosomal cause was delineated and the condition was named Down syndrome.

Chromosomal Feature	Description	Percent of Cases
Meiotic nondisjunction	Occurs in the egg in 95% of cases, and the risk increases with mother's age	96
Translocation	Usually occurs with one chromosome 21 attached to chromosome 14, 21, or 22 In 14/21 translocation, 1 of every 3 cases involves a parental carrier; in 90% of such cases, the carrier is the mother; risk of recurrence is 10–15% with a maternal carrier and 2–5% with a paternal carrier In 21/21 translocation, 1 of every 14 cases involves a parental carrier; in 50% of such cases, the carrier is the father	3–4
Mosaicism	The number of affected cells varies among persons; clinical findings vary widely; there are fewer medical complications and often less severe intellectual disability in cases characterized by mosaicism	1–2
Partial trisomy	Duplication of a delimited segment of chromosome 21 is present	<1

Table 2. Perinatal Assessment of Infants with Down Syndrome.*

Karyotype or review of amniocentesis or chorionic villus sampling
Complete blood count with differential
Blood thyrotropin level (included in newborn screening in some U.S. states)
Echocardiogram, even if obtained prenatally
Identification of gastrointestinal anomalies

Table 3. Incidence of Coexisting Medical Conditions in Patients with Down Syndrome (DS).*

Condition	Incidence	Study
	%	
Congenital heart disease	44 (Including stillbirths)	Freeman et al.[16]
Atrioventricular septal defect†	45	
Ventricular septal defect	35	
Secundum atrial septal defect	8	
Tetralogy of Fallot	4	
Patent ductus arteriosus	7	
Pulmonary hypertension	1.2–5.2	Weijerman et al.[17]
Infections, especially respiratory, due in part to immunodeficiencies	Deaths due to infection, 34–40	O'Leary et al.[18]
Hearing deficits		Kreicher et al.,[19] Park et al.[20]
Conductive	84	
Sensory	2.7	
Mixed	7.8	
Hematologic and oncologic disorders		
Transient abnormal myelopoiesis	≤10 (Resolves spontaneously but is associated with a 20–30% risk of AML)	Taub et al.[21]
Leukemia and tumors	2–3 (Patients with DS are protected against most solid tumors; only testicular cancer is more frequent in such patients than in the general population)	Hasle et al.[22]
Anemia or iron deficiency	Anemia, 2.6; iron deficiency, 10.5 (masked by macrocytosis and elevated MCH)	Dixon et al.[23]
Sleep disorders	65	Hoffmire et al.[24]
Thyroid abnormalities		Pierce et al.[25]
Congenital hypothyroidism	1–2	
Hypothyroidism and Hashimoto's disease in adults	50	
Dysphagia	55	Jackson et al.[26]
Neurodevelopmental disorders		Stafstrom et al.[27]
Seizures	5–8	
Partial seizures	2–13	
Infantile spasms	2 to 5	
Disintegrative disorder‡		Worley et al.[28]
Moyamoya disease§		Kainth et al.[29]
Dementia	At <40 yr of age, <5; by 65 yr of age, 68–80	Wiseman et al.[30]
Autism	7–16	DiGuiseppi et al.[31]
Celiac disease	5.4	Szaflarska-Popławska et al.[32]
Gastrointestinal anomalies	6	Stoll et al.[33]
Juvenile idiopathic arthritis	<1	Juj et al.[34]
Orthopedic problems	2.8	Brockmeyer,[35] Caird et al.[36]
Visual problems	56.8	Roizen et al.[37]

Transition to Adulthood

Involvement in community life has become increasingly important as persons with DS survive longer and achieve greater degrees of independence. Education involving inclusion in the classroom alongside typical students of the same age and teaching focused on the strengths of the child or adolescent enhance the progression to adulthood and provide persons with DS the chance to reach their full potential. Many transitions occur across the life span, and guidance in how they can be managed is available.

An emphasis on transitions such as employment, source of health care, and community involvement, as well as on legal issues (e.g., guardianship) and financial support (e.g., social security and trusts), has been found to be essential for the long-term well-being of persons with DS and their families. As life expectancy and quality of life for persons with DS increase, clinical research and development of evidence-based care guidelines for adults are needed.

Conclusions

The health issues and life trajectory of persons with DS are complex, and the condition is associated with many disparate medical, psychological, and social issues from infancy through adulthood. Persons with DS and their families generally have a positive attitude and express a desire for a high quality of life that builds on the strengths and skills of the affected child or adult.

A 73-Year-Old Man with Hypoxemic Respiratory Failure and Cardiac Dysfunction

The patient had been in his usual state of health until 6 days before this transfer, when a dry cough, fever, and worsening fatigue developed. Two days later, his symptoms had not resolved, and he presented to the emergency department at a local hospital. The temperature was 38.8°C, the blood pressure 94/62 mm Hg, the heart rate 91 beats per minute, the respiratory rate 12 breaths per minute, and the oxygen saturation 97% while he was breathing ambient air. On examination, he appeared well, and the lung sounds were clear. The white-cell count was 5600 per microliter (reference range, 4800 to 10,500); 56% of the cells were neutrophils and 33% were lymphocytes. A nasopharyngeal swab was submitted to the Massachusetts State Laboratory for nucleic acid testing for SARS-CoV-2 RNA. Tests for influenza A and B viruses and respiratory syncytial virus were not performed owing to a statewide shortage of nasopharyngeal swabs. Oseltamivir was prescribed for the empirical treatment of influenza, and the patient was discharged from the emergency department and instructed to self-quarantine at home. Four days later: The trachea was intubated, and mechanical ventilation was initiated. Intravenous propofol, cisatracurium, cefepime, and norepinephrine were administered, and the patient was transferred by helicopter to an academic health center in Boston for further evaluation and management of symptoms.

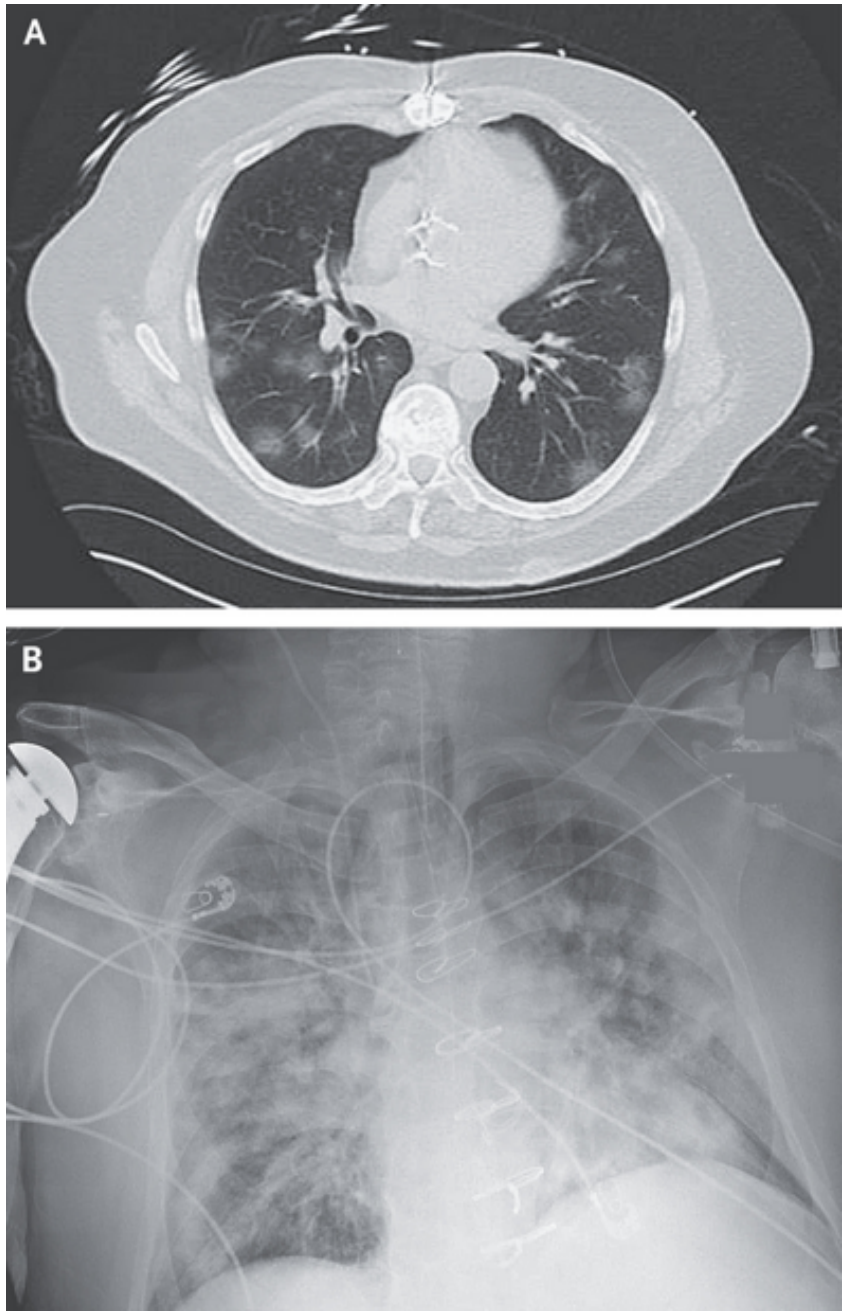

His medical history was notable for hypertension, diabetes mellitus, atrial fibrillation, and obstructive sleep apnea, for which nightly continuous positive airway pressure had been prescribed. He had undergone surgical aortic-valve replacement for severe symptomatic aortic stenosis 1 year earlier; there had been no evidence of obstructive coronary artery disease on preoperative angiography. Radiofrequency ablation for recurrent atrial flutter had been performed 2 years earlier, and he had undergone right shoulder arthroplasty. Medications included metformin, insulin lispro, atenolol, losartan, and apixaban. Multiple statin medications had previously caused myalgia with elevated creatine kinase levels.

Catheters were placed in the right internal jugular vein and the left radial artery. The central venous pressure was 4 mm Hg. The partial-thromboplastin time and blood levels of phosphorus and magnesium were normal; other laboratory test results are shown in Table 1. A blood sample was obtained for culture, and a nasopharyngeal swab was obtained for nucleic acid testing for the detection of community-acquired respiratory pathogens and SARS-CoV-2 RNA.

The patient received intravenous propofol, fentanyl, midazolam, and cisatracurium, as well as empirical intravenous vancomycin, cefepime, and doxycycline. Treatment with apixaban was discontinued, and intravenous heparin was initiated. Hydroxychloroquine was administered enterally.

Variable	Reference Range, Adults†	On Admission, Intensive Care Unit
Hemoglobin (g/dl)	13.5–17.5	15.7
Hematocrit (%)	40–51	44.5
White-cell count (per μl)	4000–10,000	18,400
Differential count (%)		
Neutrophils	34–71	82.2
Lymphocytes	19–53	11.4
Monocytes	5–13	5.3
Eosinophils	1–7	0.0
Platelet count (per μl)	150,000–400,000	222,000
Sodium (mmol/liter)	135–147	138
Potassium (mmol/liter)	3.4–5.4	4.9
Chloride (mmol/liter)	96–108	100
Carbon dioxide (mmol/liter)	22–32	16
Urea nitrogen (mg/dl)	6–25	17
Creatinine (mg/dl)	0.5–1.2	1.8
Calcium (mg/dl)	8.4–10.3	8.0
Alanine aminotransferase (U/liter)	0–40	19
Aspartate aminotransferase (U/liter)	0–40	88
Creatine kinase (U/liter)	47–322	395
Lactate (mmol/liter)	0.5–2.0	3.5
Troponin T (ng/ml)	<0.01	4.19
Central venous oxygen saturation (%)	70–80	78
N-terminal pro–B-type natriuretic peptide (pg/ml)	0–229	1298
Lactate dehydrogenase (U/liter)	94–250	572
D-dimer (ng/ml)	0–500	3838
C-reactive protein (mg/liter)	0–5.0	118.2
Ferritin (ng/ml)	30–400	2695
Prothrombin time (sec)	9.4–12.5	15.6
International normalized ratio	0.9–1.1	1.4
Arterial blood gases		
Fraction of inspired oxygen		1.0
pH	7.35–7.45	7.29
Partial pressure of carbon dioxide (mm Hg)	35–45	42
Partial pressure of oxygen (mm Hg)	80–105	118

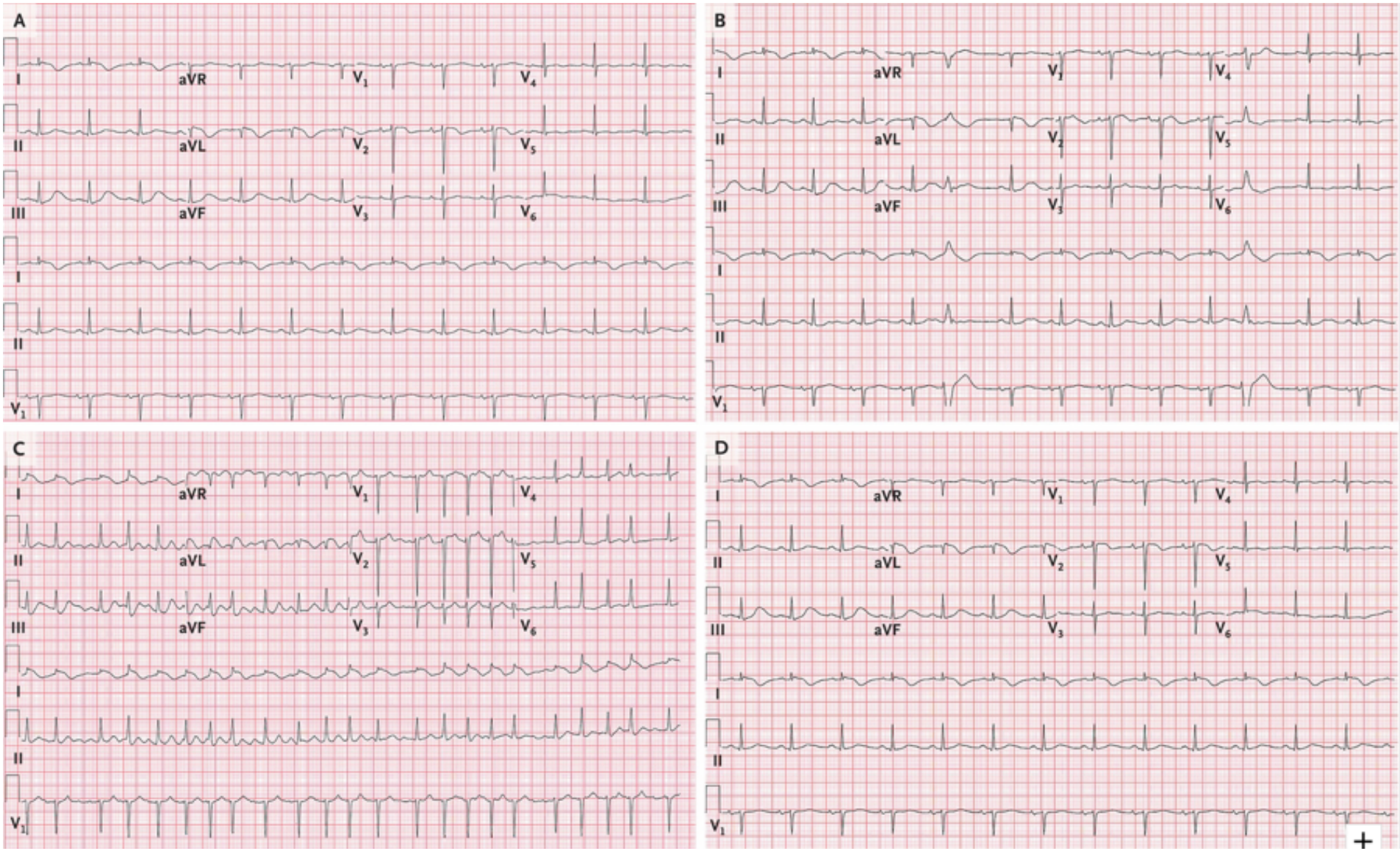
A
I
aVR
V1
V4
II
aVL
V2
V5
III
aVF
V3
V6
I
II
V1
B
I
aVR
V1
V4
II
aVL
V2
V5
III
aVF
V3
V6
I
II
V1
C
I
aVR
V1
V4
II
aVL
V2
V5
III
aVF
V3
V6
I
II
V1
D
I
aVR
V1
V4
II
aVL
V2
V5
III
aVF
V3
V6
I
II
V1

Hypoxemic Respiratory Failure with Pulmonary Infiltrates

The differential diagnosis of this patient's pulmonary findings includes cardiogenic pulmonary edema, multifocal pneumonia, and acute respiratory distress syndrome (ARDS).

Acute Respiratory Distress Syndrome

Although this patient has a history of clinically significant cardiac disease, multifocal pneumonia and ARDS are the likely causes of his hypoxemic respiratory failure. The diagnosis of ARDS is made if a patient has sudden onset (or progression) of symptoms within 1 week after a known clinical insult, bilateral pulmonary opacities on chest imaging, respiratory failure that is not fully explained by cardiac failure or fluid overload, and moderate-to-severe impairment of oxygenation; this patient met all four criteria. ARDS can be precipitated by various triggers, including infection, aspiration, trauma, transfusion-related lung injury, the use of illicit drugs, or acute pancreatitis.

Cardiac Abnormalities

This patient had an elevated troponin T level suggestive of myocardial injury, which is common among critically ill patients with SARS-CoV-2 infection. In a retrospective single-center cohort study involving 416 hospitalized patients with Covid-19 in Wuhan, China, cardiac injury, defined by a troponin T level above the 99th percentile (upper limit of the reference range), was present in 19.7% of the patients. This patient's ST-segment elevations in leads I and aVL arouse concern about an ST-segment elevation myocardial infarction (STEMI) in the lateral wall.

Coronary Angiography

Dr. Duane S. Pinto: Coronary angiography can be used to determine whether revascularization is indicated, but there are additional considerations in a critically ill patient with confirmed or suspected Covid-19. First, it is important for clinicians to maintain a high index of suspicion for diseases such as myopericarditis or stress-induced cardiomyopathy that can produce ST-segment elevation.

Myopericarditis

Dr. Kazi: Several reported cases of possible myopericarditis among patients with SARS-CoV-2 infection have been published. Some of these patients presented with localized ST-segment elevations on electrocardiography but were subsequently noted to have no evidence of obstructive coronary disease on coronary angiography.

Final Diagnosis

Severe acute respiratory syndrome coronavirus 2 (SARS-CoV-2) infection with acute respiratory distress syndrome and suspected myopericarditis.

NEJM Knowledge+

Question of the Week

An 82-year-old female nursing-home resident presents to the emergency department with dyspnea, cough, fever, and a blood pressure of 75/50 mm Hg. She is edentulous and has focal crackles in the right lower lung field. Laboratory testing reveals a leukocytosis and elevated serum creatinine and lactate levels, and a chest radiograph shows a dense opacity in the right lower lobe. She is treated with appropriate antibiotics and a 30-mL/kg bolus of lactated Ringer solution, but her blood pressure remains low and her blood lactate level remains elevated. A bedside echocardiogram shows mildly depressed systolic function, and an ultrasound shows a dilated inferior vena cava without collapse on inspiration. What is the most appropriate next therapeutic intervention for this patient?

- » Administer an additional 30-mL/kg bolus of lactated Ringer solution
- » Start dobutamine to target a mean arterial pressure goal
- Start norepinephrine to target a mean arterial pressure goal
- » Monitor central venous pressure (CVP), and administer normal saline to achieve a goal CVP
- » Initiate empiric anaerobic coverage with intravenous metronidazole

Your answer is correct.

Administer an additional 30-mL/kg bolus of lactated Ringer solution
Start dobutamine to target a mean arterial pressure goal
Start norepinephrine to target a mean arterial pressure goal
Monitor central venous pressure (CVP), and administer normal saline to achieve a goal CVP
Initiate empiric anaerobic coverage with intravenous metronidazole

Key Learning Point

View Case Presentation >

When a patient has persistent septic shock despite a 30-mL/kg fluid bolus and additional fluids are unlikely to improve the blood pressure, the most appropriate intervention is to start a norepinephrine infusion.

Detailed Feedback

This patient presents with evidence of septic shock, defined as lack of perfusion (usually due to hypotension) in the setting of infection, in this case from pneumonia. She received appropriate initial therapy, including broad-spectrum antibiotics and a 30-mL/kg crystalloid bolus. Given that she remains hypotensive with signs of lack of perfusion, she requires additional hemodynamic support. Her inferior vena cava is dilated and does not change in caliber with respirations, suggesting that she does not require additional fluids at this time.

Patientenverfügung?

nature

https://doi.org/10.1038/s415

Accelerated Article Preview

The effect of large-scale anti-contagion policies on the COVID-19 pandemic

Governments around the world are responding to the novel coronavirus (COVID-19) pandemic[1] with unprecedented policies designed to slow the growth rate of infections. Many actions, such as closing schools and restricting populations to their homes, impose large and visible costs on society, but their benefits cannot be directly observed and are currently understood only through process-based simulations[2–4]. Here, we compile new data on 1,717 local, regional, and national non-pharmaceutical interventions deployed in the ongoing pandemic across localities in China, South Korea, Italy, Iran, France, and the United States (US). We then apply reduced-form econometric methods, commonly used to measure the effect of policies on economic growth[5,6], to empirically evaluate the effect that these anti-contagion policies have had on the growth rate of infections. In the absence of policy actions, we estimate that early infections of COVID-19 exhibit exponential growth rates of roughly 38% per day. We find that anti-contagion policies have significantly and substantially slowed this growth. Some policies have different impacts on different populations, but we obtain consistent evidence that the policy packages now deployed are achieving large, beneficial, and measurable health outcomes. We estimate that across these six countries, interventions prevented or delayed on the order of 62 million confirmed cases, corresponding to averting roughly 530 million total infections. These findings may help inform whether or when these policies should be deployed, intensified, or lifted, and they can support decision-making in the other 180+ countries where COVID-19 has been reported[7].

Methods Summary

We employ well-established "reduced-form" econometric techniques[5,14] commonly used to measure the effects of events[6,15] on economic growth rates. Similar to early COVID-19 infections, economic output generally increases exponentially with a variable rate that can be affected by policies and other conditions. Here, this technique aims to measure the total magnitude of the effect of *changes in policy*, without requiring explicit prior information about fundamental epidemiological parameters or mechanisms, many of which remain uncertain in the current pandemic. Rather, the collective influence of these factors is empirically recovered from the data without modeling their individual effects explicitly (see Methods). Prior work on influenza[16], for example, has shown that such statistical approaches can provide important complementary information to process-based models.

To construct the dependent variable, we transform location-specific, subnational time-series data on infections into first-differences of their natural logarithm, which is the *per-day growth rate of infections* (see Methods). We use data from first- or second-level administrative units and data on active or cumulative cases, depending on availability (see Supplementary Information). We employ widely-used panel regression models[5,14] to estimate how the daily growth rate of infections changes over time within a location when different combinations of large-scale policies are enacted (see Methods). Our econometric approach accounts for differences in the baseline growth rate of infections across subnational locations, which may be affected by time-invariant characteristics, such as demographics, socio-economic status, culture, and health systems; it accounts for systematic patterns in growth rates within countries unrelated to policy, such as the effect of the work-week; it is robust to systematic under-surveillance specific to each subnational unit; and it accounts for changes in procedures to diagnose positive cases (see Methods and Supplementary Information).

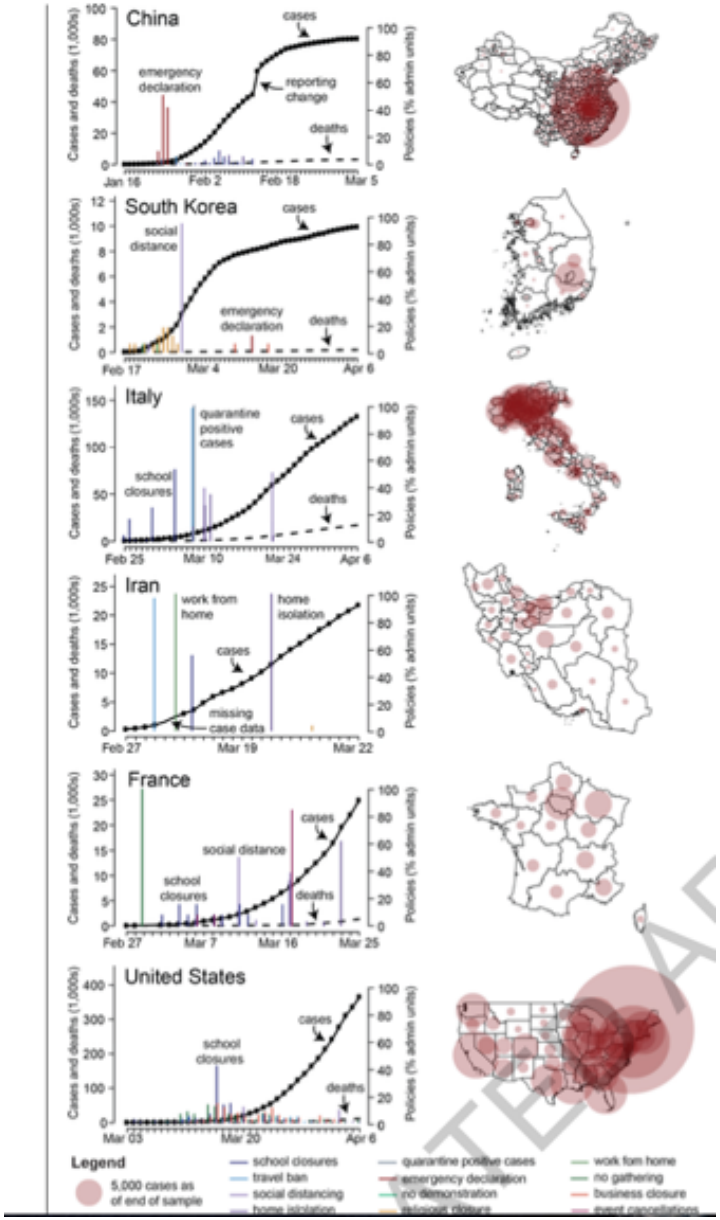

Fig. 1 | Data on COVID-19 infections and large-scale anti-contagion policies. Left: Daily cumulative confirmed cases of COVID-19 (solid black line, left axis) and deaths (dashed black line) over time. Vertical lines are deployments of anti-contagion policies, with height indicating the number of administrative units instituting a policy that day (right axis). For display purposes only, ≤ 5 policy types are shown per country and missing case data are imputed unless all sub-national units are missing. Right: Maps of cumulative confirmed cases by administrative unit on the last date of each sample.

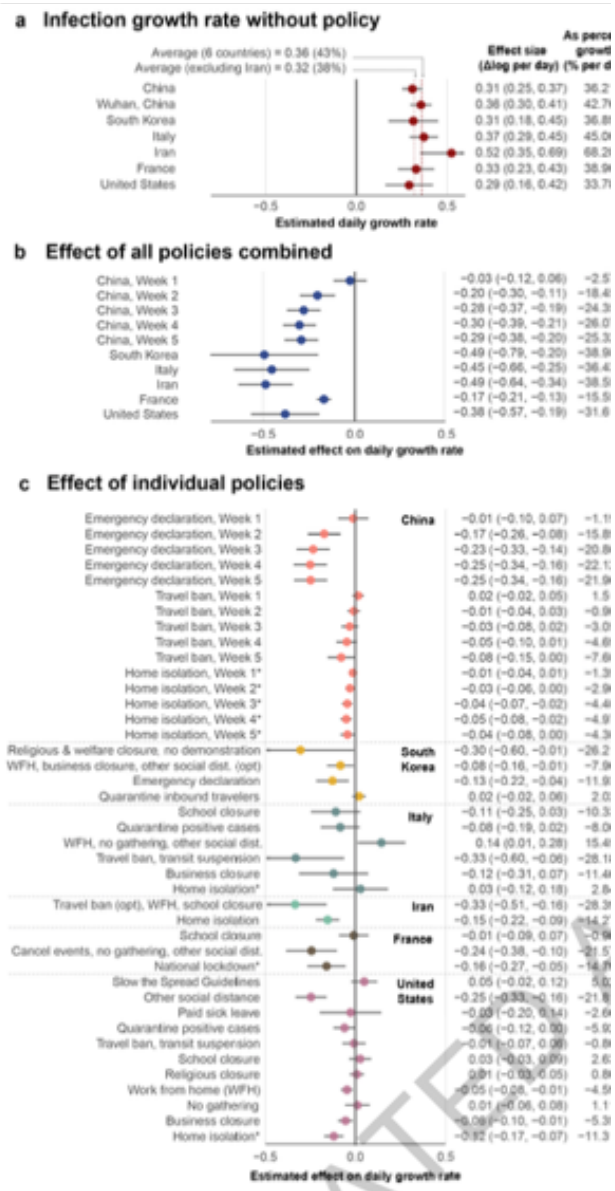

Fig. 2 | Empirical estimates of unmitigated COVID-19 infection growth ra and the effect of anti-contagion policies. Markers are country-specific estimates, whiskers are 95% CI. Columns report effect sizes as a change in the continuous-time growth rate (95% CI in parentheses) and the day-over-day percentage growth rate. (**a**) Estimates of daily COVID-19 infection growth rat in the absence of policy (dashed lines = averages with and without Iran, both excluding Wuhan-specific estimate). (**b**) Estimated combined effect of all policies on infection growth rates. (**c**) Estimated effects of individual policie or policy groups on the daily growth rate of infections, jointly estimated and ordered roughly chronologically within each country. *Reported effect of "home isolation" includes effects of other implied policies (see Methods). China: N = 3669; South Korea: N = 595, Italy: N = 2898, Iran: N = 548, France: N = 270, US: N = 1238.

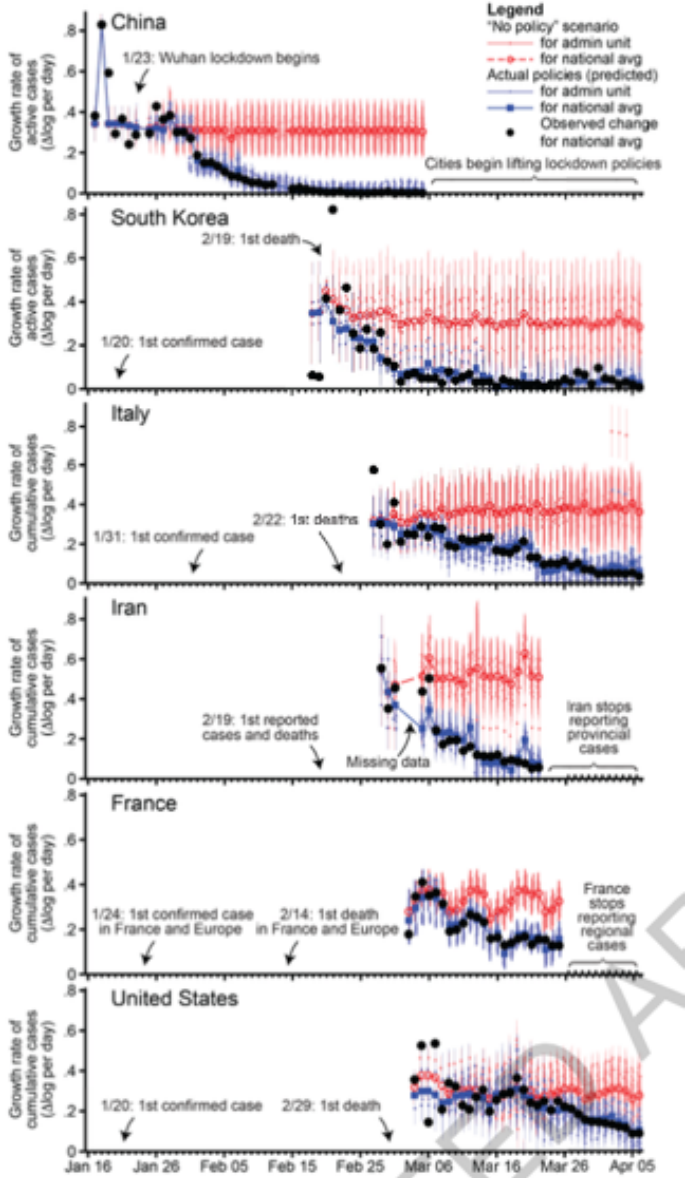

Fig. 3 | Estimated infection growth rates based on actual anti-contagion policies and in a "no policy" counterfactual scenario. Predicted daily growth rates of active (China, South Korea) or cumulative (all others) COVID-19 infections based on the observed timing of all policy deployments within each country (blue) and in a scenario where no policies were deployed (red). The difference between these two predictions is our estimated effect of actual anti-contagion policies on the growth rate of infections. Small markers are daily estimates for sub-national administrative units (vertical lines are 95% CI). Large markers are national averages. Black circles are observed daily changes in log(*infections*), averaged across administrative units. Sample sizes are the same as Figure 2.

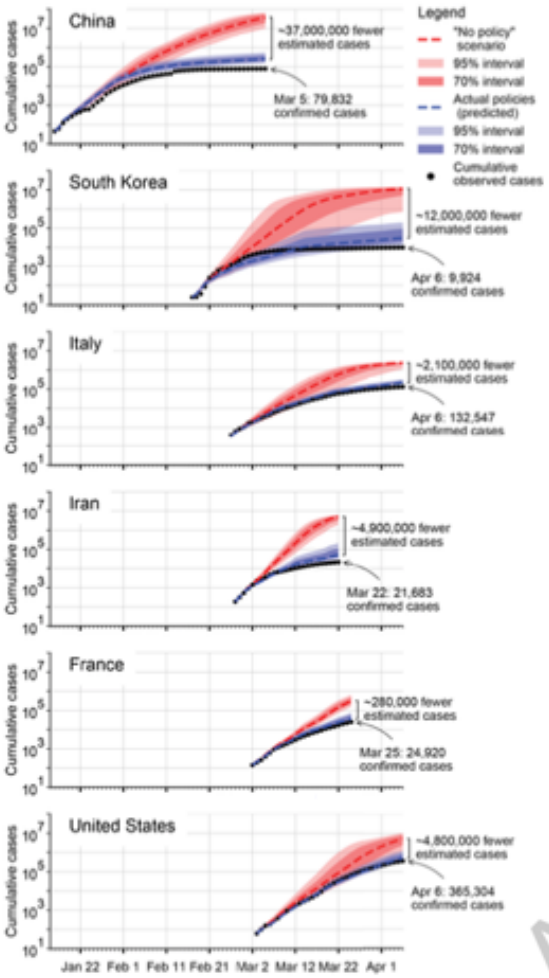

Fig. 4 | Estimated cumulative confirmed COVID-19 infections with and without anti-contagion policies. The predicted cumulative number of confirmed COVID-19 infections based on actual policy deployments (blue) and in the no-policy counterfactual scenario (red). Shaded areas show uncertainty based on 1,000 simulations where empirically estimated parameters are resampled from their joint distribution (dark = inner 70% of predictions; light = inner 95%). Black dotted line is observed cumulative infections. Infections are not projected for administrative units that never report infections in the sample, but which might have experienced infections in a no-policy scenario.

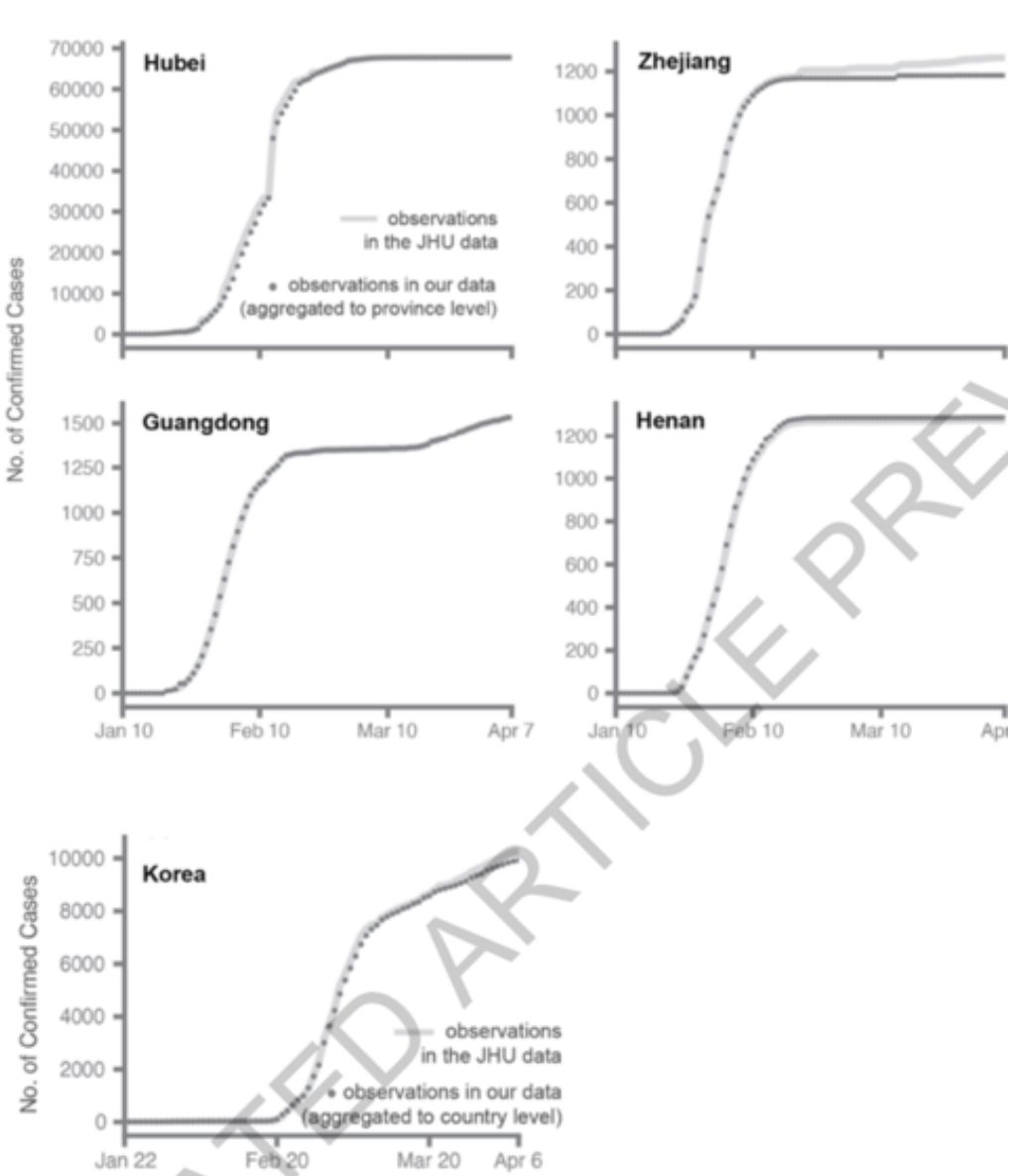

Extended Data Fig. 1 | Validating disaggregated epidemiological data against aggregated data from the Johns Hopkins Center for Systems Science and Engineering. Comparison of cumulative confirmed cases from a subset of regions in our collated epidemiological dataset to the same statistics from the 2019 Novel Coronavirus COVID-19 (2019-nCoV) Data Repository by the Johns Hopkins Center for Systems Science and Engineering (JHU CSSE)[65]. We conduct this comparison for Chinese provinces and South Korea, where the data we collect are from local administrative units that are m granular than the data in the JHU CSSE database. **a**, In China, city-level data to the province level, and **b**, in Korea we aggreg data up to the country level. Small discrepancies, especially i the outbreak, are generally due to imported cases (internatio that are present in national statistics but which we do not ass cities (in China) or provinces (in Korea).

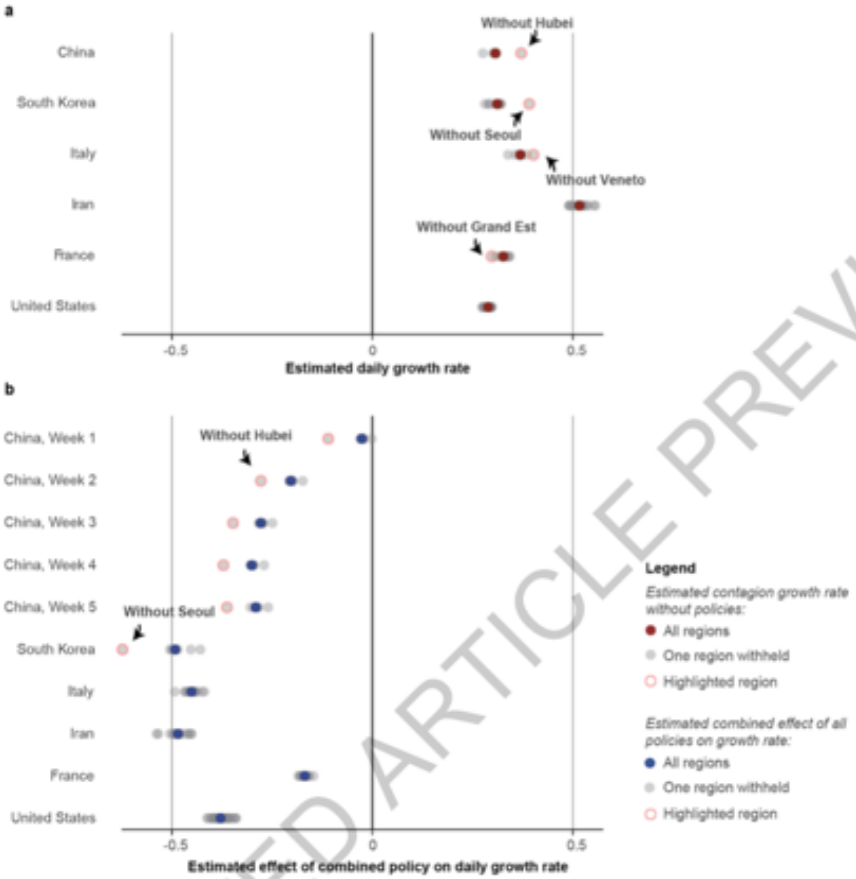

Extended Data Fig. 3 | Robustness of the estimated no-policy growth rate of infections and the combined effect of policies to withholding blocks of data from entire regions. For each country, we re-estimated Eq. 7 using real data k times, each time withholding one of the k first-level administrative regions ("Adm1," i.e. state or province) in that country. Each gray circle is either (a) the estimated no-policy growth rate or (b) the total effect of all policies combined, from one of these k regressions. Red and blue circles show estimates from the full sample, identical to results presented in panels A and B of Figure 2, respectively. For each country panel, if a single region is influential, the estimated value when it is withheld from the sample will appear as an outlier. Some regions that appear influential are highlighted with an open pink circle. As in Figure 2b of the main text, we estimate a distributed lag model for China and display each of the estimated weekly lag effects (red circle is the same "without Hubei" sample for lags). The full sample includes 3,684 observations in China, 595 in South Korea, 2,898 in Italy, 548 in Iran, 270 in France, and 1,238 in the US.

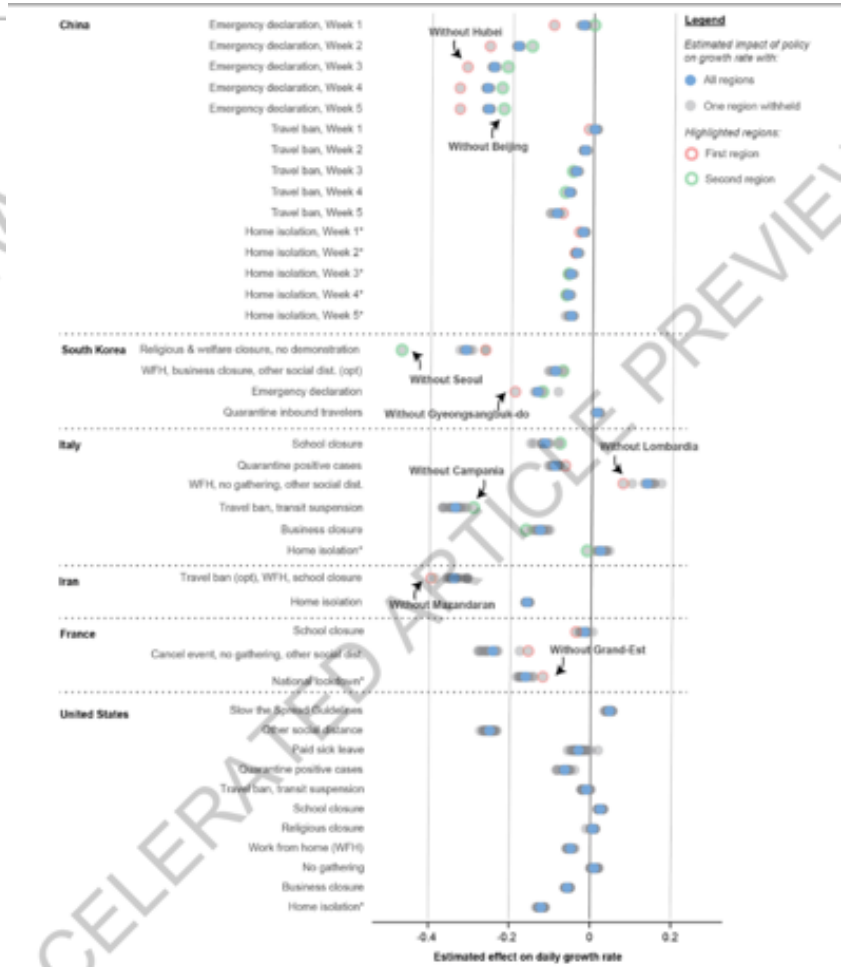

Extended Data Fig. 4 | Robustness of the estimated effects of individual policies to withholding blocks of data from entire regions. Same as Extended Data Figure 3, but for individual policies (analogous to Figure 2c in the main text). In cases where two regions are influential, a second region is highlighted with an open green circle. The full sample includes 3,669 observations in China, 595 in South Korea, 2,898 in Italy, 548 in Iran, 270 in France, and 1,238 in the US.

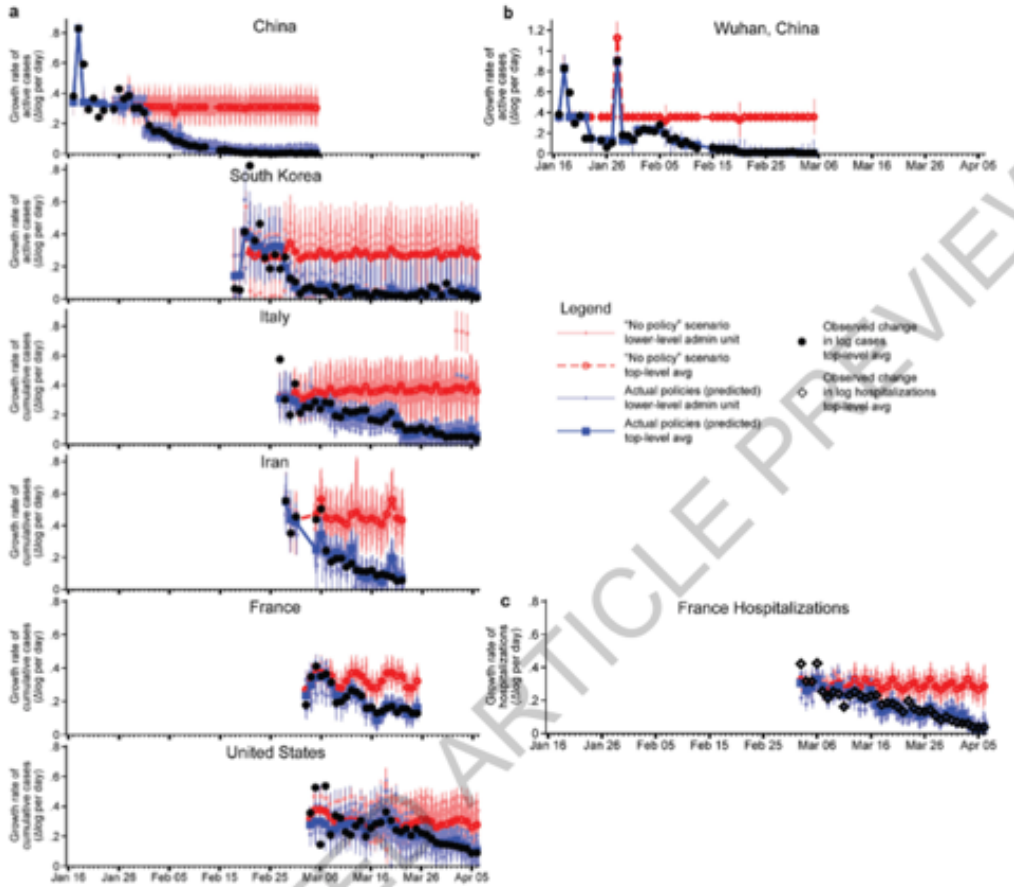

Extended Data Fig. 6 | Estimated infection or hospitalization growth rates with actual anti-contagion policies and in a "no policy" counterfactual scenario. a, The estimated daily growth rates of active (China, South Korea) or cumulative (all others) infections based on the observed timing of all policy deployments within each subnational unit (blue) and in a scenario where no policies were deployed (red). Identical to Figure 3 in the main text, but using an alternative disaggregated encoding of policies that does not group any policies into policy packages. The sample size is 3,669 in China, 595 in South Korea, 2,898 in Italy, 548 in Iran, 220 in France, and 1,238 in the US. **b**, Same as Figure 3 in the main text, but Eq. 7 is implemented for a single example administrative unit, Wuhan, China. The sample size is 46 observations. **c**, Same as Figure 3 in the main text, but using hospitalization data from France rather than cumulative cases (the French government stopped reporting cumulative cases after March 25, 2020). The sample size is 424 observations. For all panels, the difference between the with- and no-policy predictions is our estimated effect of actual anti-contagion policies on the growth rate of infections (or hospitalizations). The markers are daily estimates for each subnational administrative unit (vertical lines are 95% confidence intervals). Black circles are observed changes in log(infections) (or diamonds for log(hospitalizations)), averaged across observed administrative units.

Discussion

Our empirical results indicate that large-scale anti-contagion policies are slowing the COVID-19 pandemic. Because infection rates in the countries we study would have initially followed rapid exponential growth had no policies been applied, our results suggest that these policies have provided large health benefits. For example, we estimate that there would be roughly 465 × the observed number of confirmed cases in China, 17 × in Italy, and 14 × in the US by the end of our sample if large-scale anti-contagion policies had not been deployed. Consistent with process-based simulations of COVID-19 infections[2,4,8,9,22,26], our analysis of existing policies indicates that seemingly small delays in policy deployment likely produced dramatically different health outcomes.

While the limitations of available data pose challenges to our analysis, our aim is to use what data exist to estimate the first-order impacts of unprecedented policy actions in an ongoing global crisis. As more data become available, related findings will become more precise and may capture more complex interactions. Furthermore, this analysis does not account for interactions between populations in nearby localities[13], nor mobility networks[3,4,8,9]. Nonetheless, we hope these results can support critical decision-making, both in the countries we study and in the other 180 + countries where COVID-19 infections have been reported[7].

nature

https://doi.org/10.1038/s41586-020-2405-7

Accelerated Article Preview

Estimating the effects of non-pharmaceutical interventions on COVID-19 in Europe

Following the emergence of a novel coronavirus[1] (SARS-CoV-2) and its spread outside of China, Europe has experienced large epidemics. In response, many European countries have implemented unprecedented non-pharmaceutical interventions such as closure of schools and national lockdowns. We study the impact of major interventions across 11 European countries for the period from the start of COVID-19 until the 4th of May 2020 when lockdowns started to be lifted. Our model calculates backwards from observed deaths to estimate transmission that occurred several weeks prior, allowing for the time lag between infection and death. We use partial pooling of information between countries with both individual and shared effects on the reproduction number. Pooling allows more information to be used, helps overcome data idiosyncrasies, and enables more timely estimates. Our model relies on fixed estimates of some epidemiological parameters such as the infection fatality rate, does not include importation or subnational variation and assumes that changes in the reproduction number are an immediate response to interventions rather than gradual changes in behavior. Amidst the ongoing pandemic, we rely on death data that is incomplete, with systematic biases in reporting, and subject to future consolidation. We estimate that, for all the countries we consider, current interventions have been sufficient to drive the reproduction number R_t below 1 (probability R_t <1.0 is 99.9%) and achieve epidemic control. We estimate that, across all 11 countries, between 12 and 15 million individuals have been infected with SARS-CoV-2 up to 4th May, representing between 3.2% and 4.0% of the population. Our results show that major non-pharmaceutical interventions and lockdown in particular have had a large effect on reducing transmission. Continued intervention should be considered to keep transmission of SARS-CoV-2 under control.

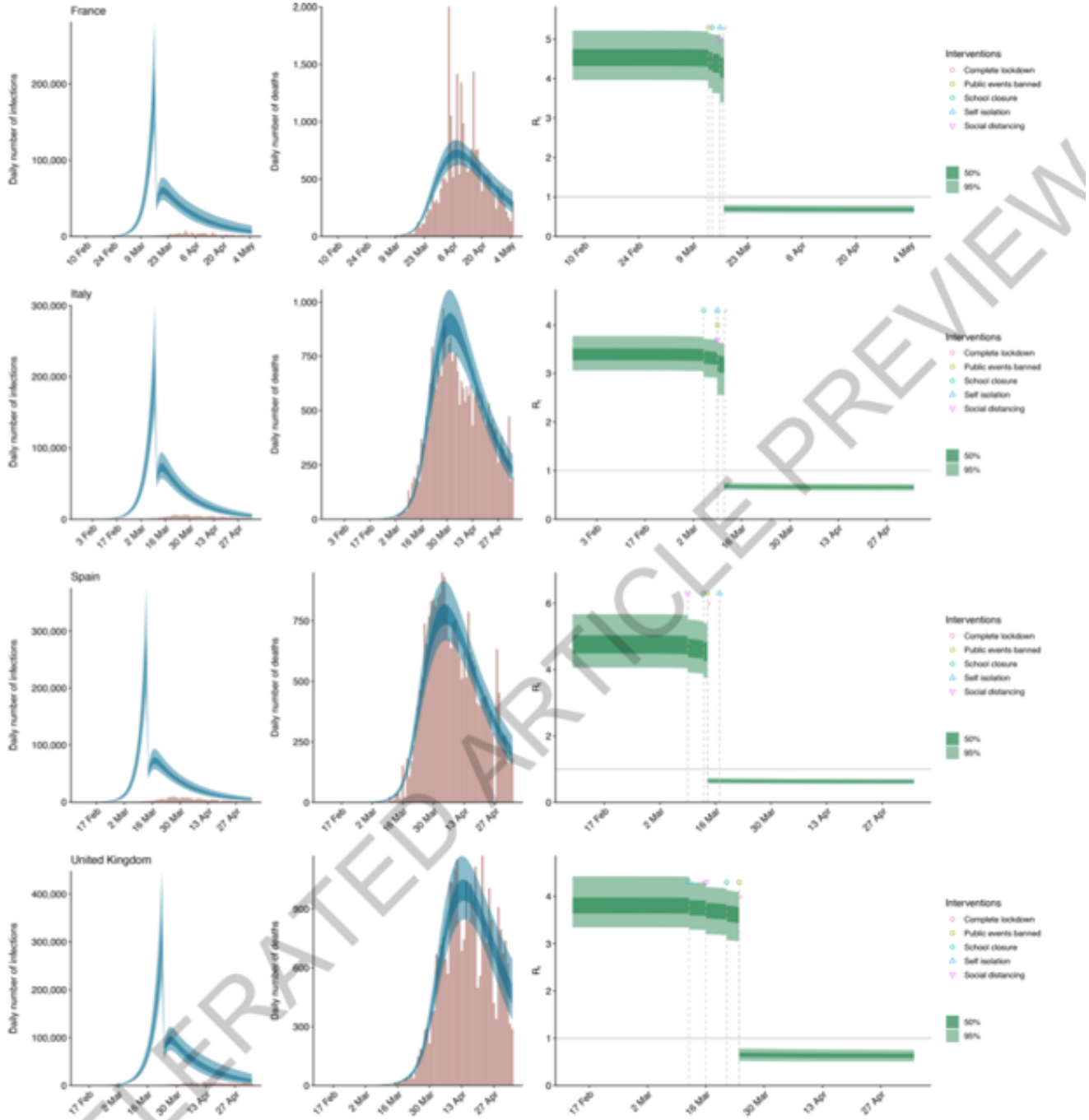

Fig. 1 | Country-level estimates of infections, deaths and R_t for France, Italy, Spain and UK. Left: daily number of infections, brown bars are reported infections, blue bands are predicted infections, dark blue 50% credible interval (CI), light blue 95% CI. The number of daily infections estimated by our model drops immediately after an intervention, as we assume that all infected people become immediately less infectious through the intervention. Afterwards, if the R_t is above 1, the number of infections will start growing again. Middle: daily number of deaths, brown bars are reported deaths, blue bands are predicted deaths, CI as in left plot. Right: time-varying reproduction number R_t, dark green 50% CI, light green 95% CI. Icons are interventions shown at the time they occurred.

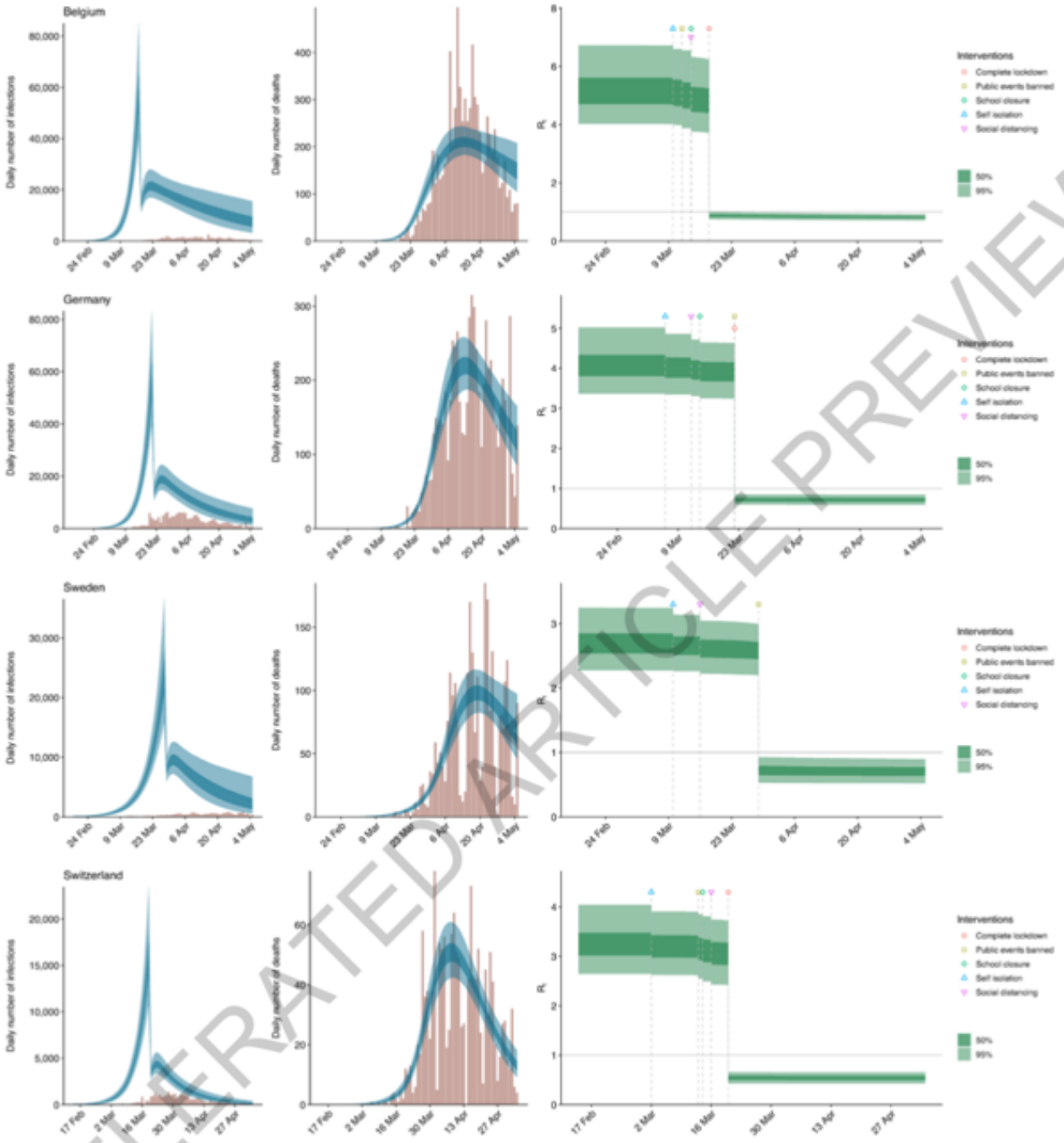

Extended Data Fig. 1 | Country-level estimates of infections, deaths and R_t for Belgium, Germany, Sweden and Switzerland. Left: daily number of infections, brown bars are reported infections, blue bands are predicted infections, dark blue 50% credible interval (CI), light blue 95% CI. The number of daily infections estimated by our model drops immediately after an intervention, as we assume that all infected people become immediately less infectious through the intervention. Afterwards, if the R_t is above 1, the number of infections will starts growing again. Middle: daily number of deaths, brown bars are reported deaths, blue bands are predicted deaths, CI as in left plot. Right: time-varying reproduction number R_t, dark green 50% CI, light green 95% CI. Icons are interventions shown at the time they occurred.

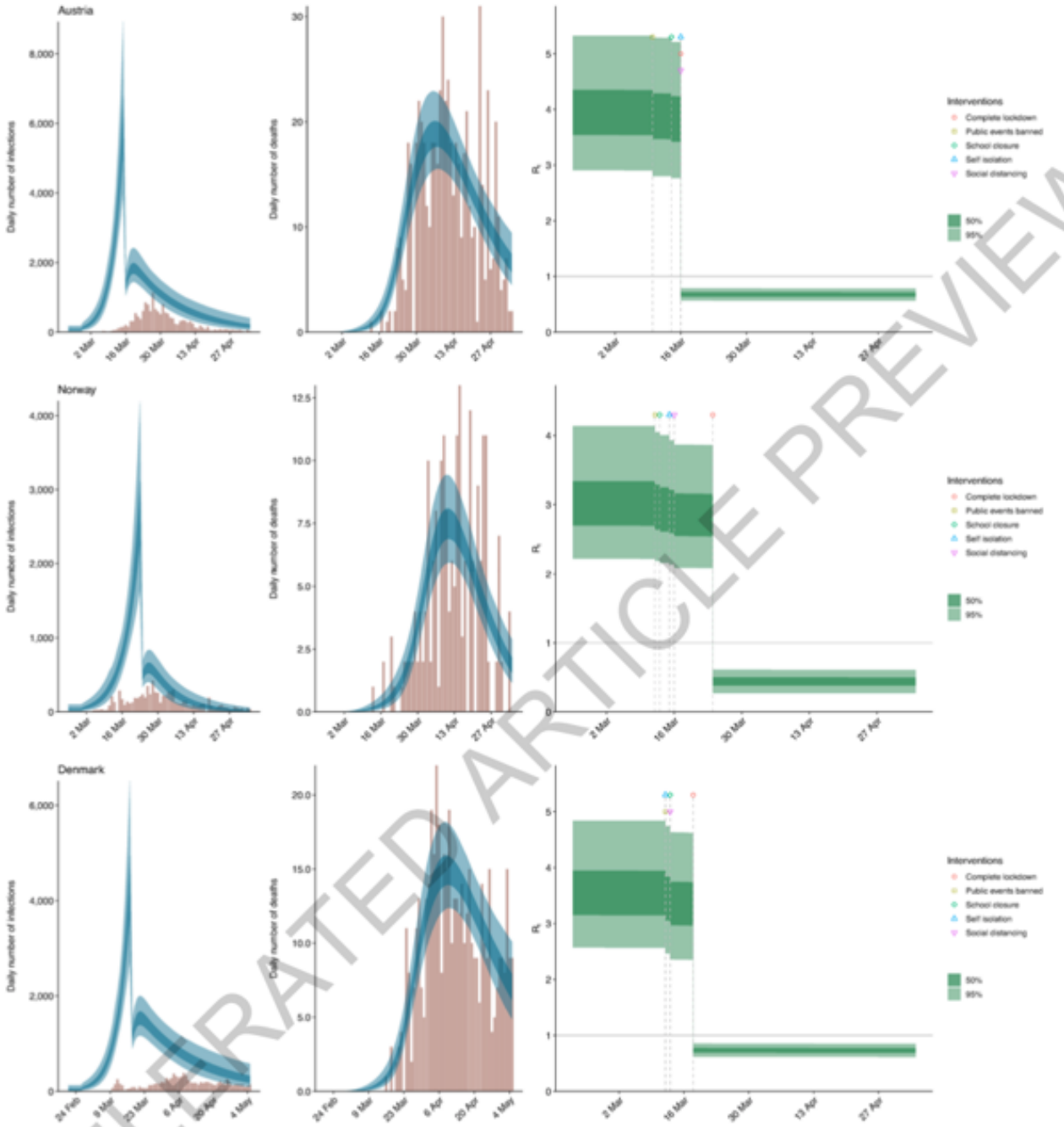

Extended Data Fig. 2 | Country-level estimates of infections, deaths and R_t for Austria, Sweden and Denmark. Left: daily number of infections, brown bars are reported infections, blue bands are predicted infections, dark blue 50% credible interval (CI), light blue 95% CI. The number of daily infections estimated by our model drops immediately after an intervention, as we assume that all infected people become immediately less infectious through the intervention. Afterwards, if the R_t is above 1, the number of infections will starts growing again. Middle: daily number of deaths, brown bars are reported deaths, blue bands are predicted deaths, CI as in left plot. Right: time-varying reproduction number R_t, dark green 50% CI, light green 95% CI. Icons are interventions shown at the time they occurred.

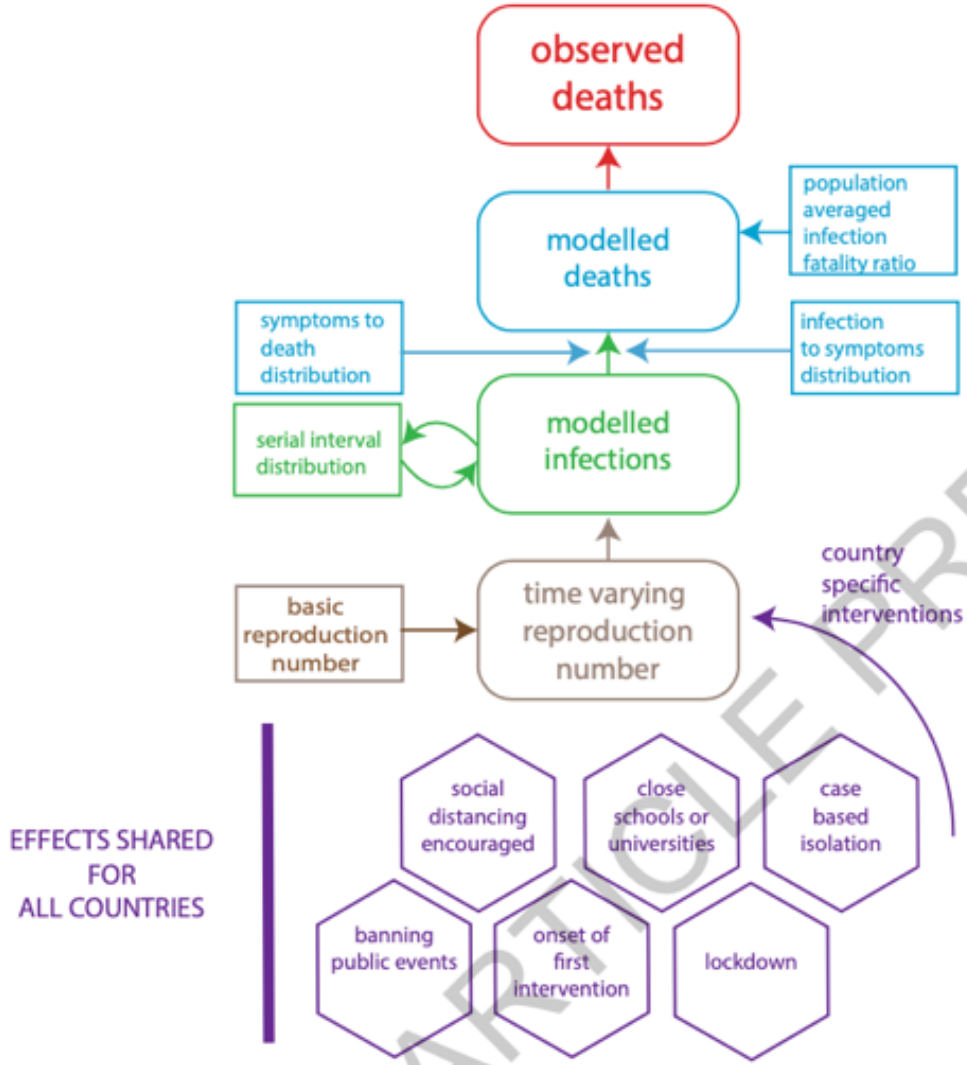

Extended Data Fig. 3 | Summary of model components.

Discussion

During ongoing transmission of coronavirus in Europe, we analyze trends in numbers of deaths to assess the extent to which transmission has been reduced. Representing the COVID-19 infection process using a semi-mechanistic, joint, Bayesian hierarchical model, we can reproduce trends observed in the data on deaths and produce empirically driven predictions which are valid over short time horizons.

We estimate that there have been many more infections than are currently reported. The high level of under-ascertainment of infections that we estimate here is likely due to the focus on testing in hospital settings which misses milder or asymptomatic cases in the community. Despite this, we estimate that only a relatively small minority of individuals in each country have been infected (Table 1). Our estimates imply that the populations in Europe are not close to herd immunity (~70% if R_0 is 3.8[14]). Further, with R_t values below 1 in all countries, the rate of acquisition of herd immunity will slow down rapidly. Our estimates for attack rates during our study period are in line with those reported from national serological studies[5]. Similarly, comparable studies estimating R_t all agree that that the number as of 4th of May 2020 is less than 1.

Modern understanding of infectious disease with a global publicized response has meant that nationwide interventions could be implemented with widespread adherence and support. Given observed infection fatality ratios and the epidemiology of COVID-19, major non-pharmaceutical interventions have had an impact in reducing transmission in all the countries we have observed. In all countries in this study we find that these interventions have reduced the reproduction number below one and have contained their epidemics at the current time. When looking at simplistic counterfactuals over the whole epidemic the number of potential deaths averted is substantial. We cannot say for certain that the current measures will continue to control the epidemic in Europe; however, if current trends continue, there is reason for optimism.

Das hereditäre non-polypöse Kolonkarzinom (korrekte Bezeichnung eigentlich: hereditäres nicht-Polyposis-assoziiertes kolorektales Karzinom) (HNPCC) oder Lynch-Syndrom ist eine erbliche Darmkrebsform ohne Polyposis, d. h. ohne Auftreten von vielen Polypen im Darm. Das hereditäre Dickdarm-Karzinom ohne Polyposis (HNPCC) ist die häufigste erbliche Darmkrebsform und betrifft etwa drei Prozent der Darmkrebsfälle. Mittlerweile sind 5 Gene (MSH2, MSH6, MLH1, PMS2, und EPCAM) bekannt, die, insofern eine pathogene Mutation vorliegt, zum Auftreten eines hereditären non-polypösen Karzinoms führen können. Diese Gene kodieren für Proteine aus der Gruppe der sogenannten DNA-Mismatch-Reparaturproteine, deren Aufgabe es ist, eventuelle Fehler bei der Replikation der DNA im Rahmen der Zellteilung zu erkennen und zu beseitigen. Das HNPCC-Syndrom wird autosomal-dominant vererbt. Das bedeutet, dass Betroffene die Erkrankung mit einer Wahrscheinlichkeit von 50 % unabhängig vom Geschlecht an ihre Kinder weitergeben.
Amsterdam Kriterien:

Alle Kriterien müssen erfüllt sein.

1. mindestens drei Familienangehörige mit HNPCC-assoziiertem Karzinom (Kolon/Rektum, Endometrium, Dünndarm, Nierenbecken/Ureter)
2. einer davon Verwandter ersten Grades der beiden anderen
3. Erkrankungen in mindestens zwei aufeinanderfolgenden Generationen
4. mindestens ein Patient mit der Diagnose eines Karzinoms vor dem 50. Lebensjahr
5. Ausschluss einer FAP (Familiäre adenomatöse Polyposis)

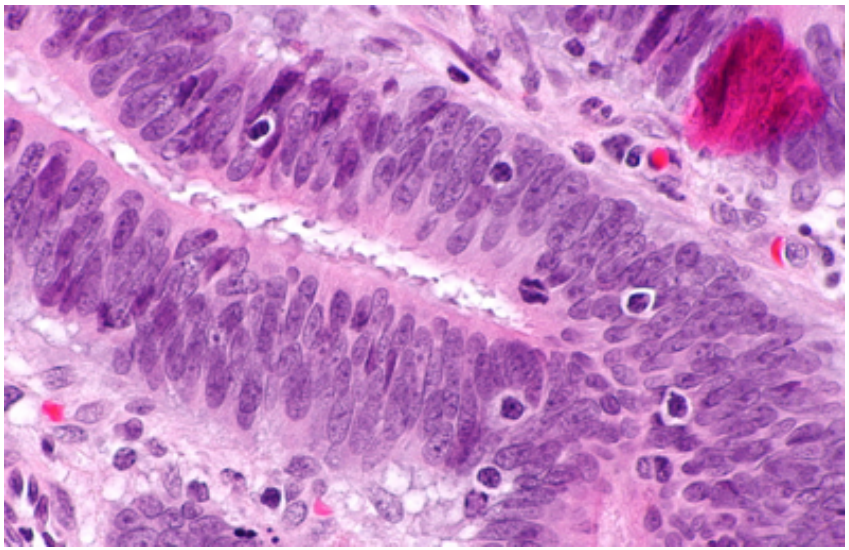

Mikrofoto von Dickdarmkrebs mit Lymphozyten im Tumor, wie es oft bei HNPCC vorkommt. HE-Färbung.

Cancer prevention with aspirin in hereditary colorectal cancer (Lynch syndrome), 10-year follow-up and registry-based 20-year data in the CAPP2 study: a double-blind, randomised, placebo-controlled trial

Summary

Background Lynch syndrome is associated with an increased risk of colorectal cancer and with a broader spectrum of cancers, especially endometrial cancer. In 2011, our group reported long-term cancer outcomes (mean follow-up 55·7 months [SD 31·4]) for participants with Lynch syndrome enrolled into a randomised trial of daily aspirin versus placebo. This report completes the planned 10-year follow-up to allow a longer-term assessment of the effect of taking regular aspirin in this high-risk population.

Methods In the double-blind, randomised CAPP2 trial, 861 patients from 43 international centres worldwide (707 [82%] from Europe, 112 [13%] from Australasia, 38 [4%] from Africa, and four [<1%] from The Americas) with Lynch syndrome were randomly assigned to receive 600 mg aspirin daily or placebo. Cancer outcomes were monitored for at least 10 years from recruitment with English, Finnish, and Welsh participants being monitored for up to 20 years. The primary endpoint was development of colorectal cancer. Analysis was by intention to treat and per protocol. The trial is registered with the ISRCTN registry, number ISRCTN59521990.

Findings Between January, 1999, and March, 2005, 937 eligible patients with Lynch syndrome, mean age 45 years, commenced treatment, of whom 861 agreed to be randomly assigned to the aspirin group or placebo; 427 (50%) participants received aspirin and 434 (50%) placebo. Participants were followed for a mean of 10 years approximating 8500 person-years. 40 (9%) of 427 participants who received aspirin developed colorectal cancer compared with 58 (13%) of 434 who received placebo. Intention-to-treat Cox proportional hazards analysis revealed a significantly reduced hazard ratio (HR) of 0·65 (95% CI 0·43–0·97; p=0·035) for aspirin versus placebo. Negative binomial regression to account for multiple primary events gave an incidence rate ratio of 0·58 (0·39–0·87; p=0·0085). Per-protocol analyses restricted to 509 who achieved 2 years' intervention gave an HR of 0·56 (0·34–0·91; p=0·019) and an incidence rate ratio of 0·50 (0·31–0·82; p=0·0057). Non-colorectal Lynch syndrome cancers were reported in 36 participants who received aspirin and 36 participants who received placebo. Intention-to-treat and per-protocol analyses showed no effect. For all Lynch syndrome cancers combined, the intention-to-treat analysis did not reach significance but per-protocol analysis showed significantly reduced overall risk for the aspirin group (HR=0·63, 0·43–0·92; p=0·018). Adverse events during the intervention phase between aspirin and placebo groups were similar, and no significant difference in compliance between intervention groups was observed for participants with complete intervention phase data; details reported previously.

Interpretation The case for prevention of colorectal cancer with aspirin in Lynch syndrome is supported by our results.

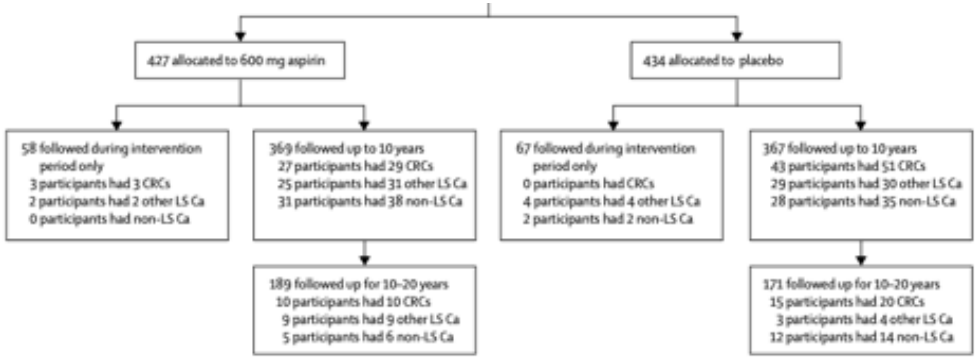

	Aspirin (n=427)	Placebo (n=434)	Total (n=861)
Time in CAPP2 intervention study (months)*	25·0 (12·5, 0·8–60·6)	25·4 (14·2, 1·1–74·4)	25·2 (13·4, 0·8–74.4)
Months between study entry and last known follow-up date*	120·4 (63·3, 1·6–238·7)	116·3 (63·7, 1·1–238·9)	118·4 (63·5, 1·1–238·9)
Years between study entry and last known follow-up date			
≤2	36 (8%)	42 (10%)	78 (9%)
>2 and ≤6	80 (19%)	87 (20%)	167 (19%)
>6 and ≤10	133 (31%)	144 (33%)	277 (32%)
>10 and ≤14	54 (13%)	43 (10%)	97 (11%)
>14 and ≤18	104 (24%)	101 (23%)	205 (24%)
>18 and ≤20	20 (5%)	17 (4%)	37 (4%)
Participants with first colorectal cancer			
Since randomisation	40 (9%)	58 (13%)	98 (11%)
Within 2 years of randomisation	10 (2%)	10 (2%)	20 (2%)
More than 2 years from randomisation	30 (7%)	48 (11%)	78 (9%)
Participants with other Lynch syndrome cancers (excluding colorectal)			
Since randomisation	36 (8%)	36 (8%)	72 (8%)
Within 2 years of randomisation	7 (2%)	9 (2%)	16 (2%)
More than 2 years from randomisation	29 (7%)	27 (6%)	56 (7%)
Participants with one or more Lynch syndrome cancers (including colorectal)			
Since randomisation	74 (17%)	89 (21%)	163 (19%)
Within 2 years of randomisation	17 (4%)	19 (4%)	36 (4%)
More than 2 years from randomisation	57 (13%)	70 (16%)	127 (15%)
Types of extracolonic Lynch syndrome cancers			
Brain	2 (<1%)	0	2 (<1%)
Stomach, duodenum	5 (1%)	6 (1%)	11 (1%)
Bile duct, pancreas	8 (2%)	3 (1%)	11 (1%)
Urinary†	7 (2%)	6 (1%)	13 (2%)
Ovarian	2 (<1%)	2 (<1%)	4 (<1%)
Endometrium–uterine	8 (2%)	17 (4%)	25 (3%)
Multiple sites	4 (1%)	2 (<1%)	6 (1%)
Participants with non-Lynch syndrome cancers			
Since randomisation	36 (8%)	42 (10%)	78 (9%)
Within 2 years of randomisation	2 (<1%)	7 (2%)	9 (1%)
More than 2 years from randomisation	34 (8%)	35 (8%)	69 (8%)

*Data are mean (SD, range) or n (%). †Urinary cancers include ureter and kidney cancers.

Table 1: The whole CAPP2 cohort at 10 years plus England, Finland, and Wales registry data to 20 years

	Hazard ratio† (95% CI)	p value	Incidence rate ratio‡ (95% CI)	p value
Colorectal cancer				
Intention-to-treat analysis (n=861, 98 events for hazard ratio analysis)				
Aspirin vs placebo	0·65 (0·43–0·97)	0·035	0·58 (0·39–0·87)	0·0085
Per-protocol analysis§ (n=509, 67 events)				
≥2 years' placebo	1·0	..	1·0	..
≥2 years' aspirin	0·56 (0·34–0·91)	0·019	0·50 (0·31–0·82)	0·0057
Cumulative aspirin dose¶ (n=861, 98 events)				
Units of 100 aspirin	0·98 (0·96–1·00)	0·079	0·98 (0·96–1·00)	0·032
Non-colorectal Lynch syndrome cancers				
Intention-to-treat analysis (n=861, 72 events)				
Aspirin vs placebo	0·94 (0·59–1·50)	0·81	1·05 (0·65–1·69)	0·84
Per-protocol analysis§ (n=509, 46 events)				
≥2 years' placebo	1·0	..	1·0	..
≥2 years' aspirin	0·75 (0·42–1·34)	0·33	0·87 (0·48–1·61)	0·67
Cumulative aspirin dose¶ (n=861, 72 events)				
Units of 100 aspirin	0·98 (0·96–1·01)	0·20	0·99 (0·97–1·02)	0·50
All Lynch syndrome cancers				
Intention-to-treat analysis (n=861, 163 events)				
Aspirin vs placebo	0·76 (0·56–1·03)	0·081	0·75 (0·56–1·02)	0·065
Per-protocol analysis§ (n=509, 107 events)				
≥2 years' placebo	1·0	..	1·0	..
≥2 years' aspirin	0·63 (0·43–0·92)	0·018	0·65 (0·44–0·94)	0·022
Cumulative aspirin dose¶ (n=861, 163 events)				
Units of 100 aspirin	0·98 (0·97–1·00)	0·033	0·98 (0·97–1·00)	0·040
All non-Lynch syndrome cancers				
Intention-to-treat analysis (n=861, 78 events)				
Aspirin vs placebo	0·81 (0·52–1·26)	0·34	0·79 (0·49–1·28)	0·34
Per-protocol analysis§ (n=509, 56 events)				
≥2 years' placebo	1·0	..	1·0	..
≥2 years' aspirin	0·81 (0·48–1·37)	0·43	0·71 (0·41–1·22)	0·21
Cumulative aspirin dose¶ (n=861, 78 events)				
Units of 100 aspirin	0·99 (0·97–1·01)	0·43	0·99 (0·96–1·01)	0·32

*Adjusted for age and gender in all participants up to 10 years and up to 20 years in England, Finland, and Wales, randomly assigned to aspirin or placebo. †Adjusted for age at consent and gender. ‡Incidence rate ratio from negative binomial regression adjusted for age at consent and gender. §The threshold for 2 years' intervention was consumption of more than 1400 aspirin tablets; rounded from a 2-year total of 1461 to allow for early scheduling of the exit colonoscopy or occasional missed dosage. ¶Units of 100 aspirin=total number of aspirin taken divided by 100.

Table 2: Cox proportional hazards and negative binomial regression analyses of cancer incidence*

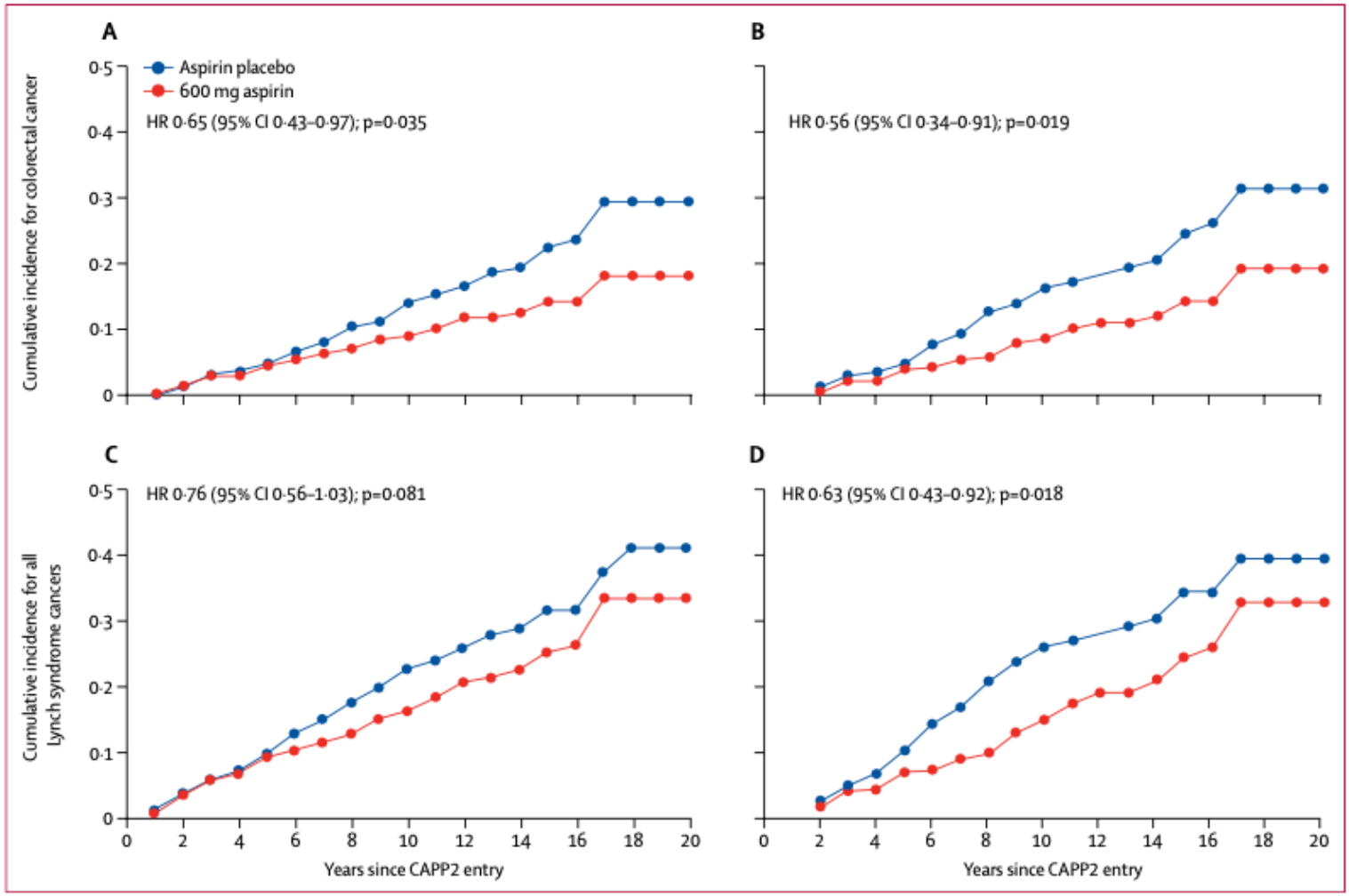

Figure 2: **Time to first colorectal cancer and time to any Lynch syndrome cancer in all CAPP2 study participants followed up for 10 years and for 20 years in England, Finland, and Wales**

Cox proportional hazards (HRs and 95% CIs) comparing those on aspirin *vs* those on placebo and depicted by Kaplan-Meier analysis (n=861). (A) Intention-to-treat analysis (n=427 aspirin, 434 placebo) by randomisation group. (B) Per-protocol analysis of all those achieving 2 years aspirin or placebo (n=259 aspirin; n=250 placebo). (C) Intention-to-treat analysis for any Lynch syndrome cancer. (D) Per-protocol analysis for any Lynch syndrome cancer. See appendix (p 16) for more details.

Research in context

Evidence before this study

There is extensive evidence from case-control studies, epidemiology, polyp prevention studies, and long-term review of historical aspirin cardiovascular prevention trials that regular intake of aspirin (acetyl salicylic acid) and other non-steroidal anti-inflammatory drugs over long periods is associated with reduced incidence of colorectal and other cancers. Two trials explored the protective effects of aspirin with cancer as a primary endpoint; the Women's Health Study showed no effect of alternate day 81 mg aspirin up to study end at 10 years, but a subsequent reduction in colorectal cancer in the second decade. The CAPP2 Study randomised 861 carriers of hereditary cancer, Lynch syndrome, average age 42 years, to 600 mg aspirin or 30 g resistant starch, or both in a factorial design. There was no effect at the end of intervention (average 2·5 years) but there was a significant per-protocol protective effect of the aspirin at an average of 4·6 years follow-up.

Added value of this study

The mechanisms of action of aspirin of relevance to colorectal cancer prevention, including for Lynch syndrome, are unknown, thus there is no insight into the time that the intervention takes to come into full effect or the period over which a time-limited intervention will allow protection. By monitoring people with known intervention and disease status, this study examines the magnitude of the effect and provides some indications as to the magnitude of the long-term effect.

The cancer histories of all participants in CAPP2 were reviewed where possible up to the planned 10-year follow-up and a subset in three countries was followed via national registries for up to 20 years. Aspirin prescription ended in 2007 at the latest. Intention-to-treat Cox proportional hazards analysis showed that aspirin protected against the primary endpoint of colorectal cancer (HR=0·65 [95% CI 0·43–0·97], p=0·035). Negative binomial regression, considering all primary cancer diagnoses in the cancer spectrum of Lynch syndrome found similar evidence of aspirin protection (incidence rate ratio 0·58, 95% CI 0·39–0·87, p=0·0085). For those who took aspirin for the planned minimum 2 years, the effect was similar; HR 0·56, CI 0·34–0·91, p=0·019.

There were half as many endometrial cancers in the aspirin group but, overall, non-colorectal cancer Lynch syndrome cancers were not significantly different in the longer follow-up. In the second decade, there was some evidence of a decline in non-Lynch syndrome cancers that did not reach significance.

Implications of all the available evidence

Two standard aspirins per day for 2 years results in a significant reduction in colorectal cancer incidence in Lynch syndrome carriers, which persists for over a decade but does not become apparent until about 5 years from commencement. During intervention, serious adverse events did not differ significantly from the placebo group in this relatively young group. The ongoing CaPP3 Study is a dose non-inferiority trial which will inform optimal doses for cancer prevention versus adverse events. There is now a strong case for prescribing aspirin to young adult carriers of a germline DNA mismatch repair gene defect.

Retraction—Hydroxychloroquine or chloroquine with or without a macrolide for treatment of COVID-19: a multinational registry analysis

Published Online
June 4, 2020
https://doi.org/10.1016/
S0140-6736(20)31324-6

After publication of our *Lancet* Article,[1] several concerns were raised with respect to the veracity of the data and analyses conducted by Surgisphere Corporation and its founder and our co-author, Sapan Desai, in our publication. We launched an independent third-party peer review of Surgisphere with the consent of Sapan Desai to evaluate the origination of the database elements, to confirm the completeness of the database, and to replicate the analyses presented in the paper.

Our independent peer reviewers informed us that Surgisphere would not transfer the full dataset, client contracts, and the full ISO audit report to their servers for analysis as such transfer would violate client agreements and confidentiality requirements. As such, our reviewers were not able to conduct an independent and private peer review and therefore notified us of their withdrawal from the peer-review process.

We always aspire to perform our research in accordance with the highest ethical and professional guidelines. We can never forget the responsibility we have as researchers to scrupulously ensure that we rely on data sources that adhere to our high standards. Based on this development, we can no longer vouch for the veracity of the primary data sources. Due to this unfortunate development, the authors request that the paper be retracted.

We all entered this collaboration to contribute in good faith and at a time of great need during the COVID-19 pandemic. We deeply apologise to you, the editors, and the journal readership for any embarrassment or inconvenience that this may have caused.

MRM reports personal fees from Abbott, Medtronic, Janssen, Roivant, Triple Gene, Mesoblast, Baim Institute for Clinical Research, Portola, Bayer, NupulseCV, FineHeart, and Leviticus. FR has been paid for time spent as a committee member for clinical trials, advisory boards, other forms of consulting, and lectures or presentations; these payments were made directly to the University of Zurich and no personal payments were received in relation to these trials or other activities since 2018. Before 2018 FR reports grants and personal fees from SJM/Abbott, grants and personal fees from Servier, personal fees from Zoll, personal fees from Astra Zeneca, personal fees from Sanofi, grants and personal fees from Novartis, personal fees from Amgen, personal fees from BMS, personal fees from Pfizer, personal fees from Fresenius, personal fees from Vifor, personal fees from Roche, grants and personal fees from Bayer, personal fees from Cardiorentis, personal fees from Boehringer Ingelheim, other from Heartware, and grants from Mars. ANP declares no competing interests.

*Mandeep R Mehra, Frank Ruschitzka, Amit N Patel
mmehra@bwh.harvard.edu

Brigham and Women's Hospital Heart and Vascular Center and Harvard Medical School, Boston, MA 02115, USA (MRM); University Heart Center, University Hospital Zurich, Zurich, Switzerland (FR); Department of Biomedical Engineering, University of Utah, Salt Lake City, UT, USA (ANP); and HCA Research Institute, Nashville, TN, USA (ANP)

1 Mehra MR, Desai SS, Ruschitzka F, Patel AN. Hydroxychloroquine or chloroquine with or without a macrolide for treatment of COVID-19: a multinational registry analysis. *Lancet* 2020; published online May 22. https://doi.org/10.1016/S0140-6736(20)31180-6.

Atezolizumab, vemurafenib, and cobimetinib as first-line treatment for unresectable advanced *BRAF*^{V600} mutation-positive melanoma (IMspire150): primary analysis of the randomised, double-blind, placebo-controlled, phase 3 trial

Summary

Background IMspire150 aimed to evaluate first-line combination treatment with BRAF plus MEK inhibitors and immune checkpoint therapy in *BRAF*^{V600} mutation-positive advanced or metastatic melanoma.

Methods IMspire150 was a randomised, double-blind, placebo-controlled phase 3 study done at 112 institutes in 20 countries. Patients with unresectable stage IIIc–IV, *BRAF*^{V600} mutation-positive melanoma were randomly assigned 1:1 to 28-day cycles of atezolizumab, vemurafenib, and cobimetinib (atezolizumab group) or atezolizumab placebo, vemurafenib, and cobimetinib (control group). In cycle 1, all patients received vemurafenib and cobimetinib only; atezolizumab placebo was added from cycle 2 onward. Randomisation was stratified by lactate dehydrogenase concentration and geographical region. Blinding for atezolizumab was achieved by means of an identical intravenous placebo, and blinding for vemurafenib was achieved by means of a placebo tablet. The primary outcome was investigator-assessed progression-free survival. This trial (ClinicalTrials.gov, NCT02908672) is ongoing but no longer recruiting patients.

Findings Between Jan 13, 2017, and April 26, 2018, 777 patients were screened and 514 were enrolled and randomly assigned to the atezolizumab group (n=256) or control group (n=258). At a median follow-up of 18·9 months (IQR 10·4–23·8), progression-free survival as assessed by the study investigator was significantly prolonged with atezolizumab versus control (15·1 *vs* 10·6 months; hazard ratio [HR] 0·78; 95% CI 0·63–0·97; p=0·025). Common treatment-related adverse events (>30%) in the atezolizumab and control groups were blood creatinine phosphokinase increased (51·3% *vs* 44·8%), diarrhoea (42·2% *vs* 46·6%), rash (40·9%, both groups), arthralgia (39·1% *vs* 28·1%), pyrexia (38·7% *vs* 26·0%), alanine aminotransferase increased (33·9% *vs* 22·8%), and lipase increased (32·2% *vs* 27·4%); 13% of patients in the atezolizumab group and 16% in the control group stopped all treatment because of adverse events.

Interpretation The addition of atezolizumab to targeted therapy with vemurafenib and cobimetinib was safe and tolerable and significantly increased progression-free survival in patients with *BRAF*^{V600} mutation-positive advanced melanoma.

	Atezolizumab + vemurafenib + cobimetinib (n=256)	Placebo + vemurafenib + cobimetinib (n=258)
Median age, years (range)	54·0 (44·8–64·0)	53·5 (43·0–63·8)
Age		
<65 years	195 (76%)	199 (77%)
≥65 years	61 (24%)	59 (23%)
Female sex	106 (41%)	109 (42%)
Male sex	150 (59%)	149 (58%)
White race	243 (95%)	246 (95%)
Geographical region		
North America	13 (5%)	14 (5%)
Europe	203 (79%)	203 (79%)
Australia, New Zealand, or other	40 (16%)	41 (16%)
Eastern Cooperative Oncology Group performance status		
0	195 (76%)	198 (77%)
1	61 (24%)	56 (22%)
Unknown	0	4 (2%)
Disease stage		
IIIC	14 (5%)	16 (6%)
IV	242 (95%)	240 (93%)
Unknown	0	2 (1%)
Elevated lactate dehydrogenase concentration (>upper limit of normal)	84 (33%)	85 (33%)
Stage, distant metastases at study entry		
M0	13 (5%)	16 (6%)
M1A	41 (16%)	35 (14%)
M1B	56 (22%)	42 (16%)
M1C	145 (57%)	163 (63%)
Unknown	1 (<1%)	2 (1%)
Histological subtype		
Superficial spreading	85 (33%)	83 (32%)
Nodular	84 (33%)	80 (31%)
Other	86 (34%)	93 (36%)
Unknown	1 (<1%)	2 (1%)

(Table 1 continues in next column)

(Continued from previous column)

	Atezolizumab + vemurafenib + cobimetinib (n=256)	Placebo + vemurafenib + cobimetinib (n=258)
Number of lesions		
1–3	113 (44%)	111 (43%)
>3	143 (56%)	144 (56%)
Unknown	0	3 (1%)
Sum of longest diameters		
<44 mm	109 (43%)	103 (40%)
≥44 mm	147 (57%)	155 (60%)
Previously treated brain metastases	5 (2%)	8 (3%)
BRAF mutation genotype*		
V600E	197 (77%)	182 (71%)
V600K	27 (11%)	29 (11%)
V600D/R	4 (2%)	3 (1%)
Missing	28 (11%)	44 (17%)
Baseline PD-L1 status†		
Immune cells 1/2/3	160 (63%)	158 (61%)
Immune cells 0	85 (33%)	86 (33%)
Unknown	11 (4%)	14 (5%)
Previous adjuvant therapy	41 (16%)	30 (12%)

Data are n (%) or median range. Due to rounding, percentages may not add up to 100. PD-L1=programmed cell death ligand 1. *All patients are reported *BRAF*^{V600} mutation-positive status in melanoma tumour tissue by a locally approved test. *BRAF* mutation genotype is reported missing when sample was not centrally analysed owing to insufficient tumour sample. †PD-L1 positivity based on the proportion of cells per tumour area occupied by PD-L1–expressing tumour-infiltrating immune cells of any intensity (% immune cells). For percentage of immune cells, immunohistochemistry staining was scored as 0 (<1%), 1 (≥1%–<5%), 2 (≥5%–<10%), or 3 (if ≥10% of cells per area were PD-L1 positive).

Table 1: **Baseline characteristics**

Results

Between Jan 13, 2017, and April 26, 2018, 514 patients were enrolled and randomly assigned to the atezolizumab group (n=256) or the control group (n=258) and comprised the intention-to-treat analysis population. Baseline demographic and disease characteristics can be seen in table 1.

A

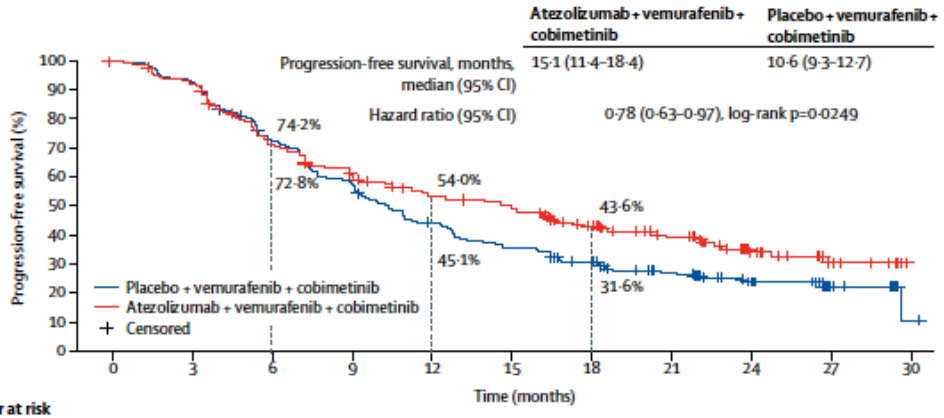

Number at risk											
Placebo + vemurafenib + cobimetinib	258	230	179	143	107	86	71	51	27	11	1
Atezolizumab + vemurafenib + cobimetinib	256	229	174	149	123	114	90	66	34	11	

B

	Atezolizumab + vemurafenib + cobimetinib (n=256)		Placebo + vemurafenib + cobimetinib (n=258)		Hazard ratio	95% Wald CI
	n	Events	n	Events		
Randomised treatment group	**256**	**148**	**258**	**179**	**0·77**	**(0·62–0·96)**
Age group, years						
<65	195	114	199	134	0·82	(0·64–1·06)
≥65	61	34	59	45	0·63	(0·40–0·99)
Race						
White	243	138	246	170	0·76	(0·60–0·95)
Non-white	13	10	12	9	1·07	(0·43–2·65)
Sex						
Male	150	81	149	101	0·75	(0·56–1·01)
Female	106	67	109	78	0·81	(0·58–1·13)
Geographical region (IWRS)						
North America	13	7	14	10	0·85	(0·32–2·27)
Europe	203	124	203	142	0·79	(0·62–1·00)
Australia, New Zealand, or other	40	17	41	27	0·69	(0·37–1·27)
Serum lactate dehydrogenase at baseline (IWRS)						
≤upper limit	172	88	173	106	0·76	(0·57–1·01)
>upper limit	84	60	85	73	0·81	(0·58–1·14)
Eastern Cooperative Oncology group performance status						
0	195	103	198	136	0·68	(0·53–0·88)
1	61	45	56	42	1·08	(0·71–1·65)
Melanoma staging						
IIIC	14	4	16	11	0·37	(0·12–1·17)
IV	242	144	240	168	0·80	(0·64–1·00)
Previous adjuvant therapy						
Yes	41	20	30	22	0·57	(0·31–1·04)
No	215	128	228	157	0·81	(0·64–1·03)
PD-L1 expression						
IC 1/2/3	160	89	158	108	0·80	(0·60–1·06)
IC 0	85	53	86	62	0·76	(0·53–1·10)
Organ involvement						
<3	205	109	197	131	0·74	(0·58–0·96)
≥3	51	39	57	48	0·94	(0·61–1·44)
Sum of longer diameter						
<44 mm	109	55	99	65	0·70	(0·49–1·01)
≥44 mm	147	93	155	114	0·83	(0·63–1·10)
Histological subtype (initial diagnosis)						
Superficial spreading	85	54	83	58	0·86	(0·59–1·24)
Nodular	84	49	80	56	0·72	(0·49–1·06)
Other	86	44	93	65	0·72	(0·49–1·07)
Distant metastasis, stage (study entry)						
M0	13	4	16	11	0·42	(0·13–1·33)
M1A	41	18	35	20	0·72	(0·38–1·37)
M1B	56	29	42	27	0·80	(0·47–1·36)
M1C	145	97	163	121	0·86	(0·66–1·13)

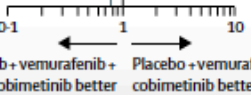

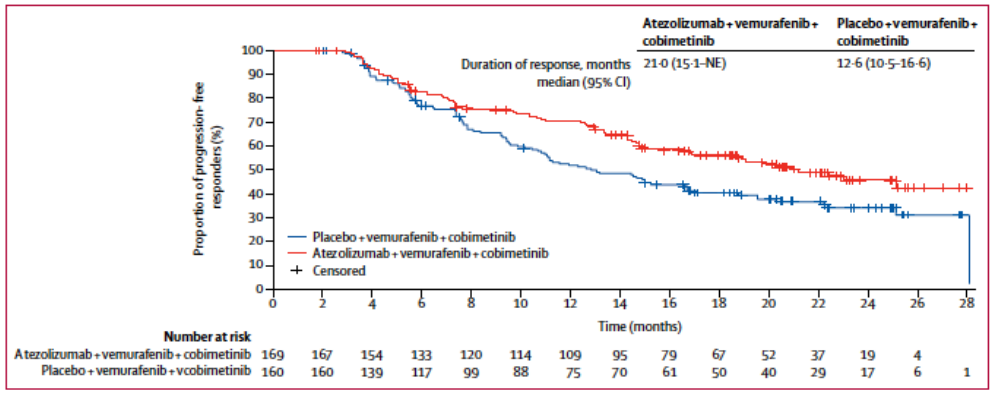

Figure 3: Kaplan-Meier estimate of duration of response in the intention-to-treat population
NE=not estimable.

	Atezolizumab + vemurafenib + cobimetinib (n=230)		Placebo + vemurafenib + cobimetinib (n=281)	
	Any grade	Grade 3–4	Any grade	Grade 3–4
Any treatment-related adverse event	228 (99%)	182 (79%)	279 (99%)	205 (73%)
Treatment-related adverse events with a prevalence ≥10%*				
Blood creatine phosphokinase increased†	118 (51%)	46 (20%)	126 (45%)	42 (15%)
Rash	94 (41%)	20 (9%)	115 (41%)	25 (9%)
Diarrhoea	97 (42%)	4 (2%)	131 (47%)	9 (3%)
Arthralgia	90 (39%)	7 (3%)	79 (28%)	6 (2%)
Pyrexia	89 (39%)	3 (1%)	73 (26%)	3 (1%)
Alanine aminotransferase aspartate increased†	78 (34%)	30 (13%)	64 (23%)	25 (9%)
Lipase increased†	74 (32%)	47 (20%)	77 (27%)	58 (21%)
Aminotransferase increased†	69 (30%)	19 (8%)	57 (20%)	12 (4%)
Fatigue	62 (27%)	3 (1%)	74 (26%)	1 (<1%)
Nausea	54 (23%)	1 (<1%)	74 (26%)	7 (2%)
Pruritus	49 (21%)	2 (1%)	45 (16%)	1 (<1%)
Myalgia	48 (21%)	2 (1%)	35 (12%)	1 (<1%)
Photosensitivity reaction	48 (21%)	2 (1%)	70 (25%)	9 (3%)
Maculopapular rash	47 (20%)	29 (13%)	53 (19%)	27 (10%)
Amylase increased	46 (20%)	23 (10%)	45 (16%)	19 (7%)
Hyperthyroidism	39 (17%)	2 (1%)	21 (8%)	0
Hypothyroidism	38 (17%)	0	17 (6%)	0
Asthenia	37 (16%)	4 (2%)	39 (14%)	2 (1%)
Blood creatinine increased	36 (16%)	0	33 (12%)	1 (<1%)
Chorioretinopathy	34 (15%)	0	37 (13%)	1 (<1%)
Blood alkaline phosphatase increased	33 (14%)	7 (3%)	38 (14%)	8 (3%)
Dermatitis acneiform	33 (14%)	5 (2%)	42 (15%)	5 (2%)
Vomiting	29 (13%)	2 (1%)	41 (15%)	5 (2%)
Anaemia	26 (11%)	3 (1%)	24 (9%)	7 (3%)
Erythema	26 (11%)	0	35 (12%)	0
Peripheral oedema	26 (11%)	0	17 (6%)	0
Sunburn	25 (11%)	0	26 (9%)	1 (<1%)
Decreased appetite	24 (10%)	0	34 (12%)	2 (1%)
Blood bilirubin increased	23 (10%)	2 (1%)	18 (6)	1 (<1%)
Dry skin	23 (10%)	0	24 (9%)	0
Pneumonitis	23 (10%)	2 (1%)	13 (5%)	0

*Listed adverse events were reported at a frequency of ≥10%, along with corresponding frequencies for grade 3–4 events. †Preferred terms for which grade 4 events were reported in either treatment group.

Table 2: **Prevalence of treatment-related adverse events**

Research in context

Evidence before this study

At the time of the drafting of these results, the approved systemic options for patients with advanced melanoma were immunotherapy (all patients) or BRAF and MEK inhibitors for the subset of patients with *BRAF* mutations in their tumours. Although immunotherapy provides durable responses, a substantial proportion of patients with melanoma have a poor response to immunotherapy; conversely, although most patients respond to MAPK pathway inhibitors, responses are often short-lived. It is clinically desirable to combine the higher response rates observed with targeted therapy with long-term clinical benefit associated with immune modulation, without compromising patient safety. On the basis of emerging preclinical and clinical evidence for potential synergy between immune checkpoint inhibition and BRAF and MEK inhibitors, IMspire150 explored whether a combination of atezolizumab, vemurafenib, and cobimetinib would prolong progression-free survival in patients with *BRAF*-mutation-positive advanced melanoma versus vemurafenib and cobimetinib. We searched PubMed for any clinical reports published until Feb 20, 2020, that explored similar systemic options. We used the search string "melanoma AND ((BRAF OR MEK inhibitor) AND (immune checkpoint inhibitor))" restricted to articles reporting on a clinical trial. We identified two previous publications reporting data from early phase clinical reports (KEYNOTE 022 and GP28384/NCT01656642) investigating this combination in melanoma, but no controlled phase 3 clinical studies.

Added value of this study

IMspire150 is the first phase 3 study to evaluate an immune checkpoint inhibitor combined with BRAF plus MEK inhibitors in patients with advanced *BRAF*^{V600} mutation-positive melanoma. The IMspire150 study met its primary progression-free survival endpoint and provided high-level evidence to show that combined inhibition with vemurafenib, cobimetinib, and atezolizumab prolongs progression-free survival in previously untreated patients with *BRAF* mutation-positive advanced melanoma. Reassuringly, the safety profile and treatment discontinuation rates with this combination were similar to those of the control group of vemurafenib and cobimetinib, which is an approved treatment option for patients with *BRAF*-mutation-positive advanced melanoma.

Implications of all the available evidence

The analysis reported here shows that atezolizumab combined with vemurafenib and cobimetinib is a safe and efficacious treatment option for patients with *BRAF* mutation-positive advanced melanoma. Survival data from this and other ongoing studies on treatment sequencing will inform the optimal treatment paradigm in this patient population.

Safety, tolerability, and immunogenicity of a recombinant adenovirus type-5 vectored COVID-19 vaccine: a dose-escalation, open-label, non-randomised, first-in-human trial

Summary

Background A vaccine to protect against COVID-19 is urgently needed. We aimed to assess the safety, tolerability, and immunogenicity of a recombinant adenovirus type-5 (Ad5) vectored COVID-19 vaccine expressing the spike glycoprotein of a severe acute respiratory syndrome coronavirus 2 (SARS-CoV-2) strain.

Methods We did a dose-escalation, single-centre, open-label, non-randomised, phase 1 trial of an Ad5 vectored COVID-19 vaccine in Wuhan, China. Healthy adults aged between 18 and 60 years were sequentially enrolled and allocated to one of three dose groups (5×10^{10}, 1×10^{11}, and $1\cdot5\times10^{11}$ viral particles) to receive an intramuscular injection of vaccine. The primary outcome was adverse events in the 7 days post-vaccination. Safety was assessed over 28 days post-vaccination. Specific antibodies were measured with ELISA, and the neutralising antibody responses induced by vaccination were detected with SARS-CoV-2 virus neutralisation and pseudovirus neutralisation tests. T-cell responses were assessed by enzyme-linked immunospot and flow-cytometry assays. This study is registered with ClinicalTrials.gov, NCT04313127.

Findings Between March 16 and March 27, 2020, we screened 195 individuals for eligibility. Of them, 108 participants (51% male, 49% female; mean age 36·3 years) were recruited and received the low dose (n=36), middle dose (n=36), or high dose (n=36) of the vaccine. All enrolled participants were included in the analysis. At least one adverse reaction within the first 7 days after the vaccination was reported in 30 (83%) participants in the low dose group, 30 (83%) participants in the middle dose group, and 27 (75%) participants in the high dose group. The most common injection site adverse reaction was pain, which was reported in 58 (54%) vaccine recipients, and the most commonly reported systematic adverse reactions were fever (50 [46%]), fatigue (47 [44%]), headache (42 [39%]), and muscle pain (18 [17%]. Most adverse reactions that were reported in all dose groups were mild or moderate in severity. No serious adverse event was noted within 28 days post-vaccination. ELISA antibodies and neutralising antibodies increased significantly at day 14, and peaked 28 days post-vaccination. Specific T-cell response peaked at day 14 post-vaccination.

Interpretation The Ad5 vectored COVID-19 vaccine is tolerable and immunogenic at 28 days post-vaccination. Humoral responses against SARS-CoV-2 peaked at day 28 post-vaccination in healthy adults, and rapid specific T-cell responses were noted from day 14 post-vaccination. Our findings suggest that the Ad5 vectored COVID-19 vaccine warrants further investigation.

	Low dose group (n=36)	Middle dose group (n=36)	High dose group (n=36)
Age, years			
18–29	9 (25%)	12 (33%)	10 (28%)
30–39	13 (36%)	14 (39%)	15 (42%)
40–49	8 (22%)	3 (8%)	7 (19%)
50–60	6 (17%)	7 (19%)	4 (11%)
Mean age, years	37·2 (10·7)	36·3 (11·5)	35·5 (10·1)
Sex			
Male	18 (50%)	19 (53%)	18 (50%)
Female	18 (50%)	17 (47%)	18 (50%)
Mean body-mass index, kg/m²	23·3 (2·7)	23·9 (2·7)	24·1 (3·1)
Underlying diseases*			
Yes	1 (3%)	2 (6%)	4 (11%)
No	35 (97%)	34 (94%)	32 (89%)
Pre-existing adenovirus type-5 neutralising antibody			
Mean GMT	168·9 (13·9)	149·5 (10·5)	115·0 (13·4)
≤200, titre	16 (44%)	17 (47%)	20 (56%)
>200, titre	20 (56%)	19 (53%)	16 (44%)

Data are n (%) or mean (SD). GMT=geometric mean titre. *Seven participants had hypertension, chronic bronchitis, gout, or were a carrier of hepatitis B virus.

Table 1: **Baseline characteristics**

	Low dose group (n=36)	Middle dose group (n=36)	High dose group (n=36)	Total (N=108)
All adverse reactions within 0–7 days				
Any	30 (83%)	30 (83%)	27 (75%)	87 (81%)
Grade 3	2 (6%)	2 (6%)	6 (17%)	10 (9%)
Injection site adverse reactions within 0–7 days				
Pain	17 (47%)	20 (56%)	21 (58%)	58 (54%)
Induration	2 (6%)	1 (3%)	1 (3%)	4 (4%)
Redness	2 (6%)	1 (3%)	1 (3%)	4 (4%)
Swelling	4 (11%)	4 (11%)	0	8 (7%)
Itch	2 (6%)	3 (8%)	0	5 (5%)
Muscular weakness	0	0	1 (3%)	1 (1%)
Systemic adverse reactions within 0–7 days				
Fever	15 (42%)	15 (42%)	20 (56%)	50 (46%)
Grade 3 fever	2 (6%)	2 (6%)	5 (14%)	9 (8%)
Headache	14 (39%)	11 (31%)	17 (47%)	42 (39%)
Fatigue	17 (47%)	14 (39%)	16 (44%)	47 (44%)
Grade 3 fatigue	0	0	2 (6%)	2 (2%)
Vomiting	1 (3%)	0	1 (3%)	2 (2%)
Diarrhoea	3 (8%)	4 (11%)	5 (14%)	12 (11%)
Muscle pain	7 (19%)	3 (8%)	8 (22%)	18 (17%)
Grade 3 muscle pain	0	0	1 (3%)	1 (1%)
Joint pain	2 (6%)	2 (6%)	5 (14%)	9 (8%)
Grade 3 joint pain	0	0	1 (3%)	1 (1%)
Throat pain	1 (3%)	3 (8%)	4 (11%)	8 (7%)
Cough	1 (3%)	2 (6%)	3 (8%)	6 (6%)
Nausea	2 (6%)	1 (3%)	3 (8%)	6 (6%)
Functional GI disorder	1 (3%)	0	0	1 (1%)
Dyspnoea	0	0	2 (6%)	2 (2%)
Grade 3 dyspnoea	0	0	1 (3%)	1 (1%)
Appetite impaired	6 (17%)	5 (14%)	6 (17%)	17 (16%)
Dizziness	1 (3%)	0	1 (3%)	2 (2%)
Mucosal abnormality	0	0	1 (3%)	1 (1%)
Pruritus	1 (3%)	1 (3%)	1 (3%)	3 (3%)
Overall adverse events within 0–28 days				
Any	31 (86%)	30 (83%)	27 (75%)	88 (81%)
Grade 3	2 (6%)	2 (6%)	6 (17%)	10 (9%)

Data are n (%). Any refers to all the participants with any grade adverse reactions or events. Adverse reactions and events were graded according to the scale issued by the China State Food and Drug Administration. Grade 3=severe (ie, prevented activity). GI=gastrointestinal.

Table 2: **Adverse reactions within 7 days and overall adverse events within 28 days after vaccination**

	Day 14				Day 28			
	Low dose group (n=36)	Middle dose group (n=36)	High dose group (n=36)	p value	Low dose group (n=36)	Middle dose group (n=36)	High dose group (n=36)	p value
ELISA antibodies to the receptor binding domain								
GMT	76·5 (44·3–132·0)	91·2 (55·9–148·7)	132·6 (80·7–218·0)	0·29	615·8 (405·4–935·5)	806·0 (528·2–1229·9)	1445·8 (935·5–2234·5)	0·016
≥4-fold increase	16 (44%)	18 (50%)	22 (61%)	0·35	35 (97%)	34 (94%)	36 (100%)	0·77
Neutralising antibodies to live SARS-CoV-2								
GMT	8·2 (5·8–11·5)	9·6 (6·6–14·1)	12·7 (8·5–19·0)	0·24	14·5 (9·6–21·8)	16·2 (10·4–25·2)	34·0 (22·6–50·1)	0·0082
≥4-fold increase	10 (28%)	11 (31%)	15 (42%)	0·42	18 (50%)	18 (50%)	27 (75%)	0·046

Data are mean (95% CI) or n (%). The p values are the result of comparison across the three dose groups. If the difference was significant across the three groups, the differences between groups were estimated with 95% CIs. SARS-CoV-2=severe acute respiratory syndrome coronavirus 2. GMT=geometric mean titre.

Table 3: **Specific antibody responses to the receptor binding domain, and neutralising antibodies to live SARS-CoV-2**

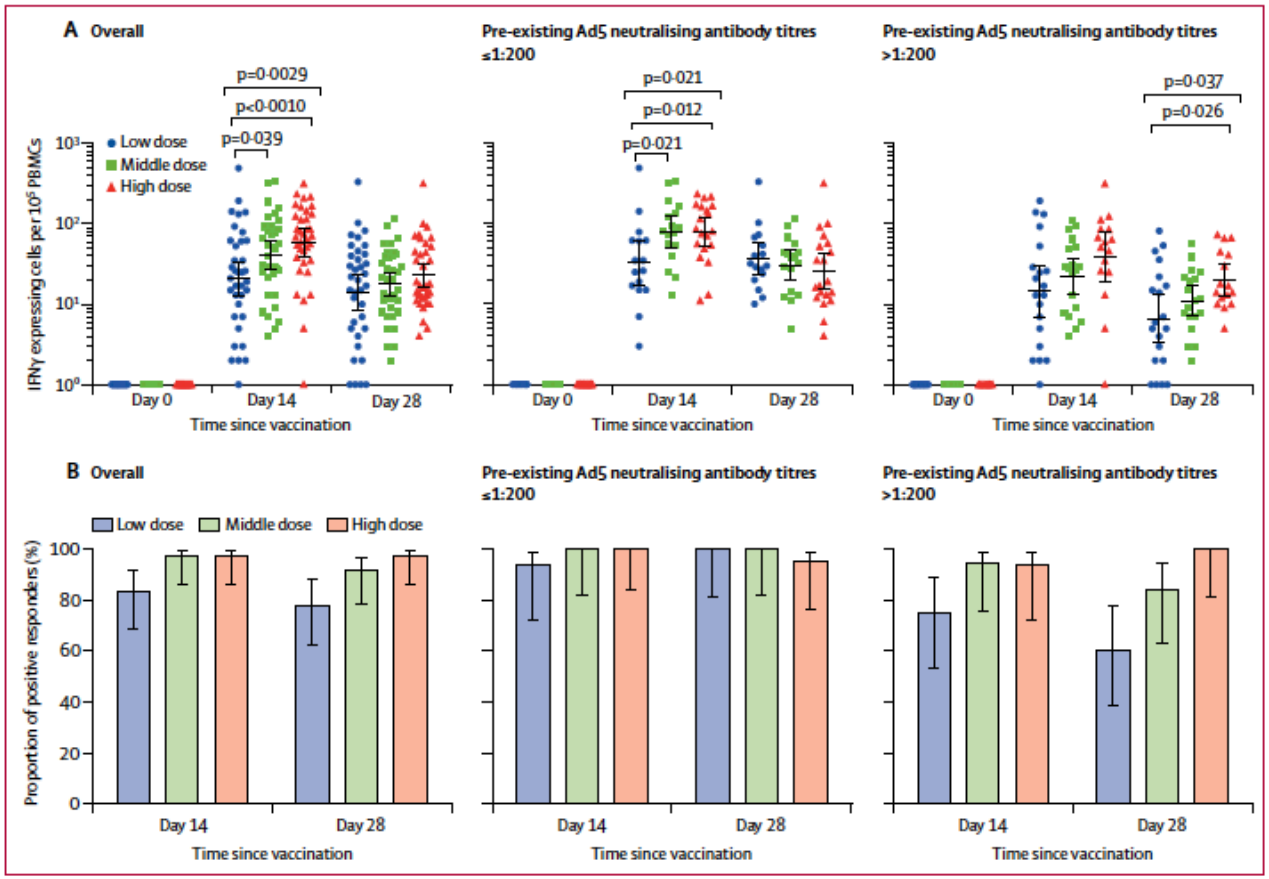

Figure 1: **Specific T-cell response measured by ELISpot**

(A) The number of specific T cells with secretion of IFNγ at days 0, 14, and 28 in all participants, and stratified by pre-existing Ad5 neutralising antibody titres. (B) The proportion of positive ELISpot responders at days 14 and 28 post-vaccination in all participants, and stratified by pre-existing Ad5 neutralising antibody titres. IFN=interferon. PBMCs=peripheral blood mononuclear cells. Ad5=adenovirus type-5. ELISpot=enzyme-linked immunospot.

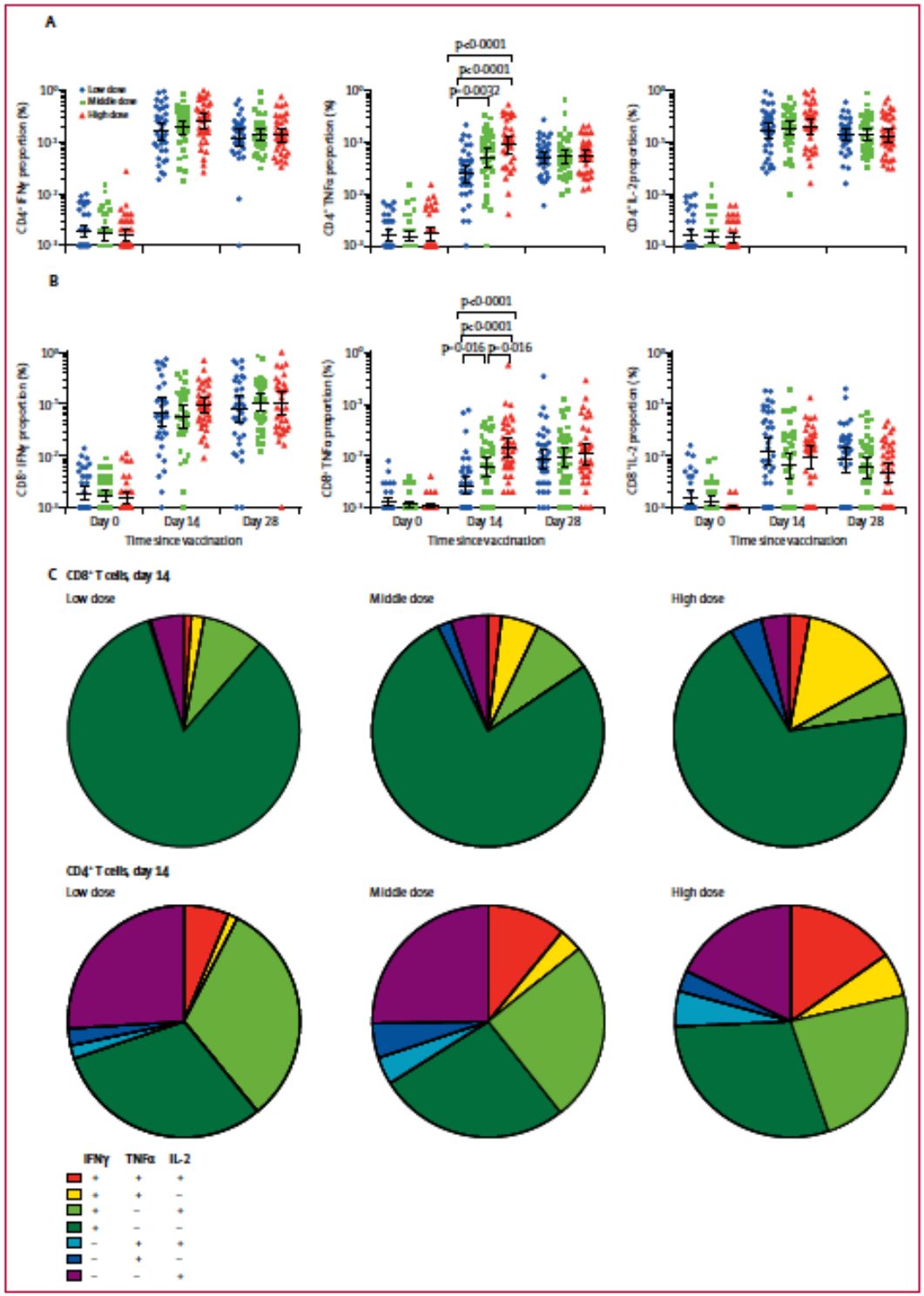

Figure 2: Flow cytometry with intracellular cytokine staining before and after vaccination

(A) Percentage of cells secreting IFNγ, TNFα, and IL-2 from CD4+ T cells. (B) Percentage of cells secreting IFNγ, TNFα, and IL-2 from CD8+ T cells. (C) The proportion of CD4+ T cells and CD8+ T cells producing any combination of IFNγ, TNFα, and IL-2. The analyses are for 108 participants, with 36 in each dose group.
IFN=interferon. TNF=tumour necrosis factor. IL=interleukin.

Research in context

Evidence before this study

We searched PubMed on May 8, 2020, for clinical trial reports with the terms "COVID-19" or "SARS-CoV-2", "vaccine", and "clinical trial" and no date or language restrictions; no other data from a human clinical trial of COVID-19 vaccine have been reported thus far, to our knowledge. We also searched the ClinicalTrials.gov registry for unpublished trials of COVID-19 vaccines, up to May 6, 2020. In addition to the adenovirus type-5 (Ad5) vectored COVID-19 vaccine reported here, seven candidate COVID-19 vaccines are in ongoing clinical trials, including Moderna's mRNA COVID-19 vaccine, Inovio Pharmaceuticals' DNA vaccine, Sinovac, Wuhan and Beijing Institute of Biological Products' inactive COVID-19 vaccines, University of Oxford's chimpanzee adenovirus-vectored vaccine, and BioNTech's mRNA COVID-19 vaccine.

Added value of this study

This first-in-human trial showed that the Ad5 vectored COVID-19 vaccine was tolerable and immunogenic in healthy adults. One dose of the vaccine at all dose concentrations (5×10^{10}, 1×10^{11}, and $1{\cdot}5 \times 10^{11}$ viral particles) tested induced both specific antibody and T-cell responses in most participants. Rapid specific T-cell responses were noted at day 14 and specific humoral responses against severe acute respiratory syndrome coronavirus 2 peaked at day 28 post-vaccination. Although we found that the high dose vaccine tended to be more immunogenic than the middle dose and low dose vaccines, it was also associated with a higher reactogenicity. Severe fever, fatigue, dyspnoea, muscle pain, and joint pain were reported in some of the recipients in the high dose group.

Implications of all the available evidence

Many vaccine candidates are in rapid development, including recombinant-protein based vaccines, replicating or non-replicating viral vector-based vaccines, DNA vaccines, and mRNA vaccines (which mostly have focused on the spike glycoprotein or receptor binding domain), live attenuated vaccines, and inactivated virus vaccines. All of these vaccine platforms have advantages and disadvantages, and it is too soon to predict which will be more successful. Our study suggests that there is potential for further investigation of the Ad5 vectored COVID-19 vaccine for prevention of COVID-19.

Meningococcal disease and sexual transmission: urogenital and anorectal infections and invasive disease due to *Neisseria meningitidis*

Shamez N Ladhani, Jay Lucidarme, Sydel R Parikh, Helen Campbell, Ray Borrow, Mary E Ramsay

Neisseria meningitidis **is an obligate human commensal bacterium that frequently colonises the upper respiratory tract. Person-to-person transmission occurs via direct contact or through dispersion of respiratory droplets from a carrier of the bacteria, and can lead to invasive meningococcal disease. Rare sporadic cases of meningococcal urogenital and anorectal infections, including urethritis, proctitis, and cervicitis, have been reported, typically following orogenital contact with an oropharyngeal meningococcal carrier. The resulting infections were clinically indistinguishable from infections caused by *Neisseria gonorrhoeae*. Over the past two decades, there have also been multiple outbreaks across North America and Europe of invasive meningococcal disease among men who have sex with men (MSM). The responsible meningococci belong to a highly virulent and predominantly serogroup C lineage, including strains that are able to express nitrite reductase and grow in anaerobic environments, such as the urogenital and anorectal tracts. More recently, a distinct clade within this lineage has expanded to cause urethritis predominantly among men who have sex with women. Evolutionary events giving rise to this clade included the loss of the ability to express a capsule, and acquisition of several gonococcal alleles, including one allele encoding a highly efficient gonococcal nitrite reductase. Members of the clade continue to acquire gonococcal alleles, including one allele associated with decreased antibiotic susceptibility. This evolution has implications for the clinical and public health management of those who are infected and their close contacts, in terms of both antibiotic treatment, and prevention through vaccination.**

	Location	Patients and characteristics	Diagnosis and outcomes
Tillet et al (1935)[3]	Baltimore, MD, USA	26 cases of acute meningococcal meningitis, including two young adults with acute epididymitis	Epididymitis resolved spontaneously within 4–5 days
Appelbaum (1937)[4]	New York City, NY, USA	15 cases of chronic meningococcal sepsis in patients aged 3–52 years, including two cases complicated by epididymitis	Epididymitis resolved spontaneously within 6–7 days
Kattwinkel (1941)[5]	MA, USA	A 22-year-old woman with a history of leucorrhoea for several years developed fever with a maculopapular rash, which was haemorrhagic in spots on the extremities	Blood cultures showed Gram-negative intracellular diplococci and she was diagnosed with gonorrhoea, although vaginal smears were negative; her condition initially improved but she developed a recurrence and was diagnosed with chronic meningococcal bacteraemia
Carpenter et al (1942)[6]	Baltimore, MD, USA	Six men with urethritis and one woman with cervicitis, none of whom had features of invasive meningococcal disease	Primary genital tract infection was initially thought to be due to *Neisseria gonorrhoeae*; MenA was isolated from the genital tract of all 7 patients
Laird (1944)[7]	Royal Army Medical Corps, UK	A 25-year-old man presented with bilateral epididymitis and no evidence of urethritis	Epididymitis gradually improved, but a few weeks later, he re-presented with a recurrence of epididymitis, malaise, and limb and joint pains; he was diagnosed with chronic meningococcal sepsis which persisted for a month
Keys et al (1971)[8]	Los Angeles, CA, USA	Case 1: a 23-year-old woman presented with fever, myalgia, painful joints, and chills; case 2: a 21-year-old woman presented with fever, rash, and arthralgia	Case 1: Gram-negative diplococci were isolated from the blood, joint, and endocervix, and subsequently confirmed as *Neisseria meningitidis*; case 2: Gram-negative diplococci were isolated from the endocervical culture and confirmed as *N meningitidis*
Volk et al (1973)[9]	Atlanta, GA, USA	Case 1: a 20-year-old man had sexual intercourse once 3 weeks previously with case 2, and was diagnosed with gonorrhoea; case 2: a 20-year-old woman was examined 7 days later with case 3 who was her regular partner; case 3: a 20-year-old asymptomatic man who was the regular partner of case 2 also attended the clinic	Cases 1 and 2 were confirmed as having gonorrhoea, while a culture of the urethral swab from case 3 identified MenB; case 3 was recalled to clinic and, although he denied symptoms, a urethral exudate was expressed and microscopy showed polymorphonuclear leucocytes and Gram-negative diplococci. Meningococcus from case 3 produced bacteriocin which showed marked growth inhibition of the gonococcus from case 2; the authors postulated that the meningococcal bacteriocin may have protected case 3 from developing gonorrhoea even after several weeks of unprotected sexual intercourse with case 2 who was known to be infectious
Beck et al (1974)[10]	London, UK	Case 1: a 30-year-old man had orogenital intercourse with his female partner two days prior to developing urethral discharge and dysuria; case 2: an adult woman presented with yellow discharge and frequency of micturition; clinical examination revealed mild cervicitis	Case 1: microscopy revealed intracellular Gram-negative diplococci which was subsequently identified as MenB; throat swab from his partner produced a scanty growth of an indistinguishable MenB strain; case 2: cultures from the urethra and cervix grew *N meningitidis*, subsequently confirmed as MenY
Givan et al (1974)[11]	Toronto, ON, Canada	Case 1: a 17-year-old woman presented with purulent vaginal discharge form the urethra and cervix; on examination, the urethral orifice, vulva, and cervix were reddened; case 2: a 21-year-old man presented with dysuria and urethral discharge 2 days after sexual contact with a female partner	Case 1: cultures of a cervical swab subsequently grew *N meningitidis*; case 2: throat and urethral cultures subsequently grew MenY
Willmott (1976)[12]	London, UK	A 19-year-old woman, contact of a man with presumptive gonococcal urethritis, complained of vaginal discharge and lower abdominal pain	Cervical smear showed extracellular Gram-negative diplococci and a presumptive diagnosis of gonococcal salpingitis was made; the cervical and throat swabs subsequently grew *N meningitidis*; she had two male sexual partners who had previously attended the same clinic with urethral discharge and both had been diagnosed and treated for gonorrhoea based on Gram staining and a positive culture for *Neisseria* sp
Givan et al (1977)[13]	Toronto, ON, Canada	Case 1: a 21-year-old woman with cervical discharge and pelvic pain was hospitalised for pelvic inflammatory disease 10 days after a copper intrauterine device was inserted; case 2: three young adult men presented with urethritis; case 3: two asymptomatic patients, a 22-year-old woman and a 28-year-old man, attending the same clinic, had cervical and urethral swabs taken	Case 1: the intrauterine coil was removed and *N meningitidis* isolated from the cervix; case 2: culture of the urethral discharge confirmed *N meningitidis* in all three patients; case 3: the swabs confirmed the presence of *N meningitidis* in both patients
Miller et al (1979)[14]	IL, USA	A 26-year-old man presented with 3 days of urethral discharge and no other symptoms	Presumptive diagnosis of gonorrhoea made after Gram-negative diplococci noted on microscopy; subsequent cultures confirmed MenX
William et al (1979)[15]	New York City, NY, USA	A 19-year-old man presented with a 4-week history of intermittent urethral discharge followed by epididymitis	Gram-negative diplococci were seen on microscopy; cultures were subsequently confirmed as MenZ9E; a contact of the case had sporadic pain during vaginal intercourse and intermittent purulent vaginal discharge; endocervical and anal cultures grew the same meningococcal strain as the case
Gregory et al (1979)[16]	Washington, DC, USA	A 27-year-old man complained of a burning sensation in the anterior urethral area but no discharge, having previously been treated for gonorrhoea	MenK was isolated from the urethral culture
Karolus et al (1980)[17]	CT, USA	A 29-year-old man presented with urethral discharge following oral sex with a female partner	He was initially diagnosed with gonorrhoea; the urethral isolate was subsequently confirmed as MenZ; his female partner attended the clinic for review and also grew MenZ from the pharynx but not the cervix
Talbot et al (1981)[18]	Sheffield, UK	A 26-year-old man presented with urethral discharge and dysuria following intercourse 12 days previously	A presumptive diagnosis of gonococcal urethritis was made after microscopy revealed intracellular Gram-negative diplococci; subsequently identified as *N meningitidis*; *N meningitidis* with identical antibiotic sensitivity was isolated from the pharynx and cervical exudate, respectively, of two asymptomatic female sexual contacts

(Table 1 continues on next page)

	Location	Patients and characteristics	Diagnosis and outcomes
(Continued from previous page)			
Lefevre et al (1985)[18]	Toulouse, France	A 28-year-old man presented with urethral discharge after sexual intercourse during the previous week	A presumptive diagnosis of gonococcal urethritis was made after Gram staining of the discharge; subsequently identified as MenB; when reviewed 10 days later, the discharge had ceased, but 5 days later he developed a new purulent discharge which was confirmed by culture as *Chlamydia trachomatis*
Hartmann et al (1988)[19]	Wurzburg, Germany	A 28-year-old man presented with urethritis 5 days after intercourse that included fellatio	A presumptive diagnosis of gonorrhoea was made; the urethral isolate was subsequently confirmed as MenB
Wilson et al (1989)[20]	London, UK	An 18-year-old man presented with a 5-day history of dysuria and urethral discharge following sexual intercourse 2 weeks previously	Gram negative diplococci were seen on microscopy and he was initially treated for gonorrhoea; urethral discharge culture subsequently identified MenA
Shanmugaratnam et al (1989)[21]	Newcastle, UK	A 25-year-old man presented with urethral discharge after receiving fellatio	The patient's urethral specimen and his girlfriend's throat specimen both grew *N meningitidis*; non-groupable and non-typeable but with identical antibiotic susceptibilities
Hay et al (1989)[22]	London, UK	A 16-year-old man presented with a 1-day history of pain in the left iliac fossa radiating to the groin, painful purulent urethral discharge, and tender swelling next to the left testicle, after receiving fellatio	Gram-negative diplococci were present on the urethral smear and subsequently confirmed as MenA
Phillips et al (1989)[23]	Sydney, NSW, Australia	A 19-year-old man presented with urethritis after sexual contact with a female approximately 1 week previously	A maltose-negative *N meningitidis* strain was identified from the urethral culture
Thangkhiew et al (1990)[24]	Rugby, England	Case 1: a 24-year-old man presented with purulent discharge and dysuria; case 2: a 19-year-old woman presented with vaginal discharge; case 3: a 54-year-old woman presented with purulent vaginal discharge; case 4: the 58-year-old male sexual contact of case 3 subsequently developed urethral discharge and testicular pain	Case 1: microscopy of the urethral exudate identified Gram-negative intracellular diplococci; case 2: microscopy of the urethral exudate identified Gram-negative intracellular diplococci and a mixed flora of extracellular organisms; the cervical swab grew *N meningitidis*, *Gardnerella vaginalis* and *Bacteroides sp*; case 3: microscopy identified Gram-negative intracellular diplococci; case 4: microscopy of the urethral exudate identified Gram-negative intracellular diplococci; all the isolates were confirmed as *N meningitidis* and the patients recovered with antibiotic treatment
Faigel (1990)[25]	MA, USA	A 20-year-old man presented with a 5-day history of penile discharge associated with dysuria, but no evidence of epididymitis or prostatitis; the patient denied vaginal or anal intercourse in the 8 weeks preceding the illness but confirmed engaging in receiving fellatio 5 days previously	MenC was confirmed from the discharge; when examined, his partner was healthy with no evidence of infection and her throat swab subsequently grew MenC
Quarto et al (1991)[17]	Bari, Italy	A 35-year-old man developed urethral discharge and dysuria 6 days after receiving fellatio	Microscopy showed intracellular Gram-negative diplococci and he was treated for presumptive gonorrhoea; the isolate was subsequently identified as MenY
Hagman et al (1991)[26]	Orebro, Sweden	Case 1: a 22-year-old man presented with urethral discharge and dysuria after sexual intercourse and receiving fellatio; case 2: a 40-year-old woman presented with vaginal discharge; case 3: a 19-year-old woman presented with lower abdominal pain and cervical discharge after having unprotected intercourse a month earlier	Case 1: treated for presumptive gonorrhoea after a positive Gram stain; the isolate was subsequently confirmed as MenB; throat swab from his female partner grew meningococcus; case 2: culture from a cervical specimen grew MenY, which was also isolated from her male partner's throat swab; case 3: culture of the cervical smear identified MenB
Conde-Glez et al (1991)[27]	Mexico City, Mexico	Five men with acute urethritis and three women with acute cervicitis were reported	All were initially treated presumptively for gonorrhoea; the isolates were subsequently identified as MenB
Kanemitsu et al (2003)[28]	Nagoya, Japan	A 48-year-old man presented with dysuria and urethral discharge one day after receiving fellatio	Gram-negative diplococci seen on microscopy and subsequently identified as *N meningitidis*
Sun et al (2004)[29]	Taipei, Taiwan	A 32-year-old man presented with generalised maculopapular and petechial skin lesions, and polyarthritis after orogenital sexual contact 3 weeks previously; he also developed acute urethritis a week later	Gram-negative diplococci were seen in the joint fluid and blood cultures yielded *N meningitidis*; the authors concluded that the route of transmission was orogenital contact manifesting as acute urethritis and arthritis-dermatitis syndrome, which is more typical of gonorrhoea
Orden et al (2004)[30]	Madrid, Spain	A 36-year-old man presented with a 2-day history of dysuria and urethral discharge, 7 days after intercourse and receiving fellatio	Microscopy of the urethral discharge identified Gram-negative intracellular diplococci and a presumptive diagnosis of gonorrhoea was made; the isolate was subsequently identified as MenC, serotype 2b:P1.5
Urra et al (2005)[31]	Madrid, Spain	A 38-year-old man presented with urethral discharge and dysuria following oral, genital, and anal sex	The urethral swab subsequently grew MenC:2a:P1; the same strain was also isolated from his partner's oropharynx and endocervix
Rodriguez et al (2005)[32]	Caracas, Venezuela	A 27-year-old man presented with a 14-day history of dysuria and urethral discharge which began 7 days after vaginal intercourse and receiving fellatio from multiple female partners	Treated for presumed gonococcal urethritis after microscopy revealed intracellular Gram-negative diplococci; the isolate was subsequently identified as MenC, which was resistant to levofloxacin, ciprofloxacin, and azithromycin
Katz et al (2011)[4]	HI, USA	A 26-year-old man presented with a 5-day history of greenish penile discharge and dysuria; he was in a mutually monogamous relationship with a 22-year-old woman with whom he had been cohabitating for the past 5 months, and having oral and vaginal sex approximately once a week	Gram stain of a urethral swab identified Gram-negative extracellular diplococci, later confirmed as *N meningitidis*

This table excludes larger outbreaks (described in the main text under "Outbreaks of meningococcal urethritis among men who have sex with women").

Table 1: Published reports of sporadic genitourinary urogenital and anorectal infections due to *Neisseria meningitidis* in people who have heterosexual sex

	Location	Patients and characteristics	Diagnosis and outcomes
Givan et al (1974)[21]	Toronto, ON, Canada	Report of four MSM attending a sexual health clinic, who were all asymptomatic apart from one case with rectal soreness	Meningococcus was isolated from the urethra in all four cases; two also had meningococcus isolated from the throat (MenB and MenC)
Beck et al (1974)[30]	London, UK	A passive MSM with a history of rectal gonorrhoea and perianal warts presented, presented with rectal discomfort and proctitis	Gram-negative diplococci were seen on a rectal swab and subsequently identified as MenB
Givan et al (1977)[22]	Toronto, ON Canada	Report of 12 MSM over a 26-month period: three had urethral discharge, one each had mild rectal burning, rectal itching, and rectal discharge; six had no symptoms	*Neisseria meningitidis* isolated from the urethra of five (three with urethritis, two with no symptoms), and from anal swabs of seven (five also had positive throat swabs)
Odegaard et al (1977)[31]	Oslo, Norway	Report of nine patients screened for gonorrhoea during 1975; of the six (four men including two MSM and two women) with clinical details, five were asymptomatic	Among six men, *N meningitidis* was isolated from the urethra (n=5) or rectum (n=1); among three women, *N meningitidis* was isolated from cervix (n=2) or urethra (n=1); the isolates were subsequently identified as MenA (n=1), MenB (n=6), and MenC (n=2); of the six with clinical details, the meningococci disappeared spontaneously in five cases, while one man with asymptomatic infection still harboured meningococci in the rectum after 1 month
Maini et al (1992)[27]	London, UK	Report of ten MSM aged 26–44 years presenting to a London genitourinary medicine clinic; seven were symptomatic, six with purulent discharge, five with dysuria, and four with both discharge and dysuria	*N meningitidis* confirmed in urethral cultures for all cases
Conde-Glez et al (1991)[29]	Mexico City, Mexico	An MSM presented to a sexual health clinic with acute urethritis	Initially diagnosed with gonorrhoea; subsequent culture confirmed MenB
Genders et al (2013)[28]	Leiden, Netherlands	A 53-year-old man presented with penile discharge and dysuria after anonymous unprotected receptive oral sex with other men; the last contact had been 5 days previously	A purulent yellow-green discharge from the urethra was present; urethral smear, with methylene blue staining, showed numerous polymorphonuclear cells with intracellular and extracellular diplococci; he was treated for presumed gonorrhoea; culture of the isolate revealed *N meningitidis* and he was also diagnosed with concurrent *Chlamydia trachomatis* urethritis
Hayakawa et al (2014)[26]	Tokyo, Japan	A 33-year-old HIV-positive MSM presented with urethral discharge for 4 days after having oral and anal sex with his male partner	Gram-negative diplococci seen on microscopy of urethral discharge and the isolate was subsequently identified as MenW (ST10651, of the ST11/ ET37 complex); the same strain was also isolated from the throat of his male partner
Jannic et al (2019)[25]	Paris, France	A 22-year-old man presented with purulent urethral discharge and pain while urinating; his last sexual intercourse occurred 3 weeks before with his stable, unique, asymptomatic partner	Urethral culture yielded growth with oxidase and Gram stain results consistent with gonococcus, but matrix-assisted laser desorption/ionization time-of-flight mass spectrometry identified *N meningitidis*; a pharyngeal swab from his partner also grew *N meningitidis*; both isolates were identical and non-groupable by slide agglutination serogrouping, and belonged to ST11 with finetype PorA 1.5,2; FetA F1-1

MSM=men who have sex with men.

Table 2: **Published reports of urogenital and anorectal infections due to *Neisseria meningitidis* in MSM**

	Location	Patients	Summary of main findings
Judson et al (1978)[42]	Denver, CO, USA	Analysis of *Neisseria* isolates from consecutive male and female patients attending a sexual health clinic during 1976–77	Anal meningococcal infection among MSM (15 [2%] of 731), was more prevalent than urethral infection among MSM (3 [<1%] of 669, p<0·01), or anal infection among women who have heterosexual sex (2 [<1%] of 1197, p<0·001); the 20 isolates with serogroup information included MenA (n=1), MenB (n=6), MenC (n=5), MenD (n=1), MenX (n=2), MenY (n=1), MenZ (n=2), and two strains were non-groupable
Janda et al (1980)[43]	Chicago, IL, USA	815 MSM attending a sexual health clinic over a 12-month period	*Neisseria meningitidis* was found mainly in the oropharynx (n=347, 43%), compared with the urethra (n=6, 1%) or the rectum (n=16, 2%); meningococcal urethral isolates were associated with urethral discharge in five of the six patients, but meningococcal carriage in the oropharynx and rectum was less likely to be associated with symptoms; *Neisseria gonorrhoeae* was more frequently isolated from the urethra (19%) and rectum (16%), and less likely from the oropharynx (6%); nearly all patients with urethral gonococcal colonisation (150 [99%] of 151) had symptoms of urethritis, whereas 89% of patients with oropharyngeal colonisation, and 62% of patients with anorectal colonisation, had no local symptoms
Faur et al (1981)[44]	New York City, NY, USA	During 1975–79, 964 meningococcal isolates were recovered from the urogenital tract or anal canal in the course of the screening programme for gonorrhoea	Most strains were isolated from anal cultures of MSM, many of whom had symptoms of urethritis and proctitis; of the 97 meningococcal isolates that were serogrouped, MenB was responsible for 48%, MenC for 22%, and MenY 13%; the rest of the isolates were distributed among all serogroups except MenD; in three cases, meningococcal colonisation was also documented in the sexual partners, including one female partner who was also symptomatic; they had infection due to serogroup 29E
Carlson et al (1980)[45]	Boston, MA, USA	663 consecutive anogenital isolates were examined, from men with a presumptive diagnosis of gonorrhoea	*N meningitidis* was identified in four (1%) of 368 *Neisseria* positive cultures from urethral specimens from men who have sex with women, compared to 15 (13%) of 114 specimens from MSM; *N meningitidis* was also more frequently isolated from urethral (six [55%] of 11) and anal specimens (16 [31%] of 52) from MSM screened at bathhouses, compared with those screened at a clinic for MSM (nine [9%] of 103 urethral specimens and 20 [16%] of 123 anal specimens); the authors speculated that MSM attending bathhouses may be more promiscuous than those attending the clinic, or that they may have experienced sexual contact shortly before screening
Salit et al (1982)[46]	Toronto, ON, Canada	383 MSM attending a sexual health clinic or a community screening clinic	*N meningitidis* was isolated from the throat in 129 (36%) of 362, rectum in eight (3%) of 316, and urethra in one (<1%) of 357, compared with isolation of gonococcus from five (1%) of 362, 29 (9%) of 316 and 0 of 357, respectively; the study also found that gonococci (mainly rectal) were 1·4 times more likely to be isolated from (mainly oropharyngeal) meningococcal carriers; overall, 14 (11%) of 134 meningococcal carriers were gonococcal culture positive, compared to 19 (8%) of 249 with negative meningococcal cultures; of the isolates with serogroup information, MenB (n=18, 13%), MenW (n=17, 12%), MenZ (n=14, 10%) and Men29E (n=10, 7%) were the most common serogroups
Jaffe et al (1983)[47]	New York City, NY, USA	92 isolates of *Neisseria* were cultured from the anogenital region of sexually active, inner-city black and Hispanic adolescents in 1981	Of the 92 isolates, 81 (88%) were *N gonorrhoeae*, eight (9%) were *N meningitidis*, and three (3%) could not be speciated
McKenna et al (1993)[48]	Edinburgh, UK	88 670 patients who were screened for anogenital gonorrhoea over a 13-year period at a genitourinary medicine unit	Non-gonococcal *Neisseria* (85% identified as *N meningitidis*) were isolated from 114 (<1%) of 88 18 69 670 patients, compared with around 9000 (10%) anogenital gonococcal infections; Non-gonococcal anogenital *Neisseria* prevalence was highest among MSM (67 [1%] of 4370), followed by women (27 [<1%] of 31 500), and men who have sex with women (20 [<1%] of 52 800); 18 men who have sex with women had meningococci isolated from their urethras, 11 (61%) of whom had urethritis; one (2%) of 49 men with rectal colonisation had proctitis; and none of nine women with cervical colonisation were symptomatic
Maini et al (1992)[37]	London, UK	5571 urethral cultures taken from MSM, 8992 urethral cultures from men who have sex with women, and 15 976 cervical cultures from women, from those attending a genitourinary medicine clinic during 1989–91	11 meningococcal isolates from 10 (<1%) of 5571 urethral cultures taken from MSM, compared to 262 (4·7%) of urethral cultures for *N gonorrhoeae*; no meningococci were isolated from 8992 urethral cultures from men who have sex with women, or from 15 976 cervical cultures; seven of the ten men with meningococcal isolates were symptomatic with purulent discharge, dysuria, or both; three of the ten men also had *N meningitidis* isolated from the oropharynx, and two of these three were also *N meningitidis* positive on rectal swab; in MSM, three (33%) of nine urethral swabs positive for *Neisseria* species were identified as *N meningitidis*, compared to only four (9%) of 46 urethral swabs from men who have sex with women (ie, meningococci contributed to a higher proportion of symptomatic urethritis among MSM, while gonococci were more prevalent among men who have sex with women and develop urethritis)
D'Antuono et al (1999)[49]	Bologna, Italy	Assessment of almost 800 men with urethritis attending an STD clinic over a 21-month period	Seven cases (four men who have sex with women, three MSM) of meningococcal urethritis (1% positivity rate) associated with unprotected orogenital intercourse with their habitual partners before the onset of symptoms; seven (88%) of eight sexual partners tested were asymptomatic oropharyngeal meningococcal carriers; 48 gonococcal positive cases (42 men who have sex with women, six MSM)

MSM=men who have sex with men. STD=sexually-transmitted disease.

Table 3: Screening, carriage, and diagnostic studies reporting *Neisseria meningitidis* isolated from the urogenital or anorectal tract

	Location, outbreak year	Number of cases (deaths, case-fatality ratio)	Summary of main findings
North America			
Tsang et al[60]	Toronto, Canada, 2001	6 (2, 33%)	MSM who had direct or indirect contact with bathhouses for males during the incubation period; outbreak due to genetic variant of MenC:NT:P1.2 (serotype 2a ET-15)
Schmink et al[61]	Chicago, IL, USA, 2003	6 (3, 50%)	MSM aged 27–42 years presented with sepsis and petechial or purpuric rash; all attended MSM-oriented social venues on Chicago's north side during the 10 days prior to the onset of illness; outbreak strains were indistinguishable and belonged to MenC ST-11, ET-15, distinct from the clone that caused the Toronto outbreak
Kratz et al[62] and Weiss et al[63]	New York City, NY, USA, 2010–13	22 (7, 32%)	MenC outbreak linked to websites and mobile phone applications that connect men with male sexual partners; seven cases of MenC in men who have sex with women were also diagnosed during the same period
Civen et al[64]	Los Angeles, CA, USA, 2012–14	35 (9, 26%); 13 MSM (5, 38%)	MenC outbreak among MSM; 13 of 35 cases self-reported as MSM including four who were also HIV-positive; annual IMD incidence among MSM was 2·39 per 100 000 vs 0·26 per 100 000 for men who have sex with women (relative risk, 9·20)
Kamiya et al[65]	Chicago, IL, USA, 2015–16	9 (1, 11%)	Seven MSM cases aged 29–54 years were diagnosed in 2015, six were black ethnicity, five were HIV-positive; outbreak was associated with anonymous sex and so-called hook-up apps; 2 additional cases were confirmed in 2016
Nanduri et al[66]	CA, USA, 2016	25 (2, 8%)	24 cases were confirmed as MenC and one due to *N meningitidis* with an undetermined serogroup
Europe			
Hellenbrand et al[67] and Marcus et al[68]	Berlin, Germany, 2012–13	5 (3, 40%)	Five cases were identified, no links to international travel between the European and US cases; outbreak due to MenC variant with the finetype P1.5-1,10-8:F3-6
Aubert et al[69]	Paris, France, 2013	36 (6, 17%)	14 MenC cases were reported in France among men aged 25–59 years, and six cases in women during the first half of 2013; between June, 2013, and December, 2014, additional MenC cases were identified among MSM living in the Paris region, and also among women and men who did not identify as MSM but attended social venues associated with the gay community; outbreak was due to MenC:P1.5-1,10-8:F3-6:cc11 (ET-15); MenC IMD incidence among MSM (2·28/100 000) was nearly ten times higher than among men who have sex with women (0·24/100 000)
Miglietta et al[70]	Tuscany, Italy, 2015–16	62 (13, 21%)	17 clusters identified, with six discos and four gay venues identified as transmission hotspots; attended by 34 of the cases in the 10 days before symptoms onset; ten cases were among MSM, three cases among bisexuals, and five cases among men who have sex with women and attended gay venues; no epidemiological link was identified, but the responsible strain was closely related to other outbreaks among MSM in Europe and the USA: MenC, P1.5-1,10–8:F3–6:ST-11 (clonal complex 11)
Rest of the world			
Sutton[71]	Melbourne, VIC, Australia, 2017	8 (deaths not reported)	Eight cases of MenC disease identified among MSM in Melbourne, Victoria, with evidence of local transmission; MenACWY vaccination offered to all MSM including bisexual men

IMD=invasive meningococcal disease. MSM=men who have sex with men.

Table 4: Outbreaks of IMD in MSM

Conclusions

N meningitidis is a well known cause of bacterial meningitis and sepsis but, in addition to other uncommon clinical manifestations, there is now increasing evidence to support that diverse strains of the pathogen cause sporadic cases of urogenital and anorectal infections among people who have heterosexual sex and, more so, among MSM. Such infections, however, have been rare, likely because meningococci in general are not adapted for transmission through oral sex or sexual intercourse, or for colonising or infecting the urogenital and anorectal tracts. Since the early 2000s, however, there have been increasing reports of clusters and outbreaks of invasive meningococcal disease among MSM and, most recently, reports of meningococcal urethritis in people who have heterosexual sex. The responsible isolates were identified as belonging to the hypervirulent ST-11 complex lineage 11.2, predominantly comprised of MenC isolates. Different members of this lineage have independently acquired the gonococcal trait of anaerobic growth owing to expression of nitrite reductase, which is usually not expressed by the majority of clonal complex 11 strains. A small cluster of urethritis-associated meningococcal isolates were observed to have lost the ability to express fHbp, while isolates capable of causing invasive disease among MSM retained this ability. Furthermore, a novel urethritis-associated meningococcal strain has also lost the ability to express a capsule and is, therefore, no longer preventable by meningococcal polysaccharide conjugate vaccines.

Natural History of Asymptomatic SARS-CoV-2 Infection

Information on the natural history of asymptomatic infection with severe acute respiratory syndrome coronavirus 2 (SARS-CoV-2) remains scarce. The outbreak of coronavirus disease 2019 (Covid-19) on the cruise ship *Diamond Princess* led to 712 persons being infected with SARS-CoV-2 among the 3711 passengers and crew members, and 410 (58%) of these infected persons were asymptomatic at the time of testing (see the Supplementary Appendix, available with the full text of this letter at NEJM.org). Here, we report the natural history of asymptomatic SARS-CoV-2 infection in part of this cohort. A total of 96 persons infected with SARS-CoV-2 who were asymptomatic at the time of testing, along with their 32 cabinmates who tested negative on the ship, were transferred from the *Diamond Princess* to a hospital in central Japan between February 19 and February 26 for continued observation. Clinical signs and symptoms of Covid-19 subsequently developed in 11 of these 96 persons, a median of 4 days (interquartile range, 3 to 5; range, 3 to 7) after the first positive polymerase-chain-reaction (PCR) test, which meant that they had been presymptomatic rather than asymptomatic. The risk of being presymptomatic increased with increasing age (odds ratio for being presymptomatic with each 1-year increase in age, 1.08; 95% confidence interval [CI], 1.01 to 1.16). Eight of 32 cabinmates with a negative PCR test on the ship had a positive PCR test within 72 hours after arrival in the hospital but remained asymptomatic. In total, data on 90 persons with asymptomatic SARS-CoV-2 infection, defined as persons who were asymptomatic at the time of the positive PCR test and remained so until the resolution of infection.

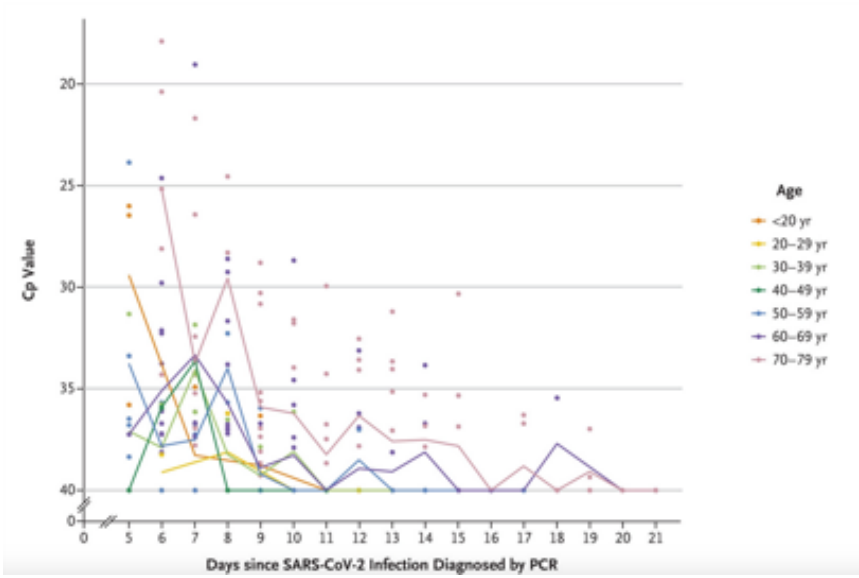

The group of persons with asymptomatic SARS-CoV-2 infection consisted of 58 passengers and 32 crew members, with median age of 59.5 years (interquartile range, 36 to 68; range, 9 to 77). A total of 24 of these persons (27%) had coexisting medical conditions, including hypertension (in 20%) and diabetes (9%). The first PCR test at the hospital was performed a mean of 6 days after the initial positive PCR test on the ship. The median number of days between the first positive PCR test (either on the ship or at the hospital) and the first of the two serial negative PCR tests was 9 days (interquartile range, 6 to 11; range, 3 to 21), and the cumulative percentages of persons with resolution of infection 8 and 15 days after the first positive PCR test were 48% and 90%, respectively. The risk of delayed resolution of infection increased with increasing age (mean delay in resolution for an increase in age from 36 to 68 years, 4.41 days; 95% CI, 2.28 to 6.53)

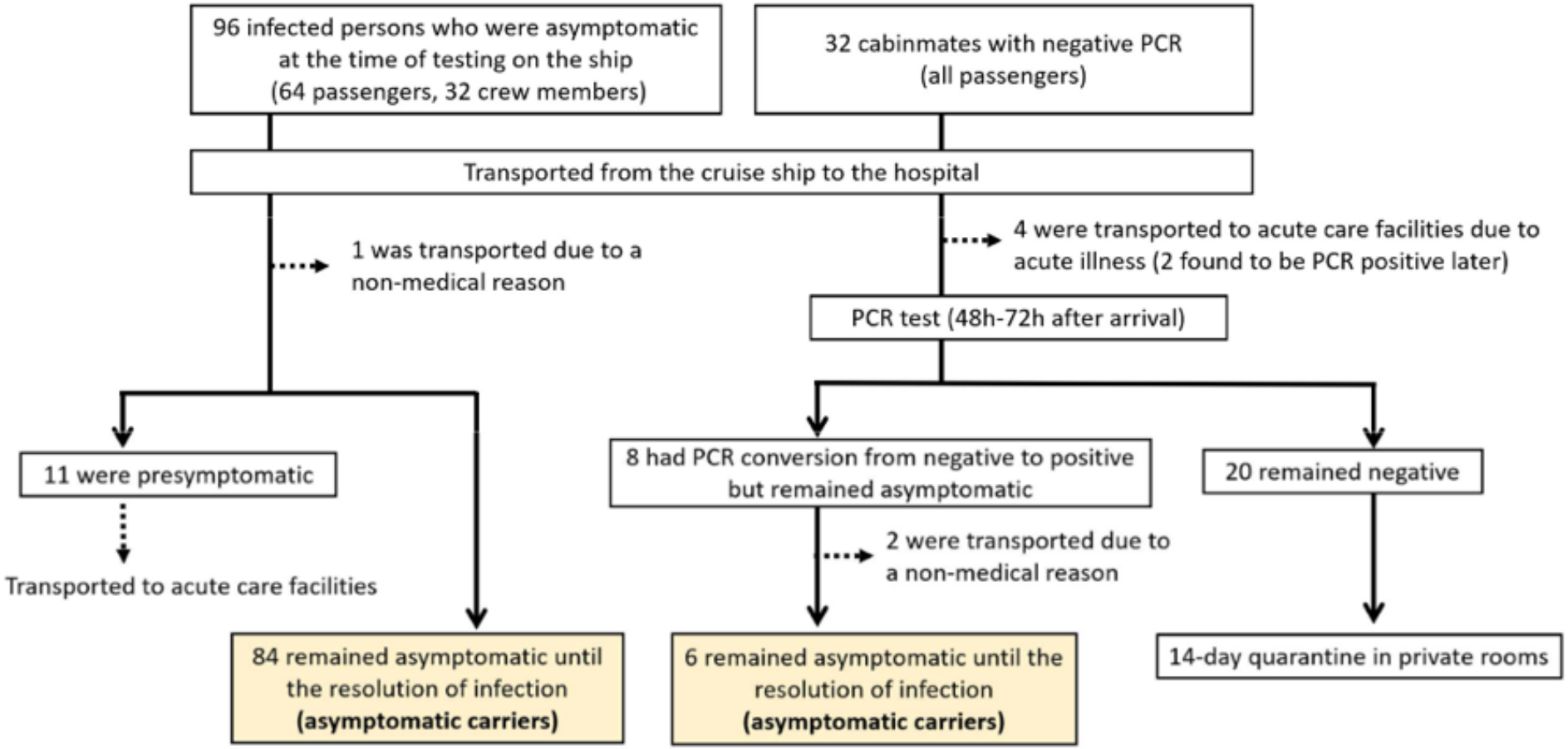

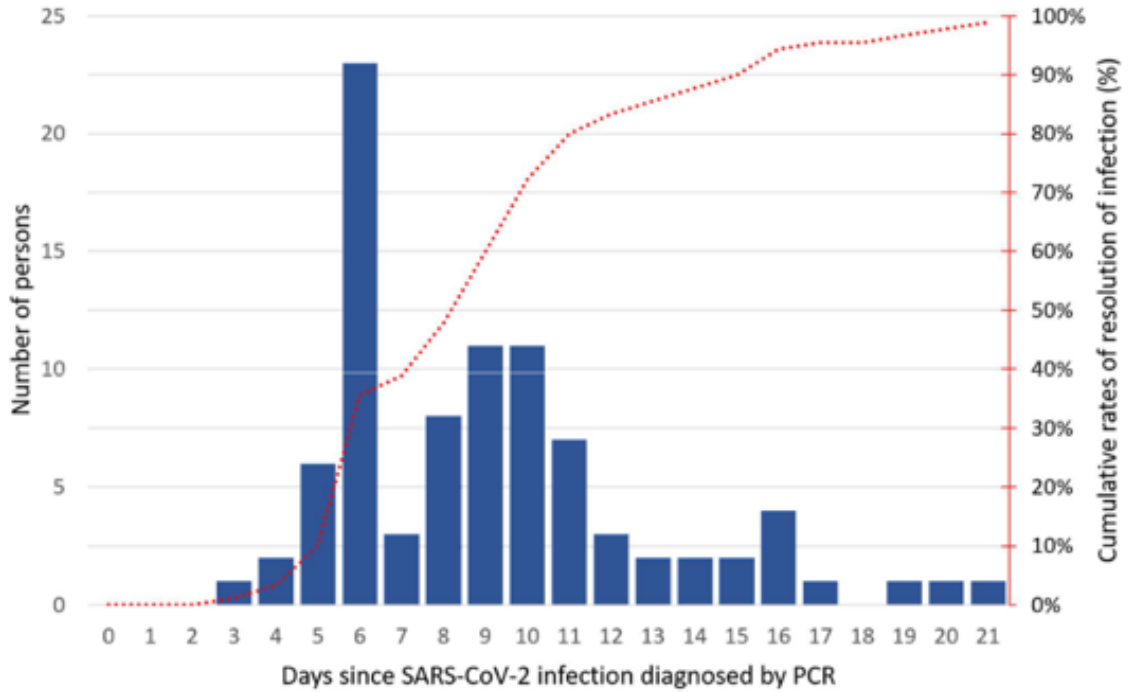

	14-Feb		15-Feb		16-Feb		17-Feb		18-Feb		19-Feb		20-Feb		21-Feb		Reasons for transfer
Patient	AM	PM	AM	PM	AM	PM	AM	PM	AM	PM	AM	PM	AM	PM	AM	PM	
1	PCR+										■XX						fever, desaturation, cough
2		PCR+									■XX						desaturation
3		PCR+									■XX						fever, lethargy
4		PCR+									■XX						fever, desaturation
5		PCR+									■				XX		cough, sputum
6				PCR+								■	XX				fever
7					PCR+						■	XX					fever, sore throat
8					PCR+							■XX					desaturation, cough, sputum
9					PCR+									■XX			fever, chest pain
10					PCR+									■XX			desaturation, cough
11							PCR+							■XX			fever

PCR+, first positive PCR on the cruise ship
■, arrival from the cruise ship to the facility
XX, onset of clinical signs or symptoms consistent with COVID-19

Supplementary Figure 5. Courses of 11 presymptomatic patients, who were asymptomatic at the time of the first positive PCR test but subsequently developed symptoms.

False Negative Tests for SARS-CoV-2 Infection — Challenges and Implications

There is broad consensus that widespread SARS-CoV-2 testing is essential to safely reopening the United States. A big concern has been test availability, but test accuracy may prove a larger long-term problem.

Diagnostic tests (typically involving a nasopharyngeal swab) can be inaccurate in two ways. A false positive result erroneously labels a person infected, with consequences including unnecessary quarantine and contact tracing. False negative results are more consequential, because infected persons — who might be asymptomatic – may not be isolated and can infect others. Third, measuring test sensitivity in asymptomatic people is an urgent priority. It will also be important to develop methods (e.g., prediction rules) for estimating the pretest probability of infection (for asymptomatic and symptomatic people) to allow calculation of post-test probabilities after positive or negative results. Fourth, negative results even on a highly sensitive test cannot rule out infection if the pretest probability is high, so clinicians should not trust unexpected negative results (i.e., assume a negative result is a “false negative” in a person with typical symptoms and known exposure). It’s possible that performing several simultaneous or repeated tests could overcome an individual test’s limited sensitivity; however, such strategies need validation.

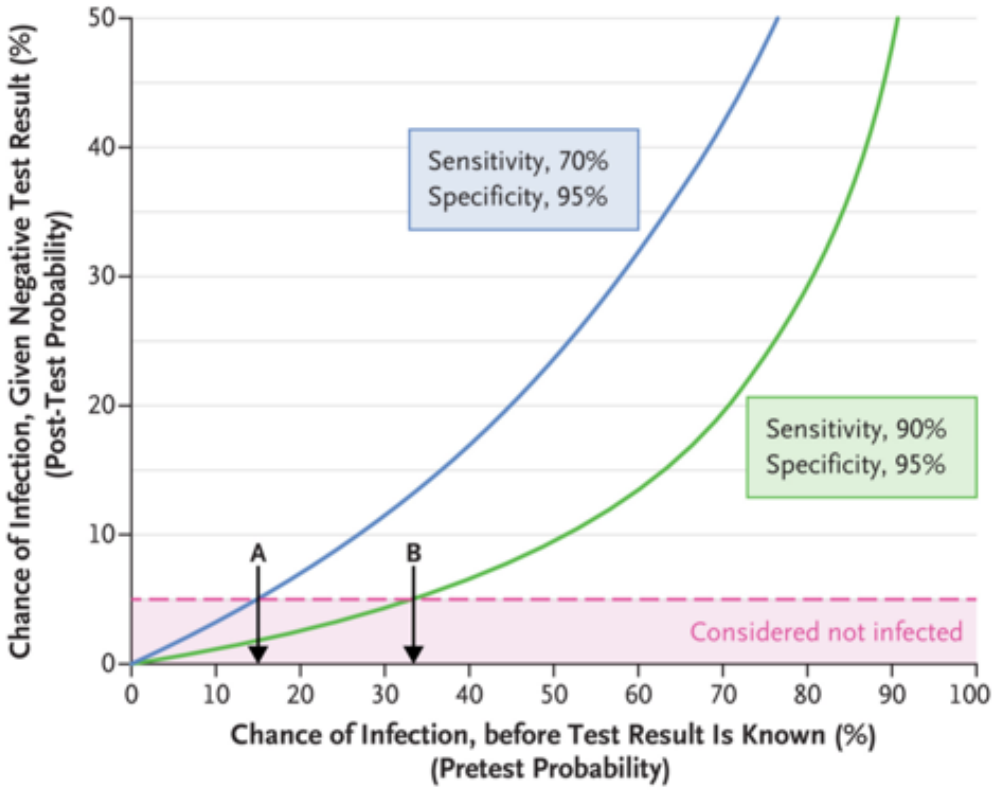

Chance of SARS-CoV-2 Infection, Given a Negative Test Result, According to Pretest Probability.

The blue line represents a test with sensitivity of 70% and specificity of 95%. The green line represents a test with sensitivity of 90% and specificity of 95%. The shading is the threshold for considering a person not to be infected (asserted to be 5%). Arrow A indicates that with the lower-sensitivity test, this threshold cannot be reached if the pretest probability exceeds about 15%. Arrow B indicates that for the higher-sensitivity test, the threshold can be reached up to a pretest probability of about 33%. An interactive version of this graph is available at NEJM.org.

Wie funktioniert die Corona-Warn-App?

Die App erfasst, welche Smartphones einander nahegekommen sind. Dazu tauschen die Geräte via Bluetooth zufällig erzeugte Krypto-Schlüssel aus. Diese Schlüssel werden nicht permanent verschickt, sondern in Abständen von zweieinhalb bis fünf Minuten als Salve von 16 Schlüsseln binnen vier Sekunden. Auf Basis der Signalstärke wird dabei die Entfernung geschätzt.

Wird ein Nutzer positiv auf Covid-19 getestet, kann kann er das Testergebnis in der App teilen, damit Nutzer, die sich in seiner Nähe aufgehalten hatten, informiert werden. Infizierte werden ausdrücklich gefragt, ob sie das Ergebnis zur Kontakt-Nachverfolgung teilen wollen. Alternativ zu der digitalen Übertragung steht eine Validierung über ein Call Center der Telekom zur Verfügung.

So funktioniert die Corona-Tracing-App
tagesschau 20:00 Uhr, 14.06.2020, Tina Petersen, NDR

Atrial septal defect and haemodynamic consequences of continuous positive airway pressure treatment

Rob Eerdekens, Sjoerd Bouwmeester

Lancet 2020; 395: 1864

Department of Cardiology, Catharina Hospital Eindhoven, Eindhoven, Netherlands
(R Eerdekens MD, S Bouwmeester MD)

Correspondence to:
Dr Rob Eerdekens, Department of Cardiology, Catharina Hospital Eindhoven, Eindhoven 5623, Netherlands
rob.eerdekens@catharinaziekenhuis.nl

A 51-year-old man was referred to our department because of reduced exercise tolerance and breathlessness on exertion. He had a medical history of obstructive sleep apnoea syndrome (OSAS), which was being treated with continuous positive airway pressure (CPAP). He had complained of snoring and a loss of concentration when he was first diagnosed with OSAS, in 2012.

The referring pulmonologist said that the patient's Apnoea–Hypopnea Index had improved from 36 events per h to 0·3 events per h after the positive pressure was increased from 4 to 8 cm water (H_2O), and for a short period there had been an improvement in the patient's problems, but then the CPAP seemed to make the situation worse—his exercise tolerance decreased further, and he reported insomnia and pronounced morning fatigue.

When we examined the patient, his oxygen saturation was 94%. On auscultation of his chest, we heard a systolic murmur at the left, second intercostal space. An echocardiogram showed a large ostium secundum atrial septal defect (ASD) and an enlarged right ventricle with preserved systolic function (figure). The patient's mean pulmonary artery pressure was 18 mm Hg (normal <25) with no CPAP, indicating no pulmonary hypertension. However, there was evidence of shunting: the pulmonary to systemic output ratio was 2·8:1 (normal 1:1; greater than 1 indicates left-to-right shunting). We therefore concluded that the augmented CPAP had led to the development of his symptoms.

As proof of concept, we took arterial blood samples both at rest and at a positive pressure of 8 cm H_2O: these showed that his arterial partial pressure of oxygen reduced from 15 to 11 kPa. We also did an echocardiogram with agitated saline while gradually increasing the positive pressure (0 cm H_2O, 8 cm H_2O, and 12 cm H_2O; appendix). The echocardiogram with the agitated saline clearly showed that the right-to-left shunting increased concomitantly with the CPAP increases: causing a reduction in arterial oxygen saturation. The patient had surgery to close the ASD and his difficulties resolved. The size of his right ventricle reduced and he was able to use his CPAP without any problems. Interestingly, at the time of the initial diagnosis of OSAS, the patient was found to have some dilatation of the right ventricle and pulmonary trunk. An echocardiogram at that time might have resulted in earlier diagnosis of the ASD and earlier surgery.

Around 10% of congenital heart defects are ASDs. Clinically, a fixed, split second heart sound and an ejection systolic murmur over the pulmonary valve can be heard; there may also be signs of right-sided heart failure. An electrocardiogram might show arrhythmias including atrial fibrillation and incomplete right bundle branch block with right—in the ostium secundum—or left—in the ostium primum—axis deviation. Late diagnosis of an ASD might lead to the development of Eisenmenger syndrome when surgery would be contraindicated (video).

See Online for appendix

See Online for video

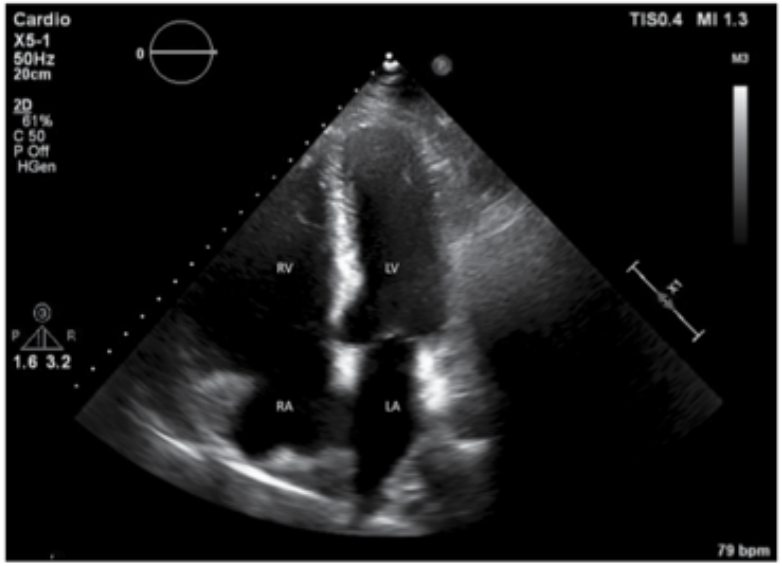

Figure: **A paradoxical response to continuous positive airway pressure treatment reveals a defect in the atrial septum**
An echocardiogram shows a large ostium secundum atrial septal defect and an enlarged right ventricle. LA=left atrium. LV=left ventricle. RA=right atrium. RV=right ventricle.

Contributors
We both contributed to caring for the patient, writing the report, and interpreting the data. Written consent for publication was obtained from the patient.

Appendix

Continuous positive airway pressure treatment and atrial septal defect

Echocardiograms with agitated saline done while gradually increasing the positive pressure: without agitated saline (A), at 0 cm H_2O (B), at 8 cm H_2O (C), and at 12 cm H_2O (D) shows right-to-left shunting increased concomitantly with the CPAP changes.

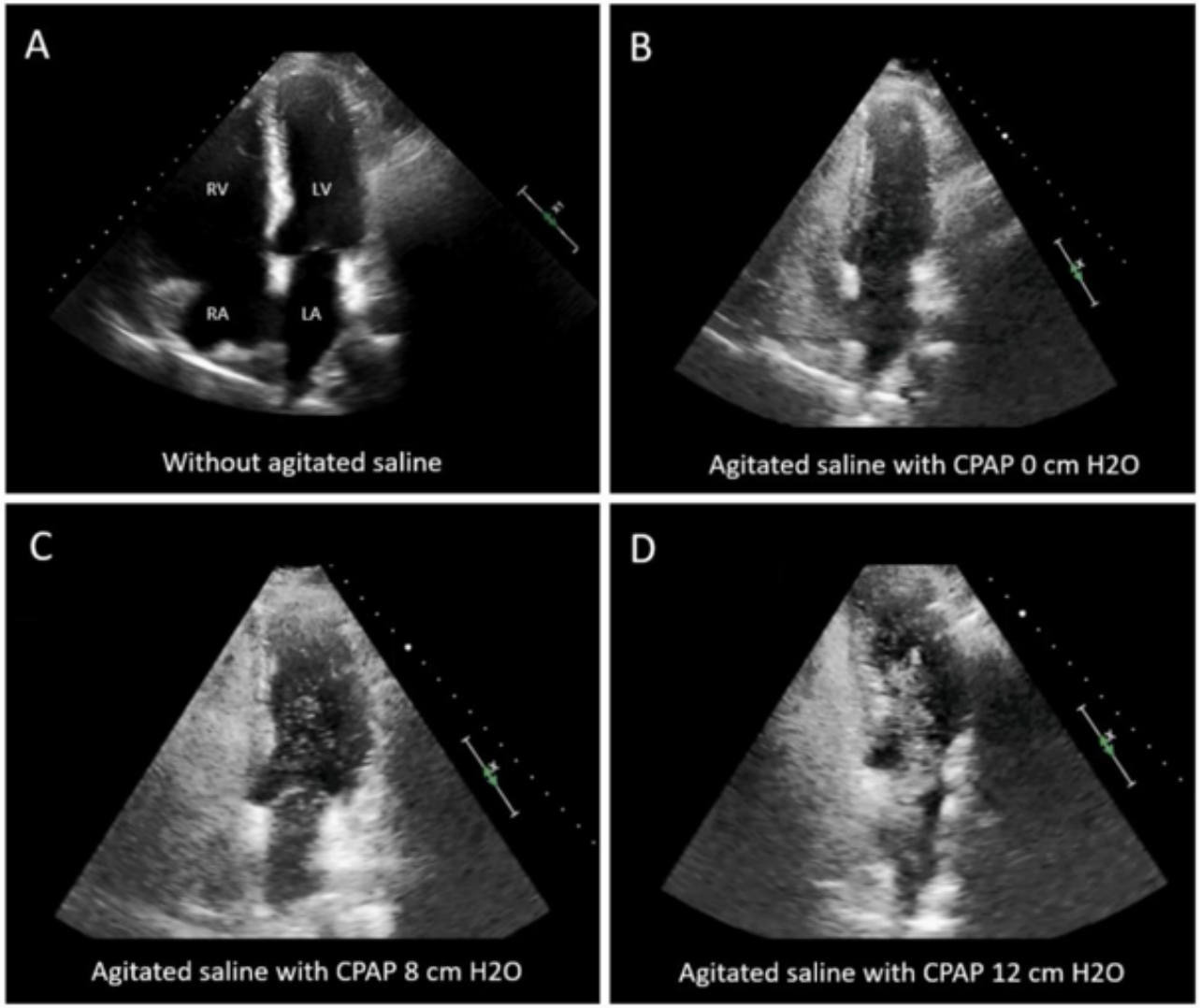

Lawyer says Buffalo activist, 75, shoved by cops suffered a brain injury when he cracked his head on a sidewalk - just days after Trump claimed he was 'an ANTIFA provocateur' who exaggerated his fall

- Activist Martin Gugino is starting physical therapy, his lawyer said Thursday
- Gugino, was shoved to the ground by police in shocking incident in Buffalo
- Catholic peace activist was hospitalized in ICU after hitting his head
- Both officers seen in the video shoving him have been charged with assault
- Trump made baseless claim Gugino was an 'antifa agent scanning cop radios'
- President claimed the activist may have faked his fall and injury to smear cops

Buffalo protester Martin Gugino has brain injury, fractured skull after being pushed by police: lawyer

Gugino, of Amherst, had been in serious but stable condition following the incident before his condition was upgraded to fair earlier this week and he was moved to Erie County Medical Center's rehabilitation floor.

On Friday, his lawyer, Kelly Zarcone, said Gugino's skull was fractured and that he hasn't been able to walk yet. She'd previously said that Gugino's brain was injured and he has started physical therapy.

Gugino said via an attorney statement Friday that it was "very unnecessary to focus on me...There are plenty of other things to think about besides me," such as helping each other and peacefully addressing societal shortcomings rather than spending energy on him, Zarcone clarified.